

EVALUATION OF CYCLIC STEAM INJECTION IN MULTI-LAYERED HETEROGENEOUS
RESERVOIR

Miss Worawanna Panyakotkaew



จุฬาลงกรณ์มหาวิทยาลัย

CHULALONGKORN UNIVERSITY

บทคัดย่อและแฟ้มข้อมูลฉบับนี้ของวิทยานิพนธ์ที่แต่งเมื่อปี ค.ศ. 2554 ที่ขึ้นชื่อในคลังข้อมูลจุฬาฯ (CUIR)

for the Degree of Master of Engineering Program in Petroleum Engineering

The abstract and full text of theses from the academic year 2011 in Chulalongkorn University Intellectual Repository (CUIR)

are the thesis authors' files submitted through the University Graduate School.

Faculty of Engineering
Chulalongkorn University

Academic Year 2014

Copyright of Chulalongkorn University

การประเมินการฉีดอัดไอน้ำแบบวัฏจักรในแหล่งกักเก็บไวรัสพันธุ์หลายชั้น

นางสาวรรรรณา ปัญญาทแก้ว



วิทยานิพนธ์นี้เป็นส่วนหนึ่งของการศึกษาตามหลักสูตรปริญญาวิศวกรรมศาสตรมหาบัณฑิต

สาขาวิชาวิศวกรรมปิโตรเลียม ภาควิชาวิศวกรรมเหมืองแร่และปิโตรเลียม

คณะวิศวกรรมศาสตร์ จุฬาลงกรณ์มหาวิทยาลัย

ปีการศึกษา 2557

ลิขสิทธิ์ของจุฬาลงกรณ์มหาวิทยาลัย

Thesis Title	EVALUATION OF CYCLIC STEAM INJECTION IN MULTI-LAYERED HETEROGENEOUS RESERVOIR
By	Miss Worawanna Panyakotkaew
Field of Study	Petroleum Engineering
Thesis Advisor	Falan Srisuriyachai, Ph.D.

Accepted by the Faculty of Engineering, Chulalongkorn University in Partial Fulfillment of the Requirements for the Master's Degree

.....Dean of the Faculty of Engineering
(Professor Bundhit Eua-arporn, Ph.D.)

THESIS COMMITTEE

.....Chairman
(Assistant Professor Jirawat Chewaroungroj, Ph.D.)

.....Thesis Advisor
(Falan Srisuriyachai, Ph.D.)

.....Examiner
(Assistant Professor Kreangkrai Maneeintr, Ph.D.)

.....External Examiner
(Witsarut Tungsunthonkhan, Ph.D.)

5671215221 : MAJOR PETROLEUM ENGINEERING

KEYWORDS: ENHANCED OIL RECOVERY / THERMAL RECOVERY / CYCLIC STEAM INJECTION / HETEROGENEITY

WORAWANNA PANYAKOTKAEW: EVALUATION OF CYCLIC STEAM INJECTION IN MULTI-LAYERED HETEROGENEOUS RESERVOIR. ADVISOR: FALAN SRISURIYACHAI, Ph.D., 109 pp.

Cyclic steam injection (CSI) is a thermal recovery technique performed by injecting periodically heated steam into heavy oil reservoir. Oil viscosity is substantially reduced by means of heat transferred from steam. Together with gas pressurization, oil recovery is greatly improved.

Effects of reservoir heterogeneity together with reservoir parameters are evaluated prior to field implementation. Judging of the best operating parameters is based on oil recovery factor and energy consumption. Steam quality of 1.0 together with soaking period of 6 days is chosen as the best condition.

Results show that reservoir heterogeneity in terms of Lorenz coefficient value slightly affects CSI process. Reservoir model with Lorenz coefficient value of 0.328 which is moderate heterogeneous model obtains benefits from well-distribution of permeability and good steam propagation. High oil recovery factor is obtained from early and later periods and low energy consumption is achieved. Higher vertical permeability is more favorable for CSI process. Better propagation of steam in upper layers and percolation of hot condensed water due to gravity results in high oil recovery factor. Higher portion of structural shale reduces performance of CSI process due to reduction of thermal conductivity of rock and hence, this condition is not favorable. Lower value of Corey's exponent favors steam propagation in top layers due to high effective permeability of fluids. Smaller irreducible water at reservoir temperature results in higher initial oil saturation. Therefore, higher portion of oil receives heat from steam, resulting in high oil recovery. Smaller residual oil at elevated temperature is favorable since oil can be maximally recovered. Coarsening upward permeability sequence leads to well development of steam chamber on top of reservoir that consequently causes percolation of hot condensed water to lower layers, whereas steam tends to expand in middle layers in fining upward sequence.

Department: Mining and Petroleum
Engineering

Student's Signature

Advisor's Signature

Field of Study: Petroleum Engineering

Academic Year: 2014

ACKNOWLEDGEMENTS

First of all, I would like to express my sincere gratitude to my thesis advisor, Dr. Falan Srisuriyachai for his invaluable help and guidance throughout my entire study. This thesis would not have been accomplished without devotion of his time, expertise and skill to me.

I would like to take this opportunity to thank all the thesis committees and all of faculty members in the Department of Mining and Petroleum Engineering for sharing their technical knowledge and giving useful advice together with recommendations to develop my work.

In addition, I would like to express special thanks to Chevron Thailand Exploration and Production, Ltd. for providing financial support for this study.

Finally, I am also grateful to my parents, family and friends for their supports and continuous encouragement throughout my thesis and my entire study as well.

CONTENTS

	Page
THAI ABSTRACT	iv
ENGLISH ABSTRACT	v
ACKNOWLEDGEMENTS	vi
CONTENTS	vii
LIST OF TABLES	x
LIST OF FIGURES	xi
LIST OF ABBREVIATIONS	xviii
LIST OF NOMENCLATURES	xx
CHAPTER I INTRODUCTION	1
1.1 Background	1
1.2 Objective	2
1.3 Outline of Methodology	3
1.4 Outline of Thesis	3
CHAPTER II LITERATURE REVIEW	5
2.1 Study of Oil Recovery Process and Reservoir Properties Altered by Cyclic Steam Injection	5
2.2 Operating Conditions and Optimization of CSI	7
2.3 Application of CSI in Pilot Scale and Oil Field	8
2.4 Effect of Heterogeneity on Thermal Recovery	8
CHAPTER III RELEVANT THEORY	10
3.1 Cyclic Steam Injection (CSI) and Oil Recovery Mechanisms	10
3.1.1 Cyclic Steam Injection Cycles	10
3.1.2 Oil Recovery Mechanisms	12

	Page
3.2 Properties Involved in Cyclic Steam Injection.....	13
3.2.1 Liquid Viscosity.....	13
3.2.2 Gas Viscosity	14
3.2.3 Relative Permeability.....	15
3.2.4 Thermal Capacity and Thermal Conductivity.....	16
3.2.5 Latent Heat of Vaporization.....	16
3.3 Displacement Mechanism.....	17
3.3.1 Hot Water Displacement	17
3.3.2 Displacement by Saturated Steam	19
3.3.3 Areal Sweep Efficiency and Stability.....	20
3.3.4 Buckley-Leverett Theory.....	22
3.4 Heterogeneous Reservoir	23
3.5 Presence of Shale	24
CHAPTER IV RESERVOIR SIMULATION MODEL AND METHODOLOGY	26
4.1 Reservoir Model.....	26
4.2 Reservoir Model with Heterogeneity	28
4.3 Pressure-Volume-Temperature (PVT) Properties	29
4.4 Special Core Analysis (SCAL) Section	33
4.5 Parameters Related to Injection and Production Wells.....	37
4.6 Thesis Methodology	39
CHAPTER V RESULTS AND DISCUSSION	43
5.1 Cyclic Steam Injection Base Case.....	43
5.1.1 Oil Recovery Mechanisms in Cyclic Steam Injection Process	43

	Page
5.1.2 Selection of Operating Soaking Period and Steam Quality	45
5.2 Effect of Reservoir Heterogeneity on Cyclic Steam Injection	53
5.3 Effect of Vertical Permeability	61
5.4 Effect of Shale Volume.....	67
5.5 Effect of Relative Permeability	71
5.5.1 Corey’s Exponent	71
5.5.2 End Point Saturations at Reservoir Temperature.....	83
5.5.3 End Point Saturations at Elevated Temperature	85
5.6 Effect of Permeability Sequence.....	87
CHAPTER VI CONCLUSION AND RECOMMENDATION.....	93
6.1 Conclusion	93
6.2 Recommendation	95
REFERENCES	96
APPENDIX.....	99
VITA.....	109

LIST OF TABLES

		Page
Table 4.1	Physical properties of reservoir model and reservoir properties.....	27
Table 4.2	Permeability values in each layer of each reservoir model with different Lorenz coefficient	28
Table 4.3	Summary of correlation for each PVT property	29
Table 4.4	Input parameters for PVT data and generated in-situ oil viscosity	30
Table 4.5	Summary of data required for construction of relative permeability curves	34
Table 4.6	Constraints of injection wells at corners of reservoir	38
Table 4.7	Constraints of injection well at center of reservoir	38
Table 4.8	Constraints of production wells at corners of reservoir	38
Table 4.9	Constraints of production well at center of reservoir	38
Table 4.10	Group event constraints of injection and production wells at corners of reservoir.....	39
Table 4.11	Group event constraints of injection and production wells at center of reservoir.....	39
Table 4.12	Cycle period of cyclic steam injection with variation of soaking period. .	39
Table 5.1	Thermal properties for reservoir rock with different structural shale volume	68
Table 5.2	End point saturations of three different cases at reservoir temperature .	83
Table 5.3	End point saturations of three different cases at elevated temperature	86
Table 5.4	Permeability values in each layer of reservoir with coarsening and fining upward sequences.....	88

LIST OF FIGURES

	Page
Figure 3.1 Illustration of Cyclic Steam Injection consisting of injection, soak and production periods [7]	11
Figure 3.2 Radial flow of cyclic steam injection steam, illustrating different radii [8].....	12
Figure 3.3 Viscosity ratio (μ_o/μ_w) as a function of temperature for three different crude oils [9]	14
Figure 3.4 Relative permeability curves of two different oils at different temperatures [9].....	15
Figure 3.5 Effects of temperature on residual oil saturation and irreducible water saturation [9]	15
Figure 3.6 Latent heat of vaporization of water as a function of temperature [9] ...	17
Figure 3.7 Two-dimensional hot water displacement resulting in downstream zone (zone II) and upstream zone (zone I) [9]	18
Figure 3.8 Comparison between temperature distributions from cases with and without heat loss to adjacent formation as a function of distance from steam injection well [9].....	18
Figure 3.9 Three zones from displacement by steam: hot steam zone, condensing zone and hot water zone [9]	19
Figure 3.10 Oil recoveries from steam, hot water and cold water [9].....	20
Figure 3.11 Oil displacement velocity ratio in z direction [9]	22
Figure 3.12 Fluid saturations as a function of dimensionless distance in the steam chamber [10].....	23
Figure 3.13 Flow capacity versus storage capacity distribution [12].....	24

	Page
Figure 3.14 Illustration of different distribution of shale in reservoir [13].....	25
Figure 4.1 Location of wells in reservoir model, representing five-spot pattern (all the wells are both injector and producer depending on cycles).....	26
Figure 4.2 Plots of 5 different Lorenz coefficient values.....	29
Figure 4.3 Dry gas formation volume factor (B_g) for reservoir model as a function of reservoir pressure.....	31
Figure 4.4 Oil formation volume factor (B_o) for reservoir model as a function of reservoir pressure.....	31
Figure 4.5 Oil viscosity (μ_o) for reservoir model as a function of reservoir pressure.....	32
Figure 4.6 Oil viscosity (μ_o) for reservoir model as a function of reservoir temperature	32
Figure 4.7 Gas-oil ratio for reservoir model as a function of reservoir pressure	33
Figure 4.8 Relative permeability curves of oil/water system for reservoir model as a function of water saturation.....	35
Figure 4.9 Relative permeability curves of gas/liquid system for reservoir model as a function of liquid saturation.....	36
Figure 4.10 Relative permeability curves of oil/water system for reservoir model at initial reservoir temperature and at steam temperature as a function of water saturation	36
Figure 4.11 Relative permeability curves of gas/liquid system for reservoir model at initial reservoir temperature and steam temperature as a function of liquid saturation	37
Figure 4.12 Thesis methodology: selection of operating conditions.....	41
Figure 4.13 Thesis methodology: study of interest parameters.....	42

	Page
Figure 5.1 Oil production rate from CSI process as a function of time.....	44
Figure 5.2 Reservoir temperature, oil viscosity and pressure profiles on top layer at different times	44
Figure 5.3 Three-phase fluid saturation profiles at different times.....	45
Figure 5.4 Oil recovery factors for cases with different soaking period and steam quality as a function of time.....	46
Figure 5.5 Summary of oil recovery factor at the end of production from whole cases	47
Figure 5.6 Actual steam-oil ratio for cases with different soaking period and steam quality as a function of time.....	48
Figure 5.7 Average steam-oil ratio for cases with different soaking period and steam quality as a function of time.....	49
Figure 5.8 Summary of cumulative steam oil ratio at the end of production from whole cases.....	50
Figure 5.9 Energy consumed per barrel of oil for cases with different soaking period and steam quality as a function of time	50
Figure 5.10 Average energy consumed per barrel of oil for cases with different soaking period and steam quality as a function of number of cycle	51
Figure 5.11 Summary of average energy consumed at the end of production from whole cases.....	52
Figure 5.12 Comparison between cumulative water injected as steam to cases of steam quality of 1.0 with soaking period of 6 and 8 days.....	53
Figure 5.13 Oil recovery factors obtained from reservoir models with different degrees of heterogeneity as a function of time.....	54
Figure 5.14 Distribution of vertical permeability of reservoir models with L_k 0.265 (minimum) and L_k 0.402 (maximum).....	55

Figure 5.15	Temperature and oil viscosity profiles from reservoir model with L_k 0.265 (minimum) and L_k 0.406 (maximum) at 500 days	56
Figure 5.16	Oil saturation and three-phase fluid saturation profiles from reservoir model with L_k 0.265 (minimum) and L_k 0.406 (maximum) at 500 days....	56
Figure 5.17	Comparison of reservoir temperature profile for reservoir models with different L_k values at the end of production.....	57
Figure 5.18	Summary of oil recovery factor for reservoir model with different L_k values at the end of production	57
Figure 5.19	Energy consumed per barrel of oil obtained from reservoir models with different degrees of heterogeneity as a function of time	58
Figure 5.20	Summary of energy consumed per barrel of oil for reservoir model with different L_k values at the end of production	59
Figure 5.21	Cumulative water injected from reservoir model with L_k value of 0.371 and 0.402 at later cycles	60
Figure 5.22	Cumulative water produced from reservoir model with L_k value of 0.371 and 0.402 at later cycles.....	60
Figure 5.23	Oil recovery factors obtained from cases with different vertical permeability values as a function of time	62
Figure 5.24	Temperature profiles of central well from reservoir models with different k_v/k_h values at different period, illustration steam propagation.....	63
Figure 5.25	Average production rates obtained cases with different vertical permeability values as a function of time	64
Figure 5.26	Three-phase fluid saturation profiles of the central well from reservoir models with different k_v/k_h values at 1,500 days, illustrating steam expansion direction and flow of condensed hot water direction.....	65

Figure 5.27	Three-phase fluid saturation profiles of reservoir models with different k_v/k_h values at 1,500 days.....	65
Figure 5.28	Energy consumed per barrel of oil obtained from reservoir models with different vertical permeability values as a function of time	66
Figure 5.29	Summary of oil recovery factor and energy consumed per barrel of oil obtained from reservoir models with different vertical permeability values at the end of production	67
Figure 5.30	Average reservoir temperatures for cases with different structural shale percent as a function of time	68
Figure 5.31	Comparison of reservoir temperature profile for reservoir models without structural shale volume and with structural shale volume of 25 percent (maximum) at the end of production	69
Figure 5.32	Oil recovery factors for cases with different structural shale percent as a function of time	70
Figure 5.33	Energy consumed per barrel of oil obtained from reservoir models with different structural shale percent as a function of time	70
Figure 5.34	Relative permeability curves of oil/water system for reservoir models with different Corey's exponent values as a function of water saturation.....	72
Figure 5.35	Relative permeability curves of gas/liquid system for reservoir models with different Corey's exponent values as a function of liquid saturation.....	72
Figure 5.36	Relative permeability curves of oil/water system for reservoir models with different Corey's exponent values at different temperature as a function of water saturation	73
Figure 5.37	Profiles of relative permeability to oil, oil saturation, three-phase fluid saturation and temperature of the central well from cases with different values of Corey's exponents after the 5 th injection cycle.....	74

Figure 5.38	Profiles of relative permeability to oil, oil saturation, three-phase fluid saturation and temperature of the central well from cases with different values of Corey's exponents after the 5 th production cycle.....	75
Figure 5.39	Profiles of relative permeability to oil, oil saturation, three-phase fluid saturation and temperature of the central well from cases with different values of Corey's exponents after the 20 th injection cycle.....	76
Figure 5.40	Profiles of relative permeability to oil, oil saturation, three-phase fluid saturation and temperature of the central well from cases with different values of Corey's exponents after the 20 th production cycle.....	76
Figure 5.41	Average oil production rates for cases with different values of Corey's exponent as a function of time.....	78
Figure 5.42	Average reservoir temperatures for cases with different values of Corey's exponent as a function of time.....	78
Figure 5.43	Oil recovery factors for cases with different values of Corey's exponent as a function of time.....	79
Figure 5.44	Energy consumed per barrel of oil obtained from reservoir models with different values of Corey's exponent as a function of time	80
Figure 5.45	Comparison of oil produced in each layer between 5 th and 30 th cycle from a case with Corey's exponent value of 2.5 in each layer.....	81
Figure 5.46	Comparison of oil produced from central well between 5 th and 30 th cycle for case with Corey's exponent value of 4.0 in each layer.....	82
Figure 5.47	Summary of oil recovery factors and energy consumed at the end of production from whole cases.....	82
Figure 5.48	Relative permeability curves of oil/water system with different end point saturations at reservoir temperature as a function of water saturation ...	84

Figure 5.49	Summary of oil recovery factors and energy consumed per barrel of oil obtained from reservoir models with different end point saturation at reservoir temperature	85
Figure 5.50	Relative permeability curves of oil/water system with different end point saturations at elevated temperature as a function of water saturation...86	86
Figure 5.51	Summary of Oil recovery factors and energy consumed per barrel of oil obtained from reservoir models with different end point saturation at elevated temperature.....	87
Figure 5.52	Comparison of temperature profiles between cases with fining and coarsening upward sequences at different time	89
Figure 5.53	Average oil production rates for cases with fining and coarsening upward sequences as a function of time.....	89
Figure 5.54	Oil recovery factors for cases with fining and coarsening upward sequences as a function of time.....	90
Figure 5.55	Cumulative water injection for reservoir models with fining and coarsening upward sequences as a function of time.....	91
Figure 5.56	Energy consumed per barrel of oil obtained from reservoir models with fining and coarsening upward sequences as a function of time	92

LIST OF ABBREVIATIONS

°API	Degree American Petroleum Institute gravity
°C	Degree Celsius
°F or F	Degree Fahrenheit
AWR	Above Well Region
bbbl	Barrel
BHP	Bottomhole pressure
BTU or Btu	British Thermal Unit
Cal/g	Kilocalorie per gram
CDOR	Calendar Day Oil Rate
CMG	Computer Modeling Group
cP	Centipoise
CSI	Cyclic Steam Injection
CSOR	Cumulative Steam Oil Ratio
CSS	Cyclic Steam Stimulation
EOR	Enhanced Oil Recovery
ft	Feet
ft ²	Square Feet
ft ³	Cubic Feet
m	Meter
mD	Millidarcy
MMBTU	Million British Thermal Unit
NWR	Near Well Region

psi	Pound per square inch
psia	Pound per square inch absolute
PVT	Pressure-Volume-Temperature
SAGD	Steam Assisted Gravity Drainage
SCAL	Special Core Analysis
SCF/STB	Standard Cubic Feet per Stock Tank Barrel
SOR	Steam-Oil Ratio
STB/D	Stock-tank barrel per day
WOR	Water-Oil Ratio



LIST OF NOMENCLATURES

ϕ	Porosity
μ	Viscosity
μ_o	Viscosity of oil
μ_{oc}	Viscosity of oil in cold zone
μ_{oh}	Viscosity of oil in heated zone
μ_w	Viscosity of water
B_g	Dry gas
B_o	Oil formation volume factor
f_s	Fractional flow of steam
h	Height
J_c	Production index before steam injection
J_h	Production index after steam injection
k	Permeability
k_d	Permeability of damage zone
k_h	Horizontal permeability to oil in gas/liquid system
k_r	Relative permeability
k_{rg}	Relative permeability to gas
k_{ro}	Relative permeability to oil
k_{rog}	Relative permeability to oil in gas/liquid system
k_{row}	Relative permeability to oil in oil/water system
k_{rw}	Relative permeability to water
k_v	Vertical permeability

L_k	Lorenz coefficient
M	Mobility ratio
N	Exponent
q_{oc}	Oil production rate at downhole conditions before steam injection
q_{oh}	Oil production rate at downhole conditions after steam injection
Q_v	Latent heat of vaporization
r_d	Drainage radius of cold zone
r_h	Drainage radius of heated zone
R_s	Solution Gas Oil ratio
S_{or}	Residual oil saturation
S_s	Steam saturation
S_{wi}	Initial water saturation
T	Absolute temperature
V	Velocity
v	Water vapor and steam
V_o	Velocity of oil
V_v	Velocity of vapor water and steam

CHAPTER I

INTRODUCTION

1.1 Background

Enhanced Oil Recovery (EOR) is one of recovery methods used to produce oil from reservoir. In general, EOR is defined as any technique implemented by injecting of absence materials into reservoir to create mechanisms that enhance oil production. The major goal of EOR is therefore to mobilize remaining oil. Effectiveness of any EOR method is mainly considered from improving oil displacement and volumetric sweep efficiencies. Nevertheless, reservoir heterogeneity, a geological factor, frequently causes failure of EOR techniques as well as difficulty in prediction of oil production. Reservoir heterogeneity could occur in permeability, porosity, thickness, fluid saturation, presence of faults fractures and depositional sequence.

Cyclic Steam Injection (CSI), also called Huff and Puff, is a thermal recovery method which involves periodical injection of steam with a purpose to heat reservoir near wellbore. One well is used as both injector and producer. A cyclic steam injection process includes three stages, injection, soaking and production. The first stage, steam is injected into the well for certain period of time to heat oil in surrounding reservoir. This injection of steam will later be allowed to create a chamber for pressure build-up in the formation. As reservoir temperature increases, oil viscosity continues to decrease, causing an increase in initial oil rate. When enough amount of steam has been injected, well is shut-in for certain period and steam is left to soak in reservoir. This stage is so-called soaking stage, well is shut-in to allow injected steam to expand chamber and heat up a larger area in formation. After soaking period, the well is re-opened and production stage is triggered by natural flow at first and then by artificial lift. Reservoir temperature returns to the level at which oil flow rate reduces. These sequences are repeated until oil production turns uneconomic. Application of CSI mainly aims to reduce residual oil saturation by means of several driving mechanisms which are mainly viscosity reduction and thermal expansion of oil, changing of relative

permeabilities and changing of rock wettability. However, these recovery mechanisms are dependent on reservoir rock and fluid properties.

In order to increase efficiency of CSI in heterogeneous reservoir, better understanding effects of various operating parameters and relationship of reservoir properties changes with CSI simulation process should be completely considered.

In this study, reservoir simulator called STARS® commercialized by Computer Modeling Group Ltd. (CMG) is used as investigation tool. A multi-layered reservoir models are constructed with various degree in heterogeneity, representing by Lorenz coefficient. Varying of permeability is mainly concerned as this property affects flow ability of reservoir and consecutively effectiveness of the process. Multi-layered sandstone formation model is generated and each horizontal layer possesses different permeabilities. Selection of operating parameters is firstly emphasized. Pre-selected parameters including well spacing, injection rate, steam temperature, steam injection period and oil production period are applied to narrow down interesting parameters. Therefore, steam quality and soaking period are varied together to identify the best values. Study is continued by performing simulation on reservoir on interest parameters are investigated after. This section includes heterogeneity index (Lorenz coefficient), vertical permeability, percent shale, relative permeability and permeability sequence are investigated. Oil recovery factor and energy consumed per barrel of oil are used as major criteria to judge the process effectiveness. Conclusion would provide preliminary concerns on both operating and reservoir parameters.

1.2 Objective

1. To select operating parameters which yields best performance of cyclic steam injection in multi-layered heterogeneous reservoir emphasizing on soaking period, and steam quality.
2. To evaluate effects of interest reservoir properties on effectiveness of cyclic steam injection in multi-layered heterogeneous reservoir, including heterogeneity index, vertical permeability, structural shale percent, relative permeability, and permeability sequence.

1.3 Outline of Methodology

1. Construct reservoir model with initial degree of heterogeneity quantifying by Lorenz coefficient value.
2. Simulate cyclic steam injection on heterogeneous reservoir constructed in previous step with variation of soaking periods and steam quality while injection period, oil production period, steam temperature, and oil production rate are maintained the same. Production rate for each cycle is varied depending on oil production rate at the end of previous cycle. The best soaking period and steam quality are obtained in this step. These selected operating parameters will be used to perform cyclic steam injection together with interest parameters.
3. Study effects interest reservoir properties on effectiveness of cyclic steam injection in multi-layered heterogeneous reservoir including;
 - Magnitude of heterogeneity (Lorenz coefficient)
 - Vertical permeability
 - Structural shale percent
 - Relative permeability at reservoir temperature and elevated temperature
 - Permeability sequence
4. Discuss the obtained results, separating in sections for each parameter.
5. Summarize new finding and indicated magnitude of sensitivity of each parameter on effectiveness of cyclic steam injection in multi-layered heterogeneous reservoir.

1.4 Outline of Thesis

This thesis is divided into six chapters as shown in following outline.

Chapter I introduces brief introduction of cyclic steam injection and indicate objectives and methodology of the study.

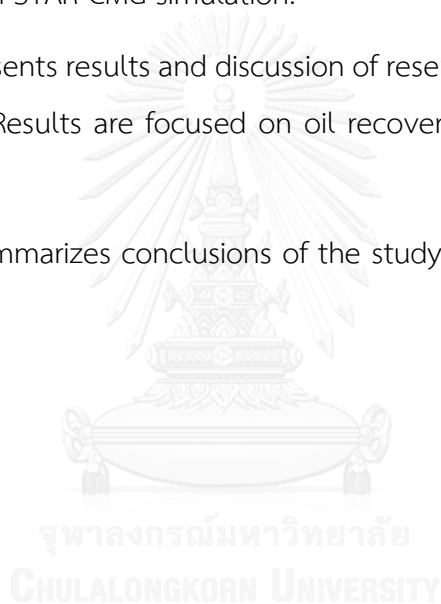
Chapter II summarizes various literature reviews related to the study of cyclic steam injection.

Chapter III presents the concepts related to cyclic steam injection process including oil recovery mechanism, displacement mechanism, involved properties and heterogeneous reservoir.

Chapter IV provides details of heterogeneous reservoir models, model dimension and input parameters in reservoir simulation model such as rock properties, Pressure-Volume-Temperature (PVT) properties of reservoir fluids, rock-fluid properties and well input data in STAR CMG simulation.

Chapter V presents results and discussion of reservoir simulation study for each interest parameters. Results are focused on oil recovery factor together with energy consumption.

Chapter VI summarizes conclusions of the study as well as recommendations for further study.



CHAPTER II

LITERATURE REVIEW

Previous studies on oil recovery process and reservoir properties altered by cyclic steam injection, effect of heterogeneity on thermal recovery, operating condition and optimization of CSI and application of CSI in pilot test are summarized in this chapter.

2.1 Study of Oil Recovery Process and Reservoir Properties Altered by Cyclic Steam Injection

Cyclic steam injection includes three important stages; injection, soaking and production. The cycle is repeated to enhance the oil production rate until the oil production turns uneconomic. Application of CSI targets to reduce formation residual oil saturation by several driving mechanism: viscosity reduction, changes in wettability and the thermal and solution gas expansion which depend on reservoir rock and fluid properties [1].

Dietirch [2] indicated that reliable relative permeability data are important to the overall planning for prospective thermal recovery projects. Cyclic steam injection process changed saturation and pressure conditions during changing imbibition and drainage cycles. The stress in grain structure of unconsolidated sand typically changed from 500 to 1,500 psi during the process. During steam injection when effective stress decreased, micro-channels were formed in porous medium and relative permeability curves of imbibition process became straight line. These channels would close during the production cycle when the effective stress increased and the relative permeability curve of drainage process became more conventional shape or curvaceous for non-segregated flow. Three-phase flow effects represented the possible mechanism on differences between imbibition and drainage relative permeability to water. During the injection when pressures were high, solution gas and distillable components remained in solution, allowing flow of water. During the production, free gas phase was continuously presented and partially blocked permeability. In conclusion, oil

production rate and thermal efficiency were sensitive to relative permeability. Effects of hysteresis from effective stress and three phase flow are compulsory to be determined in laboratory studies for unconsolidated sands.

Hascakir [3] studied Cyclic Steam Injection (CSI) in diatomaceous reservoir, using CMG reservoir simulator. The author indicated that previous laboratory had shown change in wettability of diatomite reservoir rocks depended on temperature. Water-oil and liquid-gas relative permeabilities were varied to evaluate effects on oil recovery. Relative permeability curves were collected from many literatures for diatomaceous reservoir and used for sensitivity studies. Chosen parameters were relative permeability ends points and viscosity variation with increasing temperature, rock and fluid properties (such as thermal conductivity and heat capacity), injected steam temperature, steam pressure and steam quality, bottomhole pressure for injector and producer.

First set of simulation, four different models were applied to simulate different wetting conditions on oil production. Each model presented water-oil and liquid-gas relative permeability and cumulative oil production plots. Results showed that when water-oil relative permeability curves shift to the left, becoming lesser water wetness, oil recovery decreased. In some models which water-oil relative permeability curves were fixed, production in first few years was the same, but production was affected due to differences of liquid-gas relative permeability in later period. Production slightly decreased by means of liquid-gas relative permeability created at a steam temperature. The author concluded that liquid-gas relative permeability curves have a significant impact when evaluating cyclic steam injection process at high temperature, and it is important to accurately determine gas-oil relative permeability curves for diatomite reservoirs at the exact steam temperature.

The studies of the same author showed that changes of wettability were related to relative permeability. Hascakir considered temperature-dependent relative permeability end points with two different methods. First, relative permeability end points changed with increasing temperature. Water, oil and steam saturation end points were changed with different temperature. Changes were reversible with temperature.

Second, different relative permeability curves was applied to model grid by grid and changed with different temperature in each grid block. Relative permeability curves were not allowed to reverse when temperature decreased. After the temperature-dependent relative permeability curves or end points were added to the simulation, oil production increased and recovery of the studies increased up to 40-60 percent.

Sensitivity studies showed that permeability was the most sensitive parameter. Effects of BHP and porosity were also important. Different duration of injection-soak-production periods affected timing or cycle of oil production. Optimum time for each period depended on field or section and required further study.

2.2 Operating Conditions and Optimization of CSI

Briggs [4] performed reservoir simulation to predict CSI performance in naturally fractured carbonate reservoir. Model was created as matrix-fracture system. Cubic blocks were represented rock matrix surrounded by interconnecting fractures. Simulation was also performed to study interaction between input reservoir and operating parameters. In this study, sensitivity analysis was not completely covered on relative permeability and capillary pressure curve since they affected imbibition rate, requiring more laboratory measurement and effect of temperature dependent diffusion coefficient would be the subject for further study.

Changes of reservoir parameters in this study were matrix block size, permeability, porosity and fracture porosity. Results proved that small matrix block size yielded better heat transfer, affecting oil viscosity reduction and imbibition rate. This resulted in better performance with a faster recovery rate. High matrix permeability showed similar effect as small matrix block size. Matrix porosity controlled storage capacity. Therefore, decreasing matrix porosity could cause a decrease in recovery. Fracture porosity controlled reservoir volume if rock was contacted by injected fluid and fracture porosity, affecting quantity of heat transported. So larger fracture accelerated production and improved the recovery.

The changes of operational parameter included soak period, injection period, steam slug size, steam pressure, PI or drawdown and steam quality. Increasing soak

period did not show benefit on production. Effect of injection rate with constant volume steam slug showed that heat was widely dispersed with fast injection rate. Heat losses were increased with slow injection rate. Performance was improved because since reservoir volume was heated. Increasing steam slug showed similar result as same as increasing injection rate. Range of steam pressure had no effect on performance of process. Faster offtake rate increased Calendar Day Oil Rate (CDOR) but also increased Steam Oil Ratio (SOR). Economic terms preferred to have faster offtake rate (increase of CDOR) with lower SOR, so it was important to select the optimum offtake rate. Reduction of steam quality had no effect on performance but the heating by hot water had more significant effect on production.

2.3 Application of CSI in Pilot Scale and Oil Field

Li [5] developed a thermal reservoir model to perform sensitivity studies of well configuration, well placement, inter-well spacing, steam quality, steam slug size, and cycle length. Performance of Cyclic Steam Stimulation (CSS) pilot in deep carbonate heavy oil reservoir in Oudeh field, Syria was evaluated. The CMG STARS thermal reservoir simulator was used to perform CSS possibility studies operational parameters.

This CSS pilot is currently paused for further evaluation, but there were several important conclusions from simulation study. High pressure was required to inject into deep carbonate reservoir at close to or higher than initial reservoir pressure because the latent heat of vaporization was too low, causing less efficient heating process. Steam quality at the bottomhole was low and much affected by wellbore heat loss. Only hot water reached bottomhole when steam was injected through casing annulus. Injection into tubing improved steam quality between 20 and 40 percent when wellhead steam quality was 80 percent.

2.4 Effect of Heterogeneity on Thermal Recovery

Chen et al. [6] evaluated effects of reservoir heterogeneities on Steam Assisted Gravity Drainage (SAGD), using a stochastic model of shale distribution performed by thermal reservoir simulator. Two flow regions which are Near Well Region (NWR) and

Above Well Region (AWR) were studied to separate effect of heterogeneity. Reservoir heterogeneity was represented by randomly distributed shale, thin layered shale and induced fractures created from hydraulic fracturing process. CMG star was selected as an investigation tool to perform reservoir simulation in order to study several interests which are size of NWR, and presence of shale and induced fracture in AWR.

From the study, authors found that in order to drain heated oil and condensate effectively from reservoir, it is necessary to inject steam continuously to create steam chamber. Hot fluid must pass through the NWR before being produced. A moderate size of NWR reduced fluctuation of oil production rate due to heterogeneity. Presence of shale in sand reduced vertical permeability of sand block but no effect observed on horizontal permeability. For AWR, long continuous shale layer or high fraction of shale limited development of steam chamber and consecutively reduced SAGD performance. Presence of induced fracture improved well injectivity and increased oil production rate in a poor vertical communicating formation with high percentage of shale reservoir. Comparing to the case without fracture, induced vertical fractures provided highly permeable vertical paths for steam, improving vertical development of chamber and increasing oil production rate and oil steam ratio. Orientation of induced fracture depended on the depth of the formation of interest. A vertical fracture could be parallel or perpendicular to horizontal well, depending on direction of drilling respect to direction of minimum and maximum horizontal stresses.

According to previously summarized literature reviews, it is obvious that CSI can be considered as applicable techniques for heavy oil. Nevertheless, multi-layered heterogeneous reservoir has not been studied much by means of CSI process. This study will emphasize on effects of heterogeneity together with other reservoir properties on effectiveness of CSI process. These preliminary concerns obtained from the study on both operational and reservoir parameters would yield additional considerations prior to implementation of CSI in multi-layered reservoir.

CHAPTER III

RELEVANT THEORY

3.1 Cyclic Steam Injection (CSI) and Oil Recovery Mechanisms

Cyclic steam injection (CSI) is also known as Huff and Puff process. The process consists of three important stages: injection, soaking and production periods. Steam is first injected into a well for certain period to heat oil in surrounding reservoir to a temperature that oil can flow. After sufficient amount of steam is injected, steam is left to soak for a few days to complete heat transfer from steam to oil. Heated oil is then produced from the same well. At first, oil is produced by natural flow since steam injection increases reservoir pressure. Later, oil can be produced by an aid of artificial lift. Production rate will decrease as oil cool down and once production reaches an economic limit. Several repetitions of huff-soak-puff cycle are performed but number of cycle is controlled from economic limits.

3.1.1 Cyclic Steam Injection Cycles

During steam injection period, steam is injected into a single horizontal or vertical well for a short period of time. The injected steam will create a chamber for pressure build-up in the formation. As reservoir temperature increases, oil viscosity continues to decrease which causes an increase in the initial oil production rate. There is also acceleration of production rate from increased reservoir pressure near wellbore. As steam is injected at high pressure, it could create fissures or small fractures in the formation to maximize oil contact and production. During this period, average temperature of steam chamber is assumed to be the saturated steam temperature. After that, injection well is closed for a short time and soaking period allows the building up of temperature profile while steam chamber is formed.

In soaking period, well is shut-in to allow steam to expand the chamber and to heat up a larger area in the formation. Uniformity of heat distribution within the reservoir is anticipated in order to thin the heavy oil. Most of latent heat carried by steam is transferred to formation surrounding the well and condensation of steam

occurs. The steam condensation is cooled down as it moves into reservoir and more heat is transferred by conduction. Steam chamber grows upwards as steam is lighter phase and will flow up to the top of reservoir. Oil drains downward and steam rises upward due to gravity effect as well as convection heat transfer. This counter current flow helps increasing heat transfer and improving overall process. Some factors that must be considered for the success of CSI process are recovery factor, water oil ratio (WOR) and steam oil ratio (SOR). Oil recovery factor normally increases with decreasing of soaking period.

Production period occurs after certain shutting-in period (soaking period). Heated oil near the condensation surface is allowed to drain downward due to gravity effect and pressure difference into production well and then oil is delivered to surface. Initially, temperature in heated zone is relatively high which results in high initial production rate. However, the initial rate declines with time as heat is removed with produced fluids and dissipated into non-productive formation. Production rate is greatly improves as a result of lower oil viscosity due to increase in temperature. The major mechanisms of oil production in CSI are gravity drainage and pressure drawdown. As oil is drained from reservoir toward the well, steam chamber expands to replace produces oil.

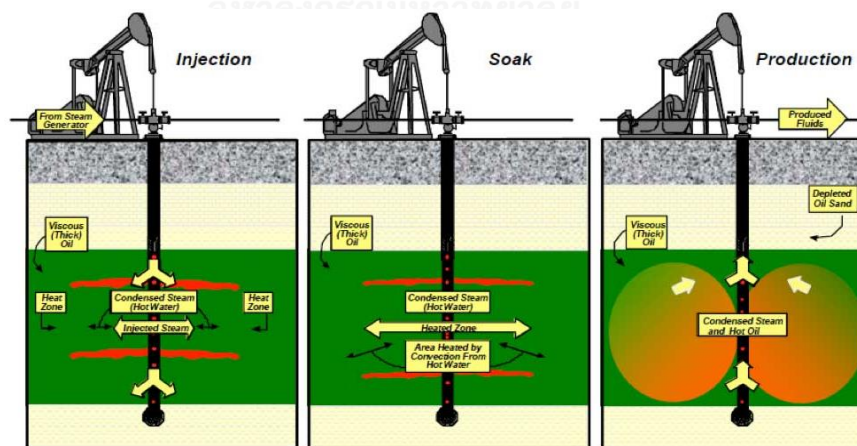


Figure 3.1 Illustration of Cyclic Steam Injection consisting of injection, soak and production periods [7]

3.1.2 Oil Recovery Mechanisms

The main oil recovery mechanism by means of cyclic steam injection process is viscosity reduction of oil, exploiting latent heat carried by steam. However, injected steam can also improve oil recovery by removing of formation damage around the wellbore, increasing flow ability of overall reservoir.

As steam is injected into reservoir, reservoir pressure is increased. Hence, pressure different from bottomhole pressure is higher and as a consequence, oil production rate is higher based on Darcy's equation. Figure 3.2 illustrated comparison of different radii in cyclic steam injection process.

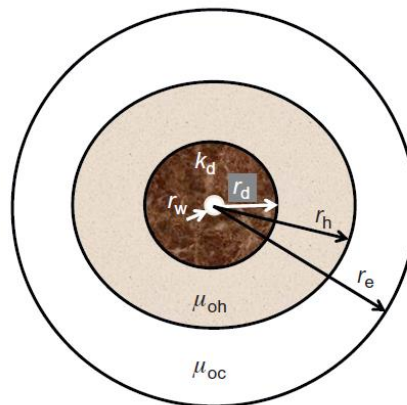


Figure 3.2 Radial flow of cyclic steam injection steam, illustrating different radii [8]

From Figure 3.2, it represents drainage radius whereas r_h and r_d are radius of heated zone and radius of damage zone, respectively. Additionally, μ_{oh} and μ_{oc} are viscosity of oil in heated zone and cold zone and k_d is permeability of damage zone. Using the steady-state Darcy's equation, production rate at the downhole conditions after steam injection, q_{oh} is:

$$\begin{aligned}
 q_{oh} &= \frac{2\pi h(p_e - p_w)}{\frac{\mu_{oc} \ln(r_e/r_h)}{k} + \frac{\mu_{oh} \ln(r_h/r_d)}{k} + \frac{\mu_{oh} \ln(r_d/r_w)}{k_d}} \quad (3.1) \\
 &= \frac{2\pi k k_d h (p_e - p_w)}{k_d \mu_{oc} \ln(r_e/r_h) + k_d \mu_{oh} \ln(r_h/r_d) + k \mu_{oh} \ln(r_d/r_w)}
 \end{aligned}$$

The production rate before steam injection, q_{oc} , is:

$$q_{oc} = \frac{2\pi h(p_e - p_w)}{\frac{\mu_{oc} \ln(r_e/r_d)}{k} + \frac{\mu_{oc} \ln(r_d/r_w)}{k_d}} = \frac{2\pi k k_d h(p_e - p_w)}{k_d \mu_{oc} \ln(r_e/r_d) + k \mu_{oc} \ln(r_d/r_w)} \quad (3.2)$$

The ratio of production index after steam injection (J_h), to that before (J_c) is:

$$\begin{aligned} \frac{J_h}{J_c} &= \frac{k_d \mu_{oc} \ln\left(\frac{r_e}{r_d}\right) + k \mu_{oc} \ln\left(\frac{r_d}{r_w}\right)}{k_d \mu_{oc} \ln\left(\frac{r_e}{r_h}\right) + k_d \mu_{oh} \ln\left(\frac{r_h}{r_d}\right) + k \mu_{oh} \ln\left(\frac{r_d}{r_w}\right)} \quad (3.3) \\ &= \frac{(k_d/k) \ln(r_e/r_d) + \ln(r_d/r_w)}{(k_d/k) \ln(r_e/r_h) + (k_d/k)(\mu_{oh}/\mu_{oc}) \ln(r_h/r_d) + (\mu_{oh}/\mu_{oc}) \ln(r_d/r_w)} \end{aligned}$$

However, if steam injection has removed formation damage after reservoir is cooled down, improvement in the productivity is significantly improved. The improvement is:

$$\frac{J_{after\ CSI}}{J_{before\ CSI}} = \frac{\log(r_e/r_d)/k + \log(r_d/r_w)/k_d}{\log(r_e/r_d)/k + \log(r_d/r_w)/k} \quad (3.4)$$

It shows that mechanism of steam injection to remove formation damage adjacent to the well will show the effect after cooling down of reservoir. Formation damage could be caused by deposition of solids, paraffin, or asphaltene near production well.

3.2 Properties Involved in Cyclic Steam Injection

3.2.1 Liquid Viscosity

Liquid viscosity reduces with increment of temperature. Relationship of liquid viscosity and temperature is in exponential form. At elevated temperature, fluid viscosity is greatly reduced. Reduction of viscosity ratio (μ_o/μ_w) with temperature is shown for two crude oils in Figure 3.3. Certain light oils show an inverse relationship (dash line on Figure 3.3) but this is however quite rare.

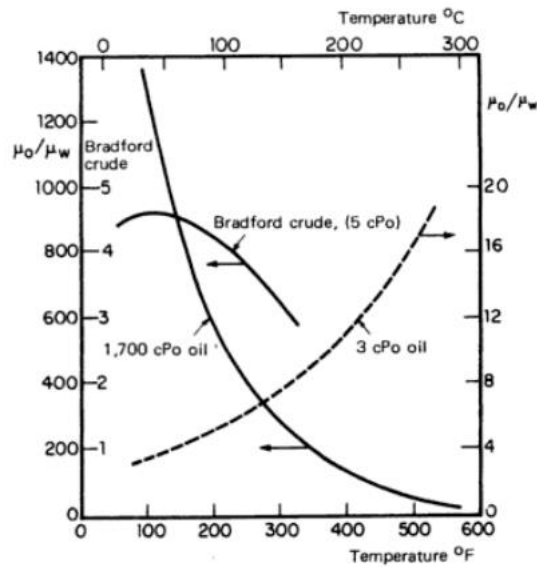


Figure 3.3 Viscosity ratio (μ_o/μ_w) as a function of temperature for three different crude oils [9]

Viscosity of liquid hydrocarbons may be reduced by solubilization of certain gases. The effect increases with quantity of dissolved gas and eventually swelling of oil by dissolved gas is occurred.

3.2.2 Gas Viscosity

According to kinetic theory of ideal gases, dynamic viscosity of any gas should be independent from pressure and should be proportional to the square root of absolute temperature. However, real gases are different from this theory. Gas viscosity tends to increase with pressure and normally increases more rapidly than the square root of the absolute temperature T . The effect of temperature on gas viscosity can be approximated by the following equation:

$$\mu = AT^n \quad (3.5)$$

where exponent n is ranging between 0.7 and 1.0 for most gases. Examples of relationship between gas viscosity and temperature are:

Steam viscosity between 0° and 400°C: $\mu = 1.7 \times 10^{-5} T^{1.116}$ cP,

Methane between 0° and 500°C: $\mu = 1.36 \times 10^{-5} T^{0.77}$ cP.

3.2.3 Relative Permeability

Many experimenters have demonstrated that relative permeability changes with temperature for diphasic oil-water flow. Relative permeability curves of two different oils at two different temperatures are shown in Figure 3.4. Figure 3.5 shows effect of increasing temperature on irreducible water saturation and residual oil saturation: irreducible water saturation increases while residual oil saturation decreases. This means that displacement efficiency is improved by thermal recovery methods.

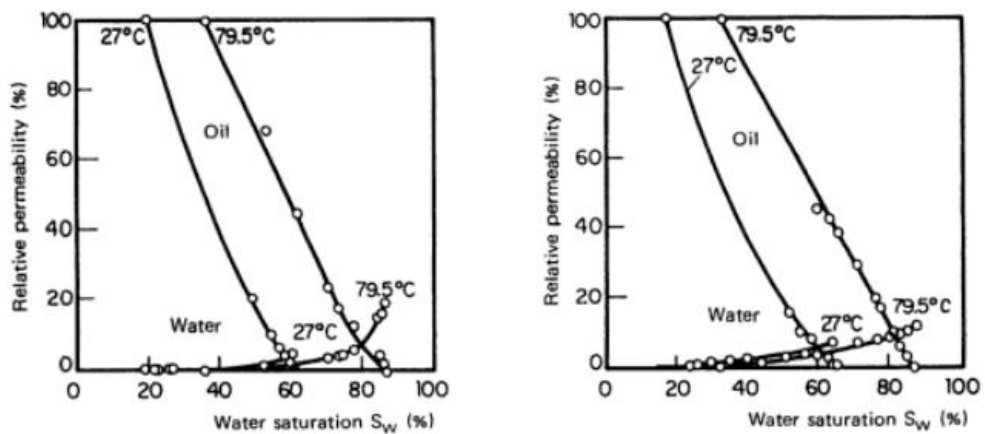


Figure 3.4 Relative permeability curves of two different oils at different temperatures

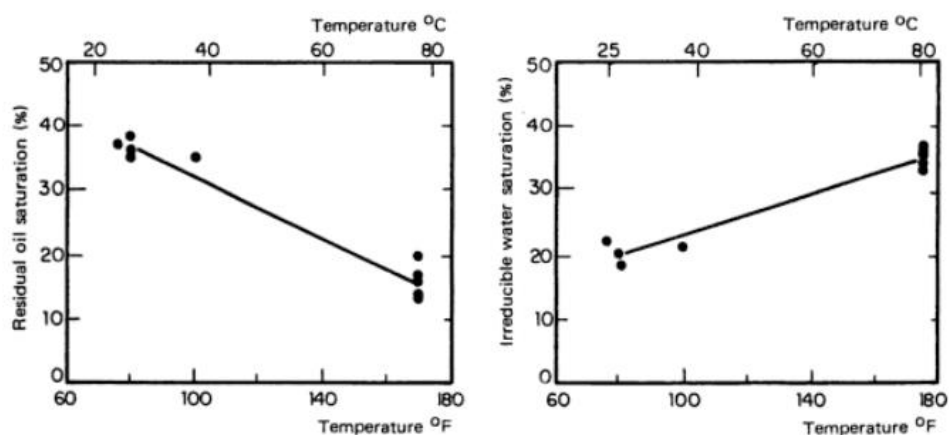


Figure 3.5 Effects of temperature on residual oil saturation and irreducible water saturation [9]

Effect of temperature on residual oil saturation and irreducible water saturation is a result from reduction of viscosity ratio and changing in physical and chemical equilibrium within porous medium at elevated temperature. Variation of ratio between relative permeability to oil and relative permeability to water (k_{ro}/k_{rw}) with temperature is less predictable than variation of residual oil saturation. Considerable change in this ratio has been observed, but the direction of the change cannot be predicted.

When gaseous phase is presented, vaporization and condensation may be added to hydrodynamic displacement on Darcy's law. There may be large heat and mass transfers which affect the lightest fraction of oil. So, residual oil saturation is lower for displacement by saturated steam than by liquid water at the same temperature. In case of high pressure, no vapor phase is formed.

3.2.4 Thermal Capacity and Thermal Conductivity

Thermal capacity per unit mass (or specific heat) of solids, liquids and gases increases with temperature and is often affected by pressure. For perfect gases, specific heat is independent from pressure but much increasingly dependent from temperature due to progressive molecular excitation. Specific heat of rocks varies slightly according to their nature. Shale in subsurface are normally fully saturated with water but there is possibility to have differences in effects of free and bound water on heat capacity. The estimation of the amount of bound water on clays is 15 percent of the total water saturation. The calculation correction of specific heat of shale might be made by multiplying 0.93 to the heat capacity of water. Thermal conductivity of gases increases with temperature, whereas thermal conductivity of liquids and solids decrease slightly with temperature. Water is an exception; its conductivity reaches the highest at around 130 °C.

3.2.5 Latent Heat of Vaporization

Latent heat of vaporization (Q_v) of a pure substance changes with temperature at which the phase change takes place. Latent heat of vaporization decreases as temperature increases and becomes zero at critical point as illustrated in Figure 3.6. Water has the highest latent heat of vaporization of about 583.2 Cal/g at 25 °C and

539 Cal/g at 100 °C. Most hydrocarbons possess latent heat of vaporization around 80-90 Cal/g at 15 °C.

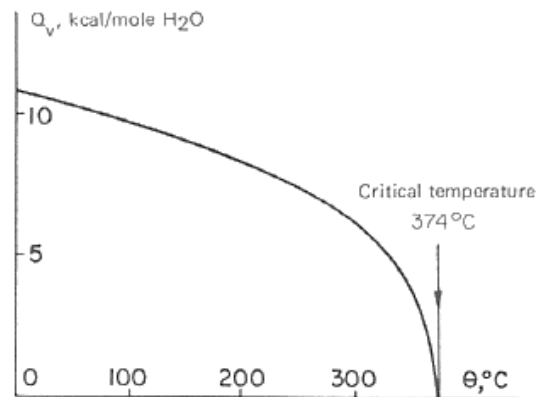


Figure 3.6 Latent heat of vaporization of water as a function of temperature [9]

3.3 Displacement Mechanism

Since water has advantages of having much higher heat transport capacity than other fluids, whether in liquid or vapor phase, water is therefore used for hot fluid displacement.

3.3.1 Hot Water Displacement

Consider a virgin homogeneous reservoir with only two-dimensional displacement where heat loss to surrounding formation is neglected, injected hot water is cooled down when it is in contact with rock and fluids in place. Under steady-state conditions, two principle zones can be observed using temperature and saturation profiles. These two zones will be described from downstream to upstream as shown in Figure 3.7.

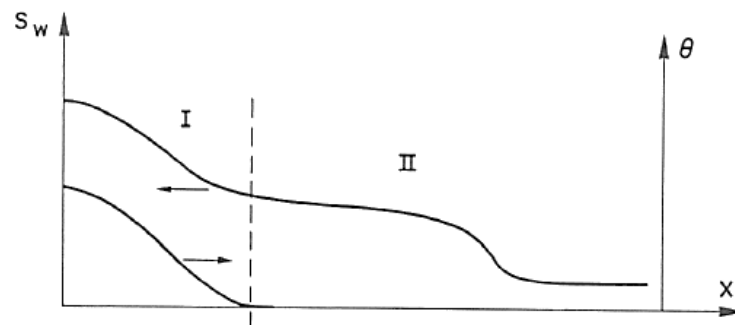


Figure 3.7 Two-dimensional hot water displacement resulting in downstream zone (zone II) and upstream zone (zone I) [9]

Zone II: Fluids in this zone is displaced by water at the same temperature. Therefore displacement by hot water suffers from the same instability problems as displacement by cold water. The residual oil saturation upstream of zone II is the same as it would be for cold water injection.

Zone I: As distance is further away from upstream temperature steadily increases. Swelling of both fluids and matrix occurs. For any given saturation, mass of oil trapped is reduced as temperature increases. If the oil contains any highly volatile hydrocarbons, certain fractions may be displaced by vaporization and condensation.

In practice, loss of heat from the hot zone to surrounding formations results in more temperature loss in the direction of flow as shown in Figure 3.8.

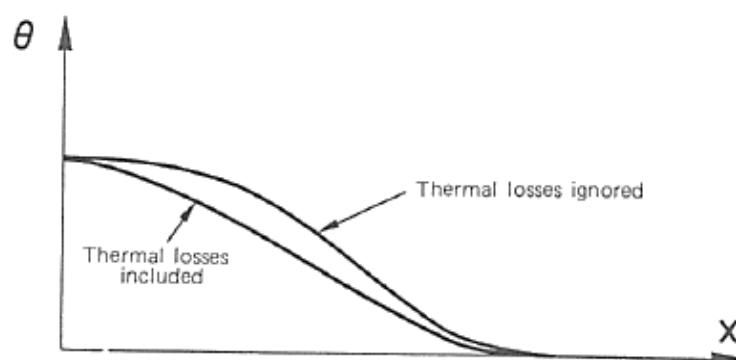


Figure 3.8 Comparison between temperature distributions from cases with and without heat loss to adjacent formation as a function of distance from steam injection well [9]

3.3.2 Displacement by Saturated Steam

With the same assumption as for hot water displacement, three principle zones can be identified as depicted in Figure 3.9. However, explanation is examined from upstream to downstream.

Zone I: At upstream of condensation zone, temperature is high and it slightly falls due to saturation of steam temperature at higher pressure. Temperature naturally declines in direction of flow. Saturations of water and vapor remain constant in this region. Oil saturation is low in this region due to vaporization of volatile component. Temperature of matrix is equal to temperature of steam. In this zone, three fluid phases exist but only water and gas phases are flowing.

Zone II: Steam comes in contact with cooler matrix and hence, condenses. Average temperature lies between temperature of the steam and matrix. During condensation, average temperature decreases and previously vaporized hydrocarbon condenses at the same time as steam.

Zone III: In this zone, displacement is done by hot water.

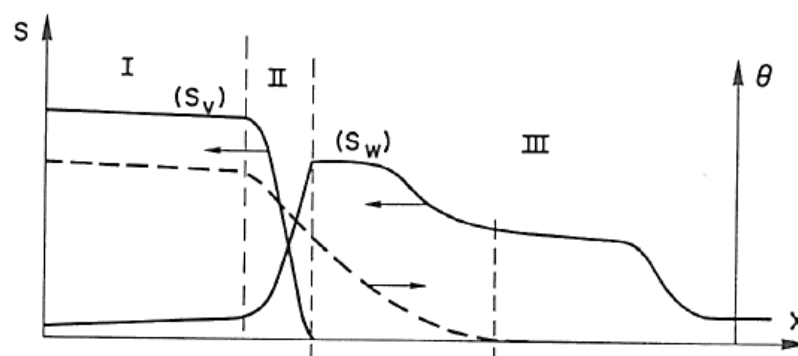


Figure 3.9 Three zones from displacement by steam: hot steam zone, condensing zone and hot water zone [9]

Comparing displacement by cold water, hot water and steam, oil recovery factors from both hot water and steam injection at breakthrough are always higher

than that of cold water injection as illustrated in Figure 3.10. After steam breakthrough, it can be observed that only oil recovered is mostly constant.

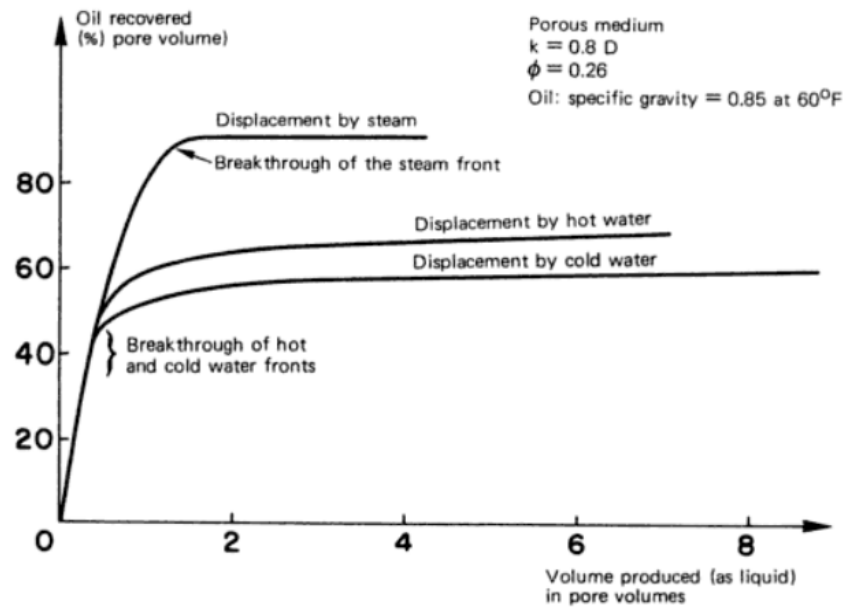


Figure 3.10 Oil recoveries from steam, hot water and cold water [9]

3.3.3 Areal Sweep Efficiency and Stability

Areal sweep efficiency during isothermal displacement and stability of displacement are highly depended on mobility ratio M . If it is assumed that relative permeability (k_r) is independent from viscosity, then areal sweep efficiency and stability will depend on viscosity ratio of oil to water (μ_o/μ_w).

Considering a hot water displacement with no mass transfer between phase and a high viscosity ratio (oil viscosity at reservoir temperature/water viscosity at injection temperature), Areal sweep will be low and displacement may become unstable.

In practice, as flood front advances, horizontal thermal conductivity, thermal capacity of rock and fluids in place and forces convection result in oil being heated and injected water cooled. This zone of gradual temperature change with distance grows with time and temperature front disappears.

If instability occurs, viscous fingering will carry heat downstream by convection and it will be conducted laterally to oil and rock. Temperature and saturation profiles will be extended further and assumption of a hydrodynamic front becomes invalid. After a certain time, oil is displaced by fluid at the same temperature, areal sweep efficiency is improved.

If steam displacement is considered while retaining thermal and hydrodynamic fronts, μ_o/μ_w will no longer useful parameter. At the saturation temperature, the ratio of specific volumes of steam and water is 86.4 at 20 bar (290 psi) and still 12.8 at 100 bar (1,450 psi). Therefore, throughout the condensation front fluid velocities cannot be equal. Velocity ratio depends on both pressure and thermal capacity of the rock. μ_o/μ_v (where subscript v refers to water vapor and steam) must be replaced by $\mu_o V_o/\mu_v V_v$, where V represents velocity.

Figure 3.11 illustrates one direction oil displacement velocities in z direction by saturated dry or superheated steam (subscript v), water at saturation temperature (subscript c) and water at reservoir temperature (subscript w). The figure shows the μV ratios at depth of 1,000 m (3,280 ft). For reservoir with 20 percent porosity, displacement by saturated steam is more efficient than by water at reservoir temperature, down to around 130 m (426 ft). Even there is low quality steam, steam displacement is better than cold water. Steam is more efficient in low porosities. Degree of instability of hot water displacement is independent from depth.

Hot water displacement flattens temperature profile with time remained for steam displacement and when fingering occurs, lateral transfer of heat by conduction has a stabilizing influence.

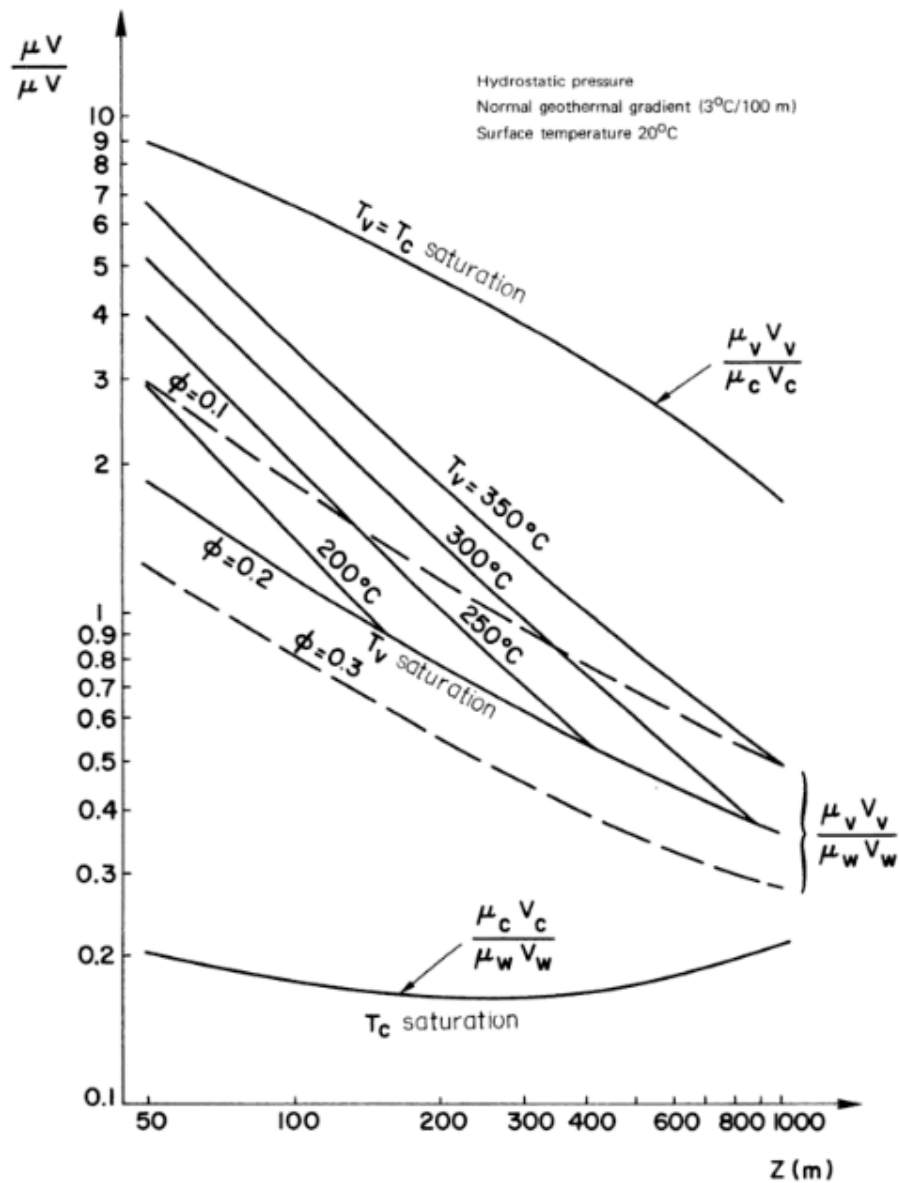


Figure 3.11 Oil displacement velocity ratio in z direction [9]

3.3.4 Buckley-Leverett Theory

Different kinds of saturation that can occur within steam chamber are shown in Figure 3.12. Dimensionless distance is equal to df_s/dS_s . Region at the upper terminal point with constant oil saturation (S_{or}) occurs if the curve of f_s is not a tangent to saturation axis. Since there is no water flow within the steam flood region, water saturation is constant at S_{wi} throughout. If the injected steam is wet, then water saturation would be higher than S_{wi} . The plot of steam saturation versus distance in

Figure 3.12 is obtained from oil in reservoir matrix with irreducible water saturation and from relative permeability data for the flow of steam [10].

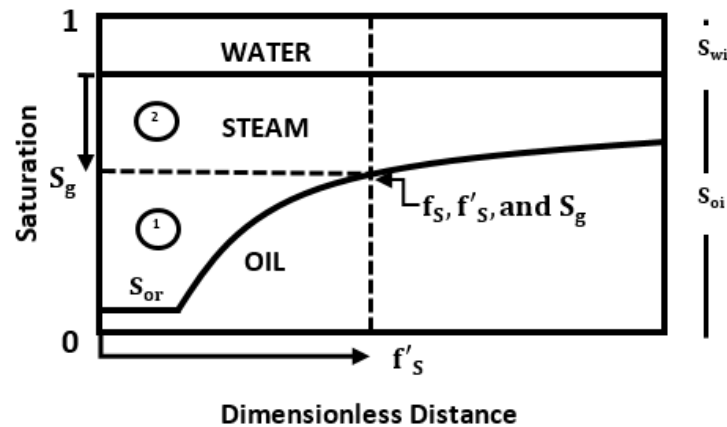


Figure 3.12 Fluid saturations as a function of dimensionless distance in the steam chamber [10]

3.4 Heterogeneous Reservoir

Reservoir heterogeneity can infer many different properties. Reservoir heterogeneity in petroleum engineering is concerned with effects created by reservoir properties expressed by flow behavior in the inter-well region. Reservoir heterogeneity can be divided into three principle types [11]:

1. Fissured reservoir: one or more fracture systems divide formation into more or less regular blocks and provide highly conductive fluid paths.
2. Layered reservoir: composes of several parallel beds where the extent is usually greater than their thickness. The beds may or may not be in communication.
3. Reservoirs with random heterogeneities: two or more types of porosity or permeability are distributed randomly.

A method to quantify reservoir heterogeneity is to generate relationship between the cumulative flow capacity and cumulative storage capacity of the reservoir as shown in Figure 3.13. The greater the deviation of this curve from 45 degree line, the greater the heterogeneity of system. The plot is constructed by arranging

permeability and porosity values from high to low, determining each intervals flow capacity (kh) and storage capacity (ϕh), summarizing these values to obtain cumulative curves, and then dividing by the maximum results in fraction or percent of flow or storage capacity. The Lorenz coefficient, L_k , was used to characterize permeability distributions. From Figure 3.13, it is defined as,

$$L_k = \frac{\text{Area } ABCA}{\text{Area } ADCA} \quad (3.6).$$

Lorenz coefficient varies from zero to one, where the uniform permeability is zero. Several permeability distribution can result the same value of L_k , so the solution is not unique. Comparison of L_k for different wells will provide a relative magnitude of heterogeneity between wells [12].

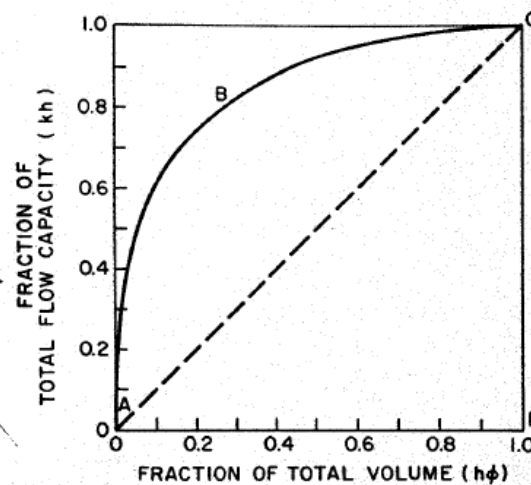


Figure 3.13 Flow capacity versus storage capacity distribution [12]

3.5 Presence of Shale

In thermal recovery, presence of shale is important since shale is generally water-saturated and has a very high specific heat. In CSI process, shale can act as storage areas for heat, reducing heat loss during injection and releasing heat to sustain a higher temperature during latter part of the steam cycle. Moreover, gravity override of steam is reduced by non-communicating barrier and this effect leads to better sweep efficiency. The distribution of shale in reservoir can be classified into three types which are 1) laminated shale: thin layers of clay between rock matrixes, 2) structural

shale: clays particles distributed within rock matrix, and 3) dispersed shale: clay in open spaced between grains of rock matrix. Differences of these three type of shale are illustrated in Figure 3.14.

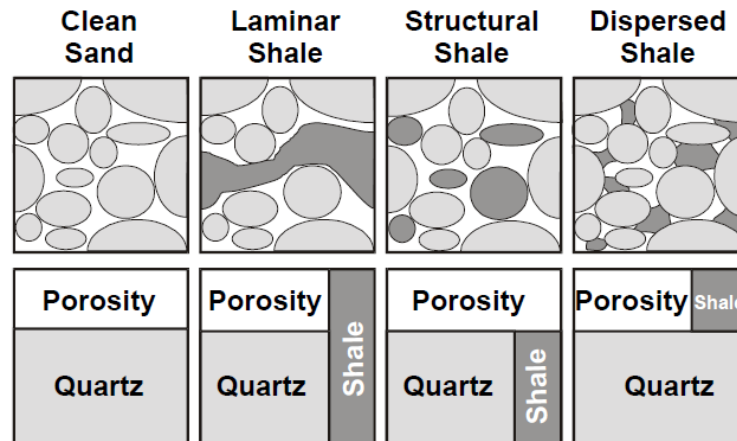


Figure 3.14 Illustration of different distribution of shale in reservoir [13]

From Figure 3.14, it can be seen that distribution of laminated shale and structural shale results in becoming part of rock structure. Porosity of reservoir with types of shale remains the same. As dispersed shale occupies the space between rock matrixes, porosity is reduced as a result of higher dispersed shale volume.

CHAPTER IV

RESERVOIR SIMULATION MODEL AND METHODOLOGY

4.1 Reservoir Model

Reservoir model is constructed with Cartesian grid type. The model is 165, 165 and 63 ft in x-,y- and z-directions. Each direction of reservoir model is divided into grid blocks of 33x33x9 grid blocks in three directions. Total grid block is 9,801 blocks which is still less than maximum grid block provided by educational package of CMG STAR. Total area of model is 0.625 acre with thickness of 63 ft. Wells are located in model on five-spot pattern. Figure 4.1 illustrates dimensions of reservoir together with location of all wells.

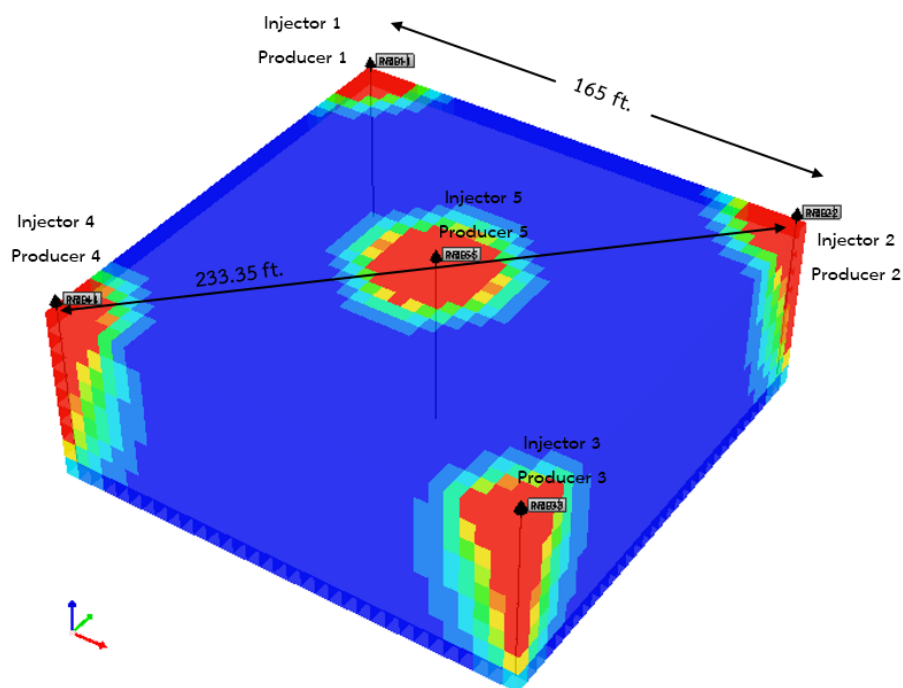


Figure 4.1 Location of wells in reservoir model, representing five-spot pattern (all the wells are both injector and producer depending on cycles)

First, heterogeneous reservoir models with average permeability value of 1,600 millidarcies are constructed using Lorenz coefficient to quantify degree of heterogeneity. Models are constructed to have different Lorenz coefficients which are

0.265, 0.296, 0.328, 0.371 and 0.402. Detail of permeability values of each heterogeneous model are shown in the following section.

Physical properties and required reservoir parameters for constructing basic reservoir model are summarized in Table 4.1.

Table 4.1 Physical properties of reservoir model and reservoir properties

Parameter	Value	Unit
Grid dimension	33×33×9	Block
Grid size	5×5×7	ft
Top of reservoir	1,640	ft
Reservoir thickness	63	ft
Effective Porosity	0.30	Fraction
Horizontal permeability	Varied in each layer	mD
Vertical permeability	0.1×kh	mD
Average horizontal permeability	1,600	mD
Maximum permeability	3,000	mD
Minimum permeability	200	mD
Initial oil saturation	0.8	Fraction
Initial water saturation	0.2	Fraction
Reservoir pressure	725	psia
Reservoir temperature	77	°F
Oil gravity	9	°API
Formation type	Sandstone	

For heterogeneous base case model, CSI is performed in heterogeneous model with middle value of Lorenz coefficient which is 0.328. As CSI process is favorable in not very deep reservoir, top layer of reservoir model is constructed at depth of 1,640 ft. This depth corresponds to initial reservoir pressure of about 725 at top of reservoir based on pressure gradient of 0.433 psi/ft. Maximum bottomhole pressure of 900 psi is calculated and limited for injection process to prevent undesired fracture based on Ben and Eaton's equation. As reservoir is located in shallow depth, average

permeability can be as high as 1,600 millidarcies. However, heterogeneous reservoir has variation of maximum permeability at top layer of 3,000 millidarcies and minimum value of 200 millidarcies. This variation of permeability represents coarsening upward sequence.

4.2 Reservoir Model with Heterogeneity

Lorenz coefficient (L_k) is used to quantify heterogeneity of reservoir models in this study. Values of permeability in each layer for each heterogeneity degree are summarized in Table 4.2.

Table 4.2 Permeability values in each layer of each reservoir model with different Lorenz coefficient

Layer	Permeability in millidarcies for different Lorenz Coefficient				
	0.265	0.296	0.328	0.371	0.402
1	3,000	3,000	3,000	3,000	3,000
2	2,200	2,500	2,650	2,800	2,950
3	2,000	2,000	2,300	2,500	2,900
4	1,800	1,900	1,950	2,300	2,300
5	1,600	1,600	1,600	1,600	1,600
6	1,400	1,400	1,250	1,200	800
7	1,200	1,100	900	500	400
8	1,000	700	550	300	250
9	200	200	200	200	200

From permeability values shown in Table 4.2 together thickness and porosity of each layer, Lorenz coefficient curves of all models plotted between cumulative flow capacity versus cumulative storage capacity which is intensively described in chapter III, are illustrated in Figure 4.2.

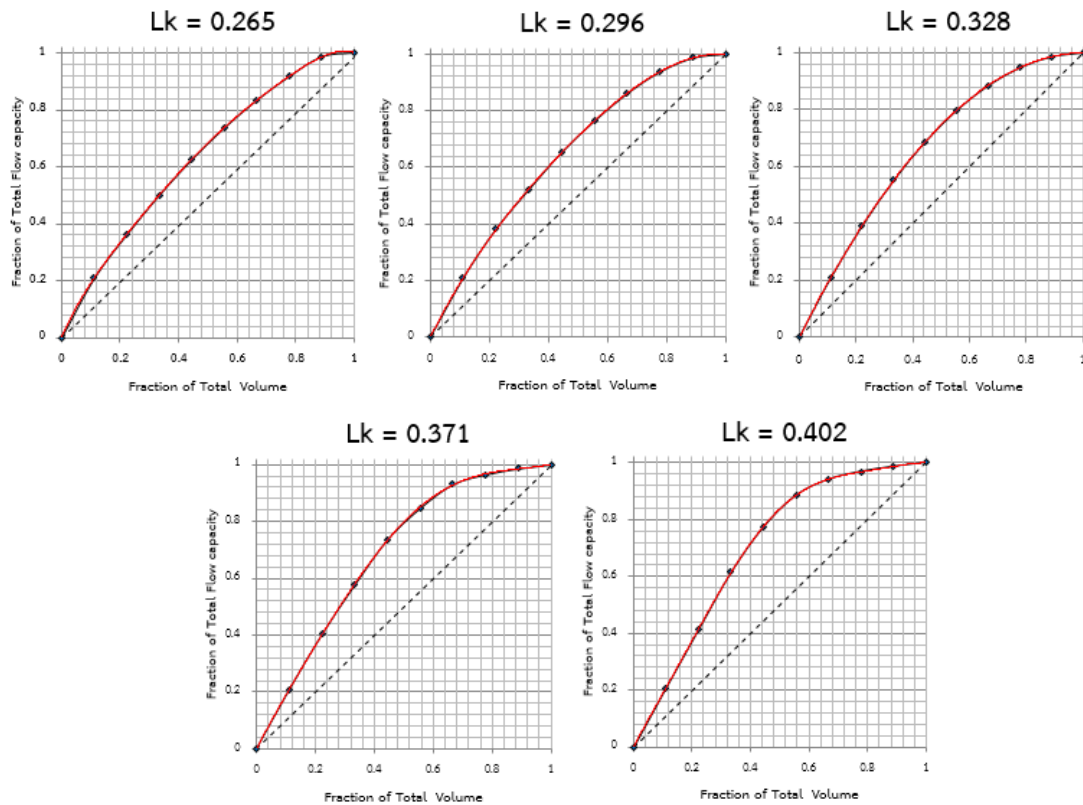


Figure 4.2 Plots of 5 different Lorenz coefficient values

4.3 Pressure-Volume-Temperature (PVT) Properties

Pressure-Volume-Temperature (PVT) properties of reservoir fluid are specified by using several correlations. Summary of correlation used for each PVT properties is shown in Table 4.3.

Table 4.3 Summary of correlation for each PVT property

Parameter	Option
Oil properties (bubble point, R_s , B_o) correlation	Standing
Oil compressibility correction	Glaso
Dead oil viscosity correlation	Ng and Egbogah
Live oil viscosity correlation	Beggs and Robinson
Gas critical properties correlation	Standing

In order to generate PVT properties several properties are required to initiate PVT functions which are oil gravity, bubble point pressure and solution gas-oil ratio. From these data, in-situ oil viscosity is obtained. Initial input parameters and generated oil viscosity are summarized in Table 4.4.

Table 4.4 Input parameters for PVT data and generated in-situ oil viscosity

Parameter	Value	Unit
Oil gravity	9	°API
Bubble Point Pressure	294.86	psi
Solution Gas-Oil Ratio	45.86	SCF/STB
In-situ Oil Viscosity	1217.8	cP

Figures 4.3 to 4.7 depicts dry gas formation volume factor (B_g) as a function of pressure, Oil formation volume factor (B_o) as a function of pressure, oil viscosity (μ_o) as a function of pressure, oil viscosity (μ_o) as a function of temperature, and solution gas-oil ratio (R_s) as a function of pressure. As pressure affects liberation of solution gas, most properties are therefore plotted with pressure.

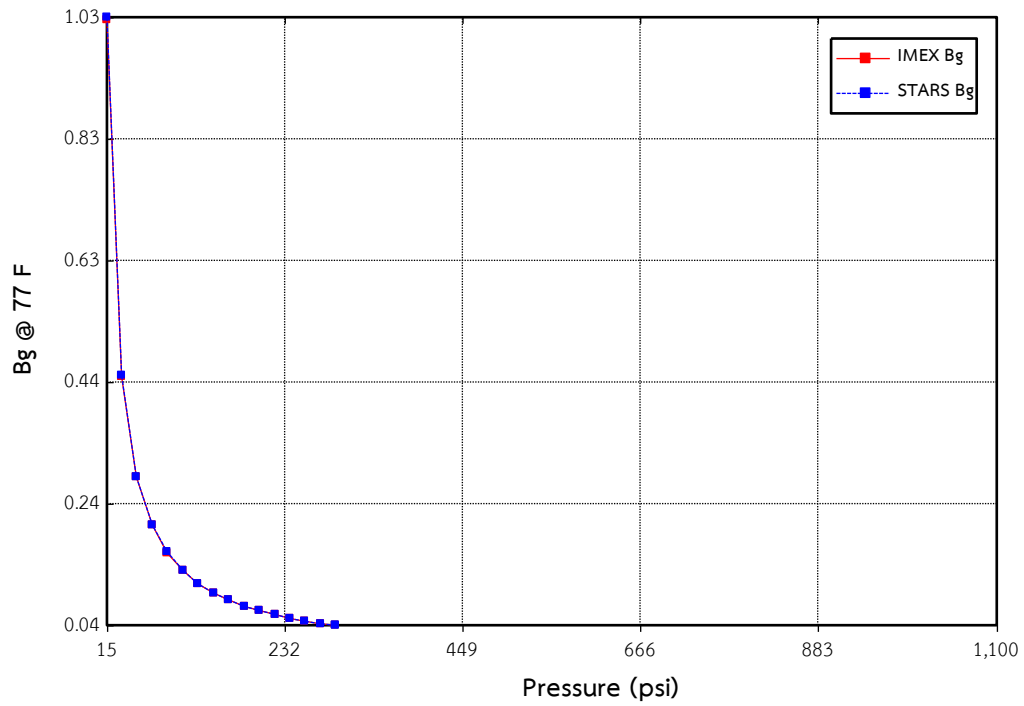


Figure 4.3 Dry gas formation volume factor (B_g) for reservoir model as a function of reservoir pressure

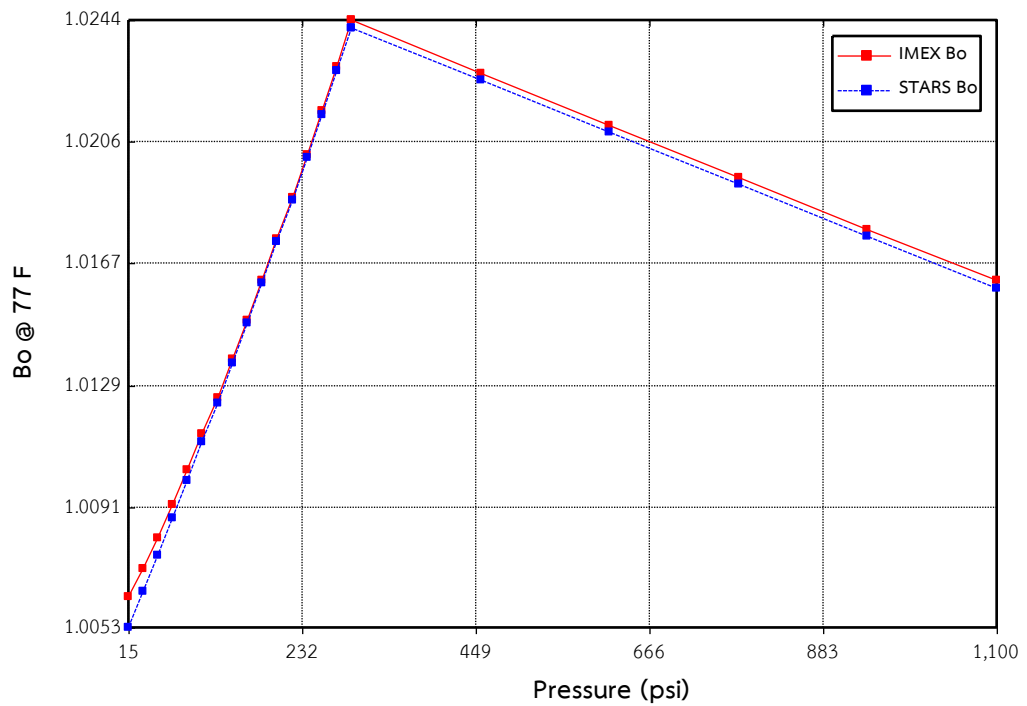


Figure 4.4 Oil formation volume factor (B_o) for reservoir model as a function of reservoir pressure

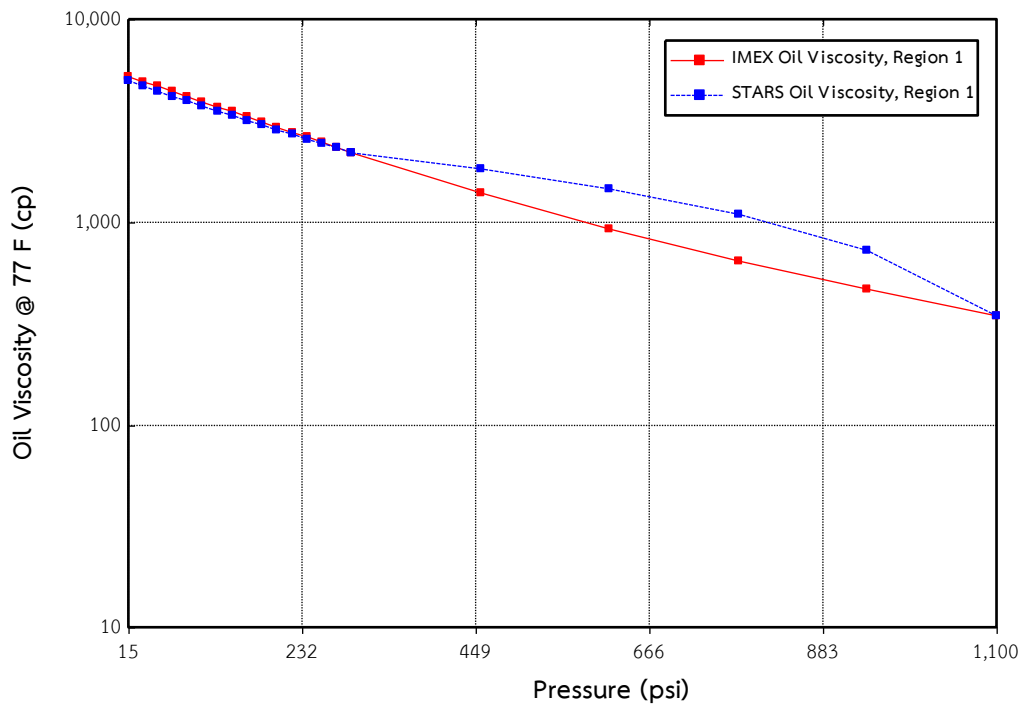


Figure 4.5 Oil viscosity (μ_o) for reservoir model as a function of reservoir pressure

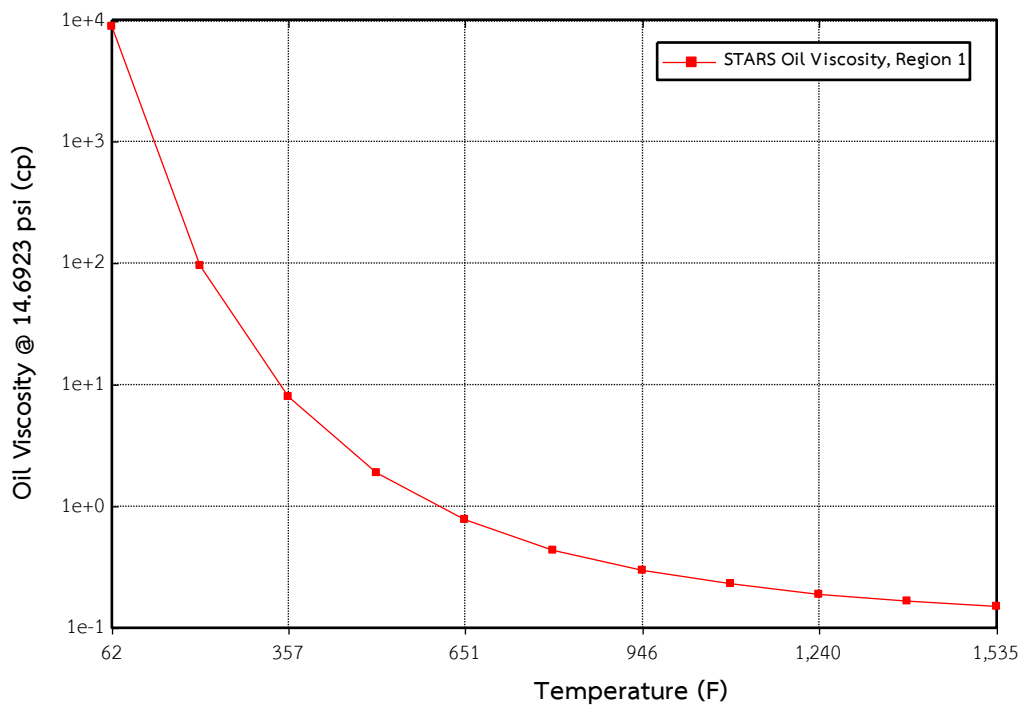


Figure 4.6 Oil viscosity (μ_o) for reservoir model as a function of reservoir temperature

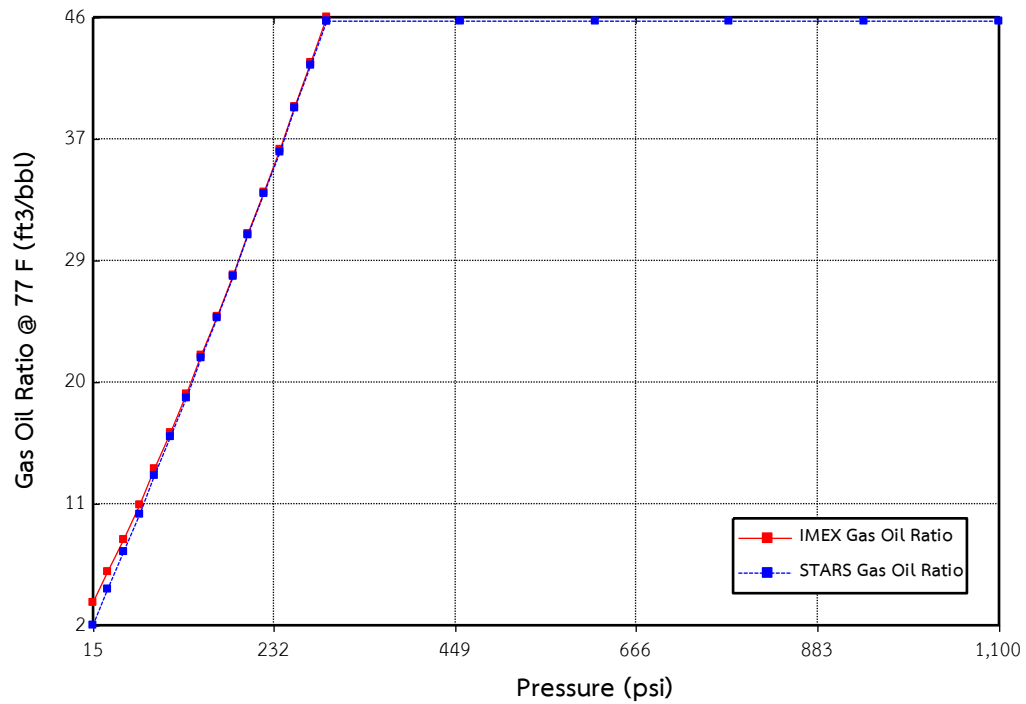


Figure 4.7 Gas-oil ratio for reservoir model as a function of reservoir pressure

PVT property plotted with reservoir pressure possesses two functions. The blue color stands for correlation using in STAR simulator while red color represents correlation using in IMEX simulator. In this study, blue color is utilized due to the simulations of this study are cyclic steam injection processes and STAR simulator is compatible for thermal reservoir simulation.

4.4 Special Core Analysis (SCAL) Section

End-point data are compulsory for generating water/oil and gas/oil relative permeability curves, using Corey's correlation equipped within STAR simulator. Table 4.5 summarizes required end-point data and other requirements for SCAL section.

Table 4.5 Summary of data required for construction of relative permeability curves

Parameter	Value
SWCON - Endpoint Saturation: Connate Water	0.2
SWCRIT - Endpoint Saturation: Critical Water	0.2
SOIRW - Endpoint Saturation: Irreducible Oil for Water-Oil Table	0.2
SORW - Endpoint Saturation: Residual Oil for Water-Oil Table	0.2
SOIRG - Endpoint Saturation: Irreducible Oil for Gas-Liquid Table	0
SORG - Endpoint Saturation: Residual Oil for Gas-Liquid Table	0.2
SGCON - Endpoint Saturation: Connate Gas	0
SGCRIT - Endpoint Saturation: Critical Gas	0
KROCW - kro at Connate Water	0.7
KRWIRO - krw at Irreducible Oil	0.3
KRGCL - krg at Connate Liquid	0.8
Exponent for calculating krw from KRWIRO	3
Exponent for calculating krow from KROCW	3
Exponent for calculating krog from KROGCG	3
Exponent for calculating krg from KRGCL	3

Figures 4.8 and 4.9 show relative permeability curves of oil-water and liquid-gas systems respectively. These relative flow abilities are properties at reservoir temperature which is 77 °F. Since relative permeability is a function of temperature, additional sets of relative permeability curves are generated. Figure 4.10 and Figure 4.11 illustrate relative permeability of oil-water and liquid-gas systems respectively in comparison between reservoir temperature (77°F) and at elevated reservoir temperature (500°F) which is steam temperature. For gas relative permeability shown in Figure 4.11, two lines are represented. This can be explained that before performing CSI the reservoir temperature is at initial reservoir temperature and relative permeability curve for oil/water system is the same as in Figure 4.8 but after steam enters, heating the reservoir, temperature is increased and average reservoir temperature is in between initial and steam temperature. Thus, relative permeability

curve for oil/water system is shifted as shown in Figure 4.10. At any temperature after CSI process, relative permeability curve is interpolated between these two defined curves. In this model, the composition of gas phase will be determined in every grid block in each time step. If composition of gas contains steam less than 20 percent (base in mole fraction) the first interpolation set (set#1 in Figure 4.11) is used. If the composition of gas contains steam greater than 60 percent, the second interpolation set (set#2 in Figure 4.11) will be used. For any composition between these values a linear interpolation of the different sets of curves is performed.

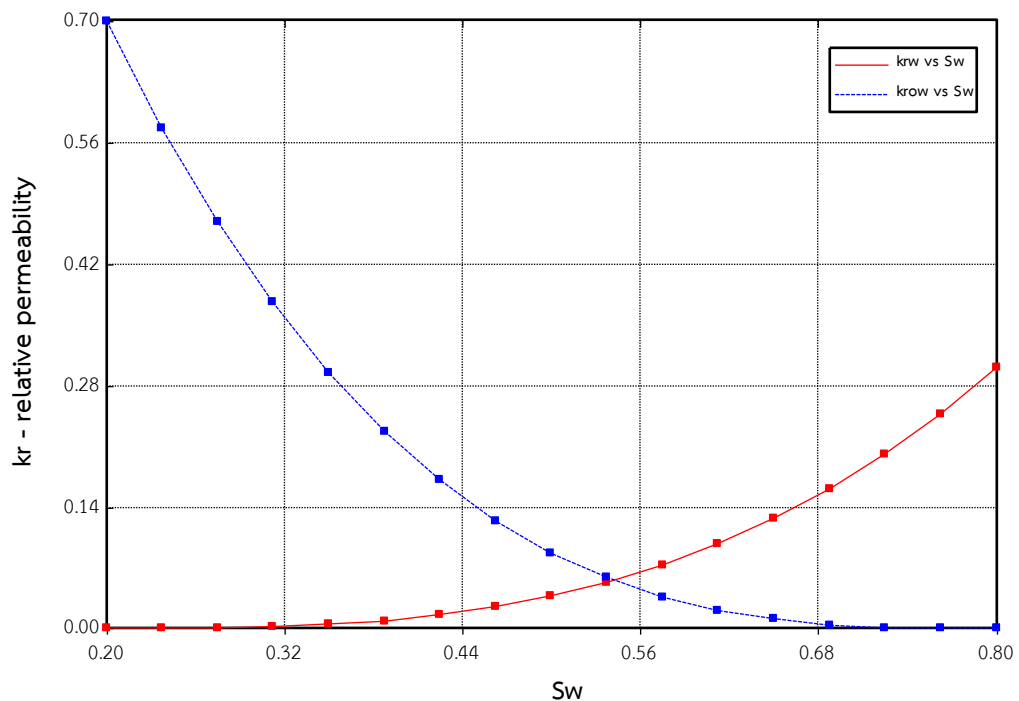


Figure 4.8 Relative permeability curves of oil/water system for reservoir model as a function of water saturation

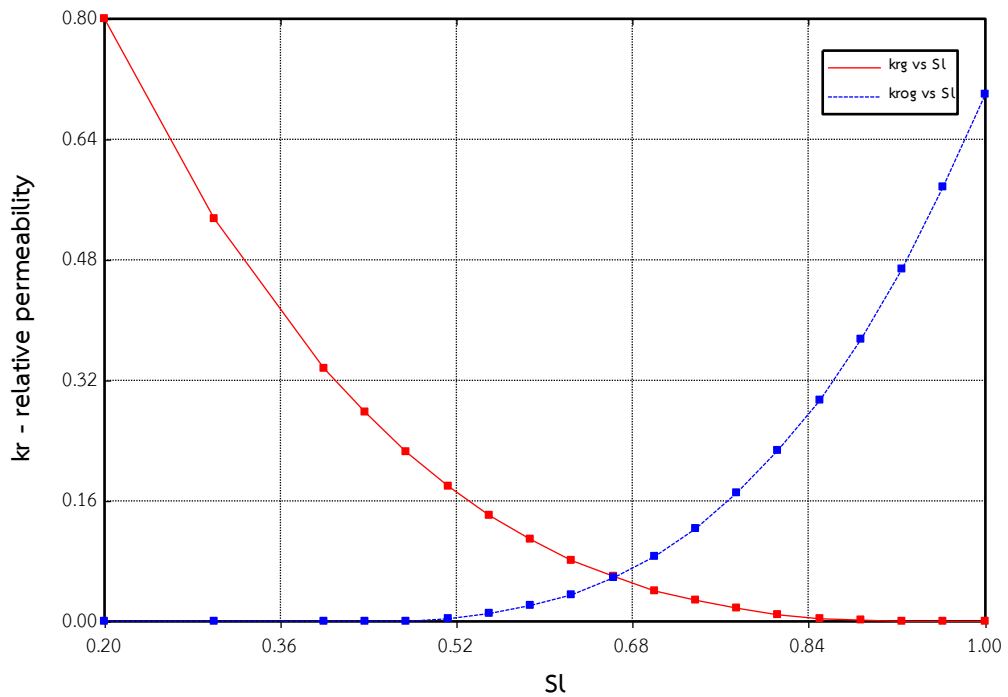


Figure 4.9 Relative permeability curves of gas/liquid system for reservoir model as a function of liquid saturation

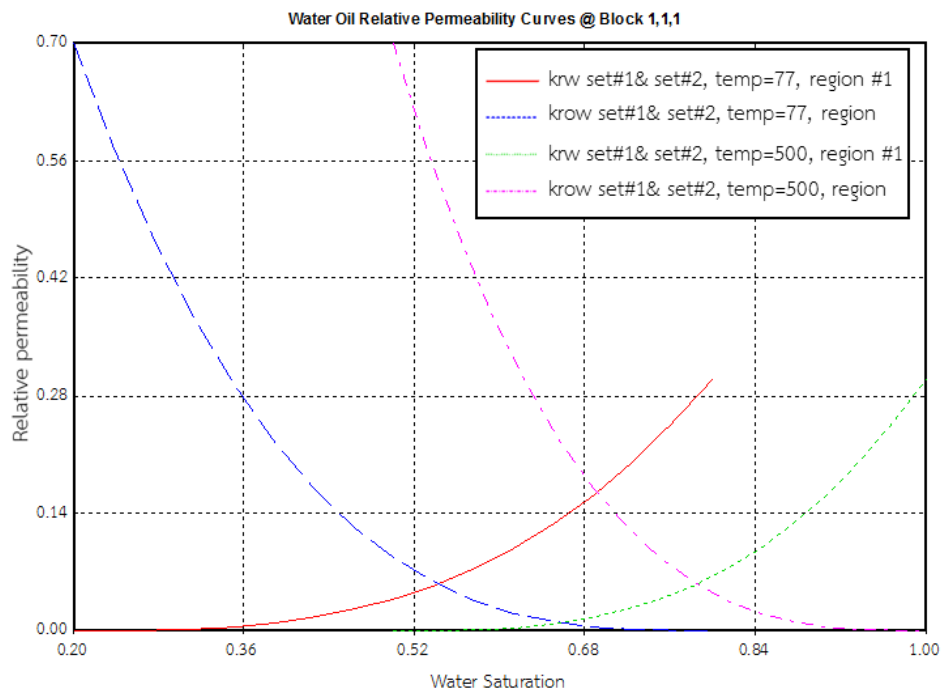


Figure 4.10 Relative permeability curves of oil/water system for reservoir model at initial reservoir temperature and at steam temperature as a function of water saturation

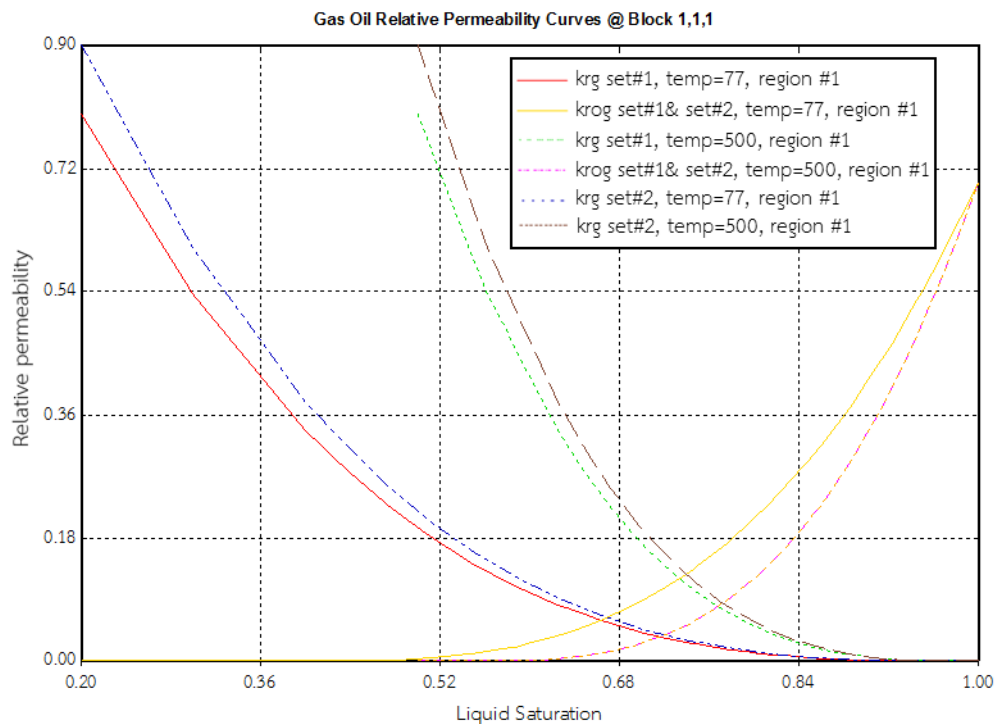


Figure 4.11 Relative permeability curves of gas/liquid system for reservoir model at initial reservoir temperature and steam temperature as a function of liquid saturation

4.5 Parameters Related to Injection and Production Wells

Wellbore radius of injection and production well is 0.25 ft. and skin factor is assumed to be zero. Both injection and production wells of all groups are fully-perforated along reservoir thickness. Wells are placed in 5-spot pattern, having one well located at the middle and other four wells at the corners of reservoir model. Location of wells is illustrated in Figure 4.1. Steam injection rate is determined in a unit of STB/D which is equivalent of liquid volume. Soaking period and steam quality are varied. Selected parameters of both soaking period and steam quality are utilized for the entire study. Injection and production constraints are listed in Table 4.5 to Table 4.8. In first cycle, steam cannot be easily injected into reservoir due to high oil saturation, viscosity and pressure. Low liquid production rate could help maintaining heat in the reservoir in early cycles to reduce oil viscosity. Since steam can be better injected into reservoir and oil can flow more readily in later cycles, liquid production rate is increasingly adjusted to achieve higher oil production. Group events of injection

and production constraints for cyclic steam injection are listed in Tables 4.9 and 4.10. Total operating period is around 4 years (1,500 days) with 30 of 50 days life cycle. Soaking period is varied in this study therefore production period is automatically adjusted to keep cycle length constant. Cycle periods with variation of soaking periods are shown in Table 4.12.

Table 4.6 Constraints of injection wells at corners of reservoir

Parameter	Value	Unit
Maximum bottom hole pressure	900	psi
Maximum injection water rate	250	STB/D
Steam Temperature	500	°F
Steam quality	Varied (0.5, 0.8, 1.0)	fraction

Table 4.7 Constraints of injection well at center of reservoir

Parameter	Value	Unit
Maximum bottom hole pressure	900	psi
Maximum injection water rate	1,000	STB/D
Steam Temperature	500	°F
Steam quality	Varied (0.5, 0.8, 1.0)	Fraction

Table 4.8 Constraints of production wells at corners of reservoir

Parameter	Value	Unit
Minimum bottom hole pressure	300	psi
Maximum liquid rate	50	STB/D

Table 4.9 Constraints of production well at center of reservoir

Parameter	Value	Unit
Minimum bottom hole pressure	300	psi
Maximum liquid rate	200	STB/D

Table 4.10 Group event constraints of injection and production wells at corners of reservoir

Cycle	Parameter	
	Maximum injection rate (STB/D)	Maximum liquid production rate (STB/D)
1 - 20	250	25
21 - 25	250	37.5
26 - 30	250	50

Table 4.11 Group event constraints of injection and production wells at center of reservoir

Cycle	Parameter	
	Maximum injection rate (STB/D)	Maximum liquid production rate (STB/D)
1 - 20	1,000	100
21 - 25	1,000	150
26 - 30	1,000	200

Table 4.12 Cycle period of cyclic steam injection with variation of soaking period.

Parameter	Value			Unit
Injection period	10	10	10	days
Soaking period	4	6	8	days
Production period	36	34	32	days

4.6 Thesis Methodology

1. Reservoir model with different degrees of heterogeneity are constructed to have different Lorenz coefficients of 0.265, 0.296, 0.328, 0.371 and 0.402.
2. First reservoir model with medium value of Lorenz coefficient (0.328) is selected to perform CSI process with reservoir parameters summarized Table 4.1 and all operation parameters from Table 4.6 to Table 4.12. Different three soaking period and three steam quality results in nine combination cases. These cases are performed with the same cycle length for comparing all cases

appropriately. Selection of best soaking period and steam quality is considered based on recovery factor and energy consumed per barrel of oil produced. These selected operating parameters will be utilized to perform CSI for the entire study. Details of selection of operating parameters are as followed:

- Soaking period (4, 6 and 8 days) with 10 days of injection period,
 - Steam quality (0.5, 0.8, and 1.0).
3. Perform CSI process using selected operational parameters obtained from step 2 on reservoir model with different Lorenz coefficients (0.265, 0.296, 0.328, 0.371 and 0.402) to study effects of reservoir heterogeneity. These heterogeneous models are constructed under the same controlled values which are average permeability, maximum permeability, minimum permeability and median permeability and these models represent coarsening upward sequence.
 4. Perform study of interest parameters including vertical permeability, shale percent, relative permeability, and permeability sequence on reservoir model with Lorenz coefficient of 0.328. Details of interest parameters are as followed:
 - a) Vertical permeability (k_v/k_h) (0.001, 0.01, 0.1 and 0.2),
 - b) Structural shale percent (10%, 15%, 20% and 25%),
 - c) Relative permeability
 - Corey's exponent (2.5, 3.0, 3.5 and 4.0),
 - End point saturations at reservoir temperature $[(S_{wi}= 0.15, S_{or}= 0.25), (S_{wi} = 0.20, S_{or} = 0.20)$ and $(S_{wi} = 0.25, S_{or} = 0.15)]$,
 - End point saturations at elevated temperature $[(S_{wi} = 0.40, S_{or} = 0.10), (S_{wi}= 0.45, S_{or} = 0.05)$ and $(S_{wi}= 0.50, S_{or} = 0)]$,
 - d) Permeability sequence (coarsening upward and fining upward).

5. Compare and discuss results from simulation outcomes mainly based on oil recovery factor, energy consumed per barrel of oil produced and steam/oil ratio and conclude new finding from the study.

This methodology is illustrated and described in figure as shown in Figure 4.12 and Figure 4.13.

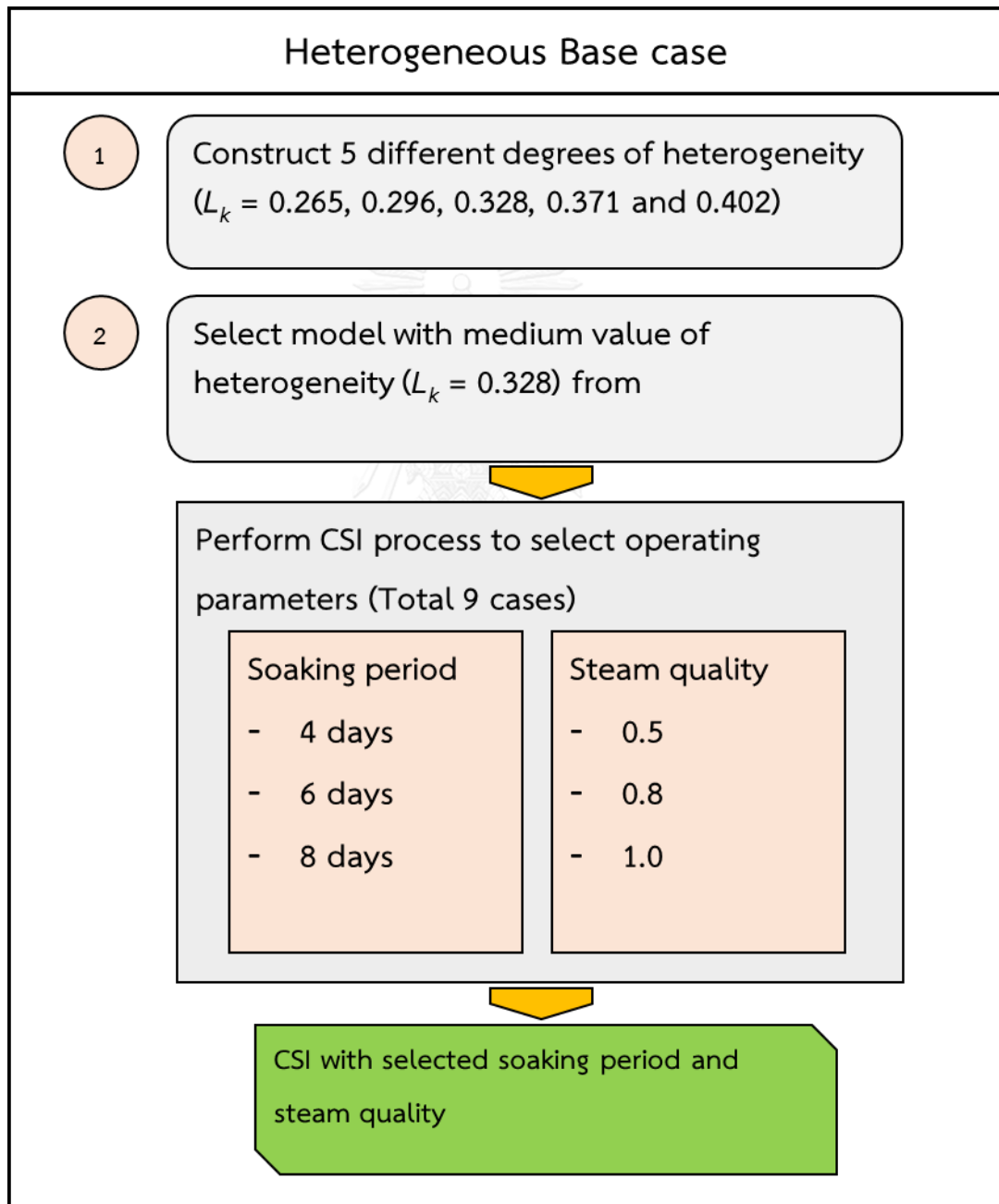


Figure 4.12 Thesis methodology: selection of operating conditions

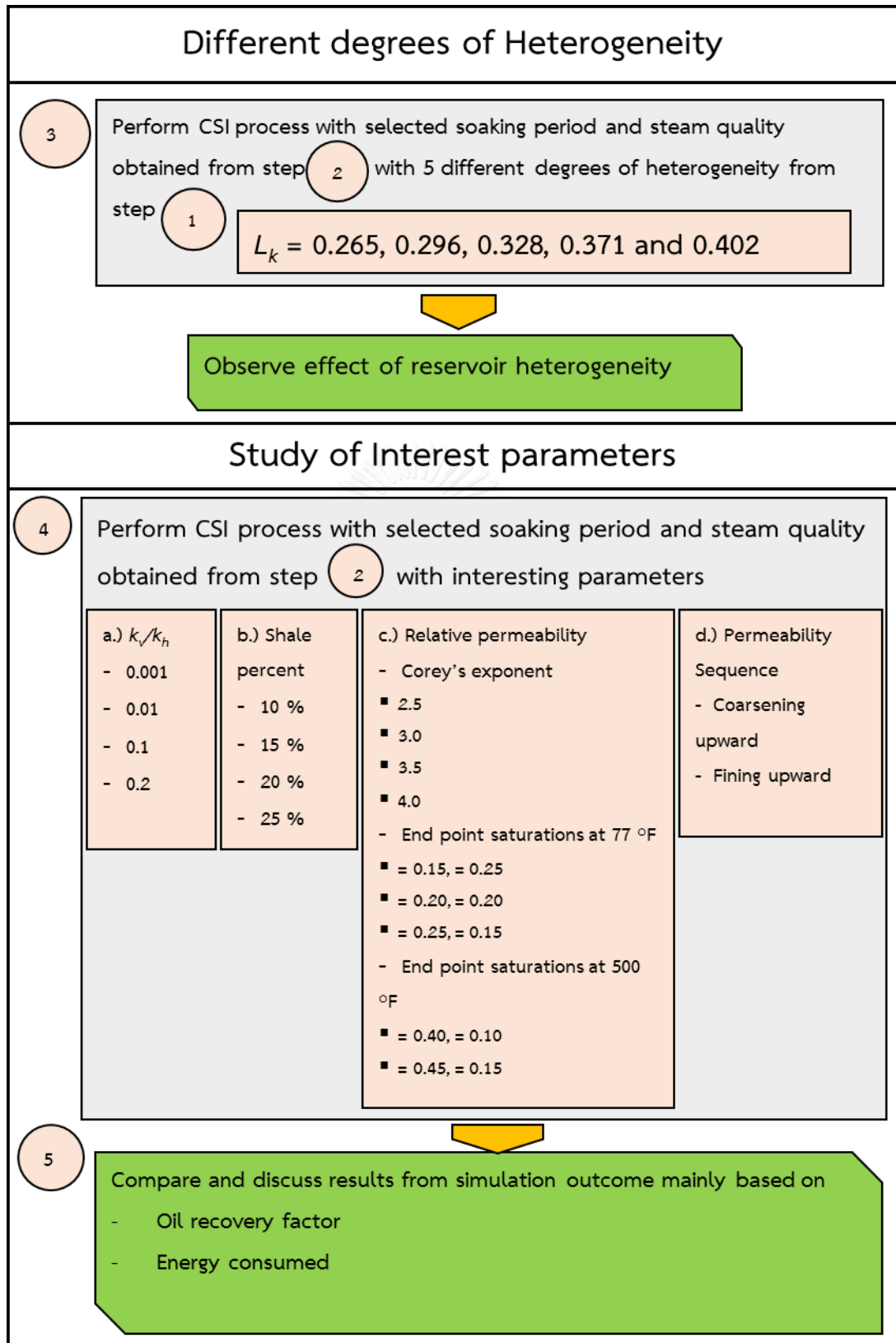


Figure 4.13 Thesis methodology: study of interest parameters

CHAPTER V

RESULTS AND DISCUSSION

After heterogeneous reservoir model is constructed with all selected properties, cyclic steam injection simulation is performed on the first reservoir model with variation of operating parameters to obtain proper values of soaking period and steam quality. Then reservoir heterogeneity is varied to investigate the sensitivity on effectiveness of CSI in heterogeneous reservoir. Middle value of heterogeneity ($L_k = 0.328$) is selected to perform CSI simulation on other interest properties consist of vertical permeability, shale percent, relative permeability and permeability sequence. Oil recovery factor and enthalpy consumed per barrel of oil are used to discuss the effectiveness of the process.

Set of operating parameters is kept constant for every case. Maximum steam injection and cycle length are constant in every cycle while maximum production rate is varied and increased proportionally in later cycles. During Injection period, injection wells are controlled from maximum bottomhole pressure of 900 psi to prevent undesired fractures and the pressure is also maintained during soaking period. After that the well are switched to production wells and controlled by minimum bottomhole pressure of 300 psi. Total production period is 4 years (1,500 days) to represent proper period for cyclic steam injection process.

5.1 Cyclic Steam Injection Base Case

5.1.1 Oil Recovery Mechanisms in Cyclic Steam Injection Process

There are several oil recovery mechanisms during CSI process. In early cycles, reservoir pressure is increased as steam is injected into reservoir with high pressure. Oil is produced at higher rates due to this driving force. As injected heat steam contacts reservoir rock and fluid and heat is transferred deep into reservoir, oil viscosity is reduced together with improvement of oil mobility. At later time during production period, oil rate is reduced as a result of reservoir depletion due to production. Typical oil production profile of CSI process is shown in Figure 5.1. From the figure it can be

observed that oil production rate is high in early period of production period and decreased in later time in each cycle. The peak of oil rate represents rate at which oil is drained to production well from steam pressurization. After that the rate starts to decline. Period that oil production rate is zero represents injection and soaking period. Reservoir temperature, oil viscosity and pressure profiles at different times are shown in Figure 5.2.

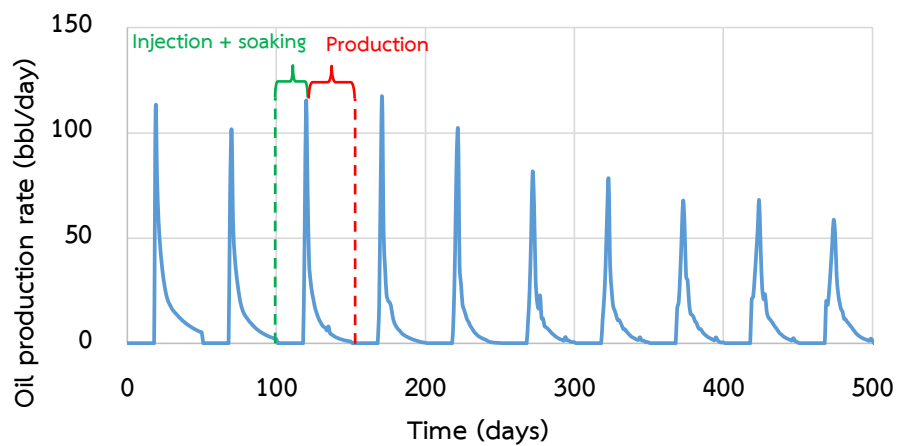


Figure 5.1 Oil production rate from CSI process as a function of time

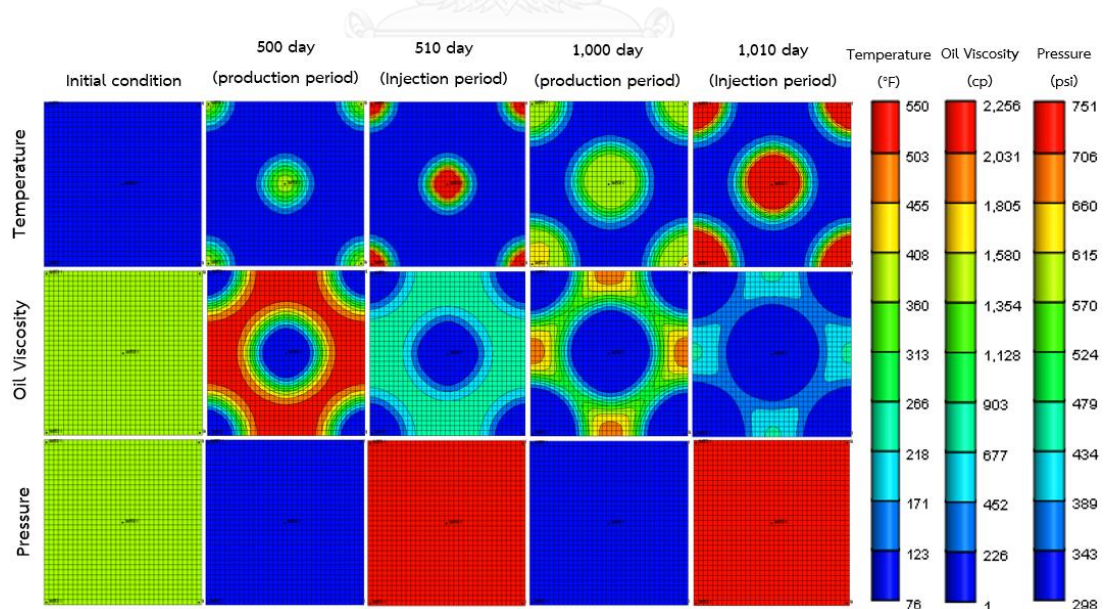


Figure 5.2 Reservoir temperature, oil viscosity and pressure profiles on top layer at different times

From Figure 5.2 it can be obviously seen that reservoir temperatures increases with larger extent with longer time. Due to the fact that steam is injected from all the wells in the same time, steam therefore penetrates slowly into reservoir due to high reservoir pressure during injection period. As a result, propagation of temperature slowly develops. The area affected from steam temperature obviously results in low oil viscosity which is greatly reduced. It can be noticed that. Oil viscosity in the area that is not affected from steam temperature is much higher during production period where reservoir pressure is decreased and much lower during injection period where reservoir pressure is increased. As oil viscosity is depended on pressure, fluctuation of oil viscosity can be observed during different phases since reservoir pressure is fluctuated from steam pressurization and production periods.

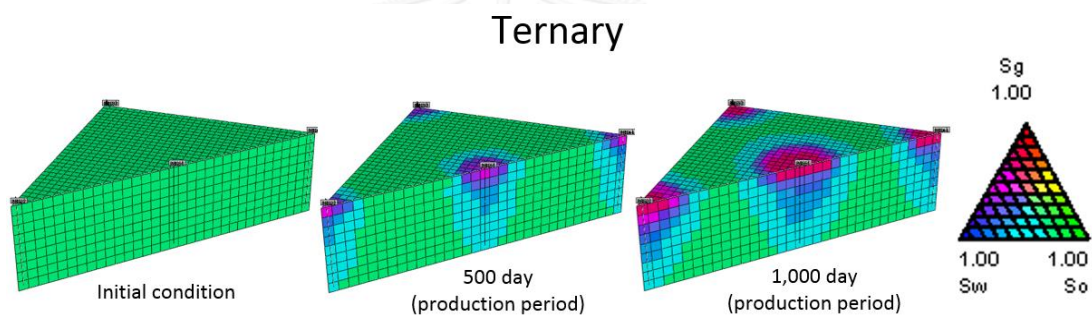


Figure 5.3 Three-phase fluid saturation profiles at different times

From Figure 5.3 high water saturation is observed around the wellbore. This is water that is condensed from injected steam and it is locked up in pores due to irreducible water saturation. Gas saturation is also observed around the wellbore but only in top layers of reservoir. Due to production period that could cause reservoir pressure to become lower than bubble point pressure, solution gas is liberated. The upper layer of reservoir where pressure is lower compared to the rest location together with low density of gas and residual gas saturation, gas therefore occupies around the wellbore only in top layers.

5.1.2 Selection of Operating Soaking Period and Steam Quality

Cyclic steam injection is first simulated with various soaking period and steam quality to obtain the best operating parameters on reservoir with median degree of

heterogeneity (Lorenz coefficient of 0.328). CSI is performed in 5-spot pattern consisting of 5 wells with 4 wells located at corners of reservoir and the rest well is located in the middle of reservoir. Maximum steam injection and maximum liquid production rate are remained the same for wells at the corner, whereas both values are four times higher for the central well. Cycle length is kept constant for all 5 wells. Oil recovery factor, energy consumed and steam-oil ratio (SOR) are concerned and used to compare effectiveness of CSI process for each case. Energy consumed is defined as enthalpy used to produce one unit volume of oil and SOR is also defined as volume of steam required to produce one unit volume of oil. Process with low SOR value is therefore more efficient than ones with high SOR.

Soaking period is an important operating parameter affecting heat transfer efficiency. Too short soaking period, heat efficiency is lower compared to longer soaking period. However, too long period leads to heat loss to overburden and underburden area that consecutively leads to low heat efficiency.

Results of different soaking period together with steam quality are shown in Figure 5.4 to Figure 5.10.

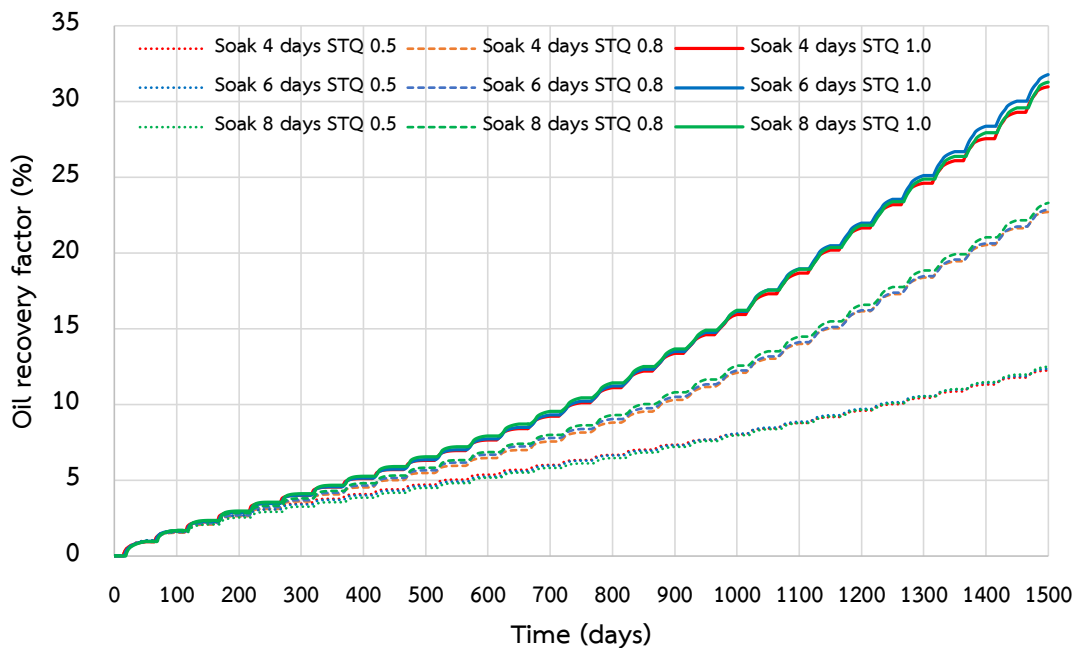


Figure 5.4 Oil recovery factors for cases with different soaking period and steam quality as a function of time

From Figure 5.4 it can be observed that at the same steam quality, there is no significant difference of oil recovery factor among three different soaking periods. Initially, all cases yield almost the same oil recovery due to low injectivity from high reservoir pressure. Therefore, steam is injected with limited amount. After that, different steam quality starts to affect oil recovery rate. Higher steam quality results in faster rate of increment of oil recovery factor due to higher amount of heat carried by steam. Comparing among the same steam quality, it shows soaking period does not yield exactly related trend on oil recovery factor. Summary of oil recovery factor at the end of production from whole cases is shown in Figure 5.4.

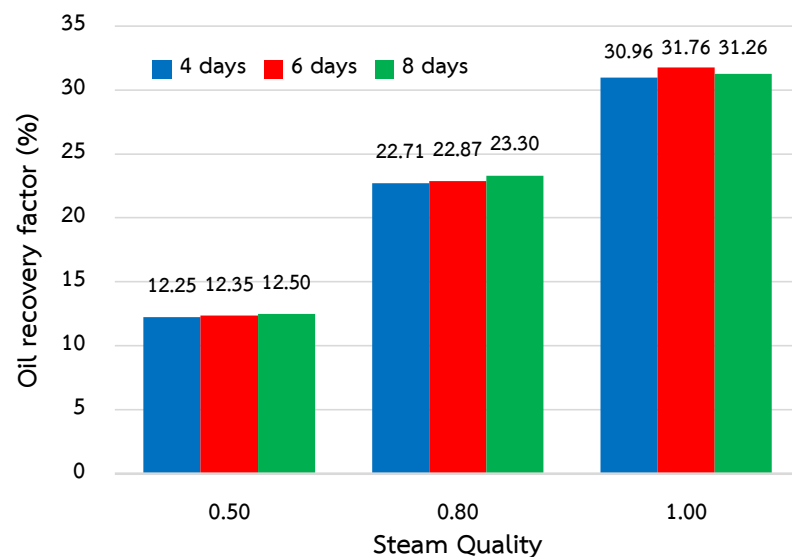


Figure 5.5 Summary of oil recovery factor at the end of production from whole cases

From Figure 5.5, it shows that at lower steam quality, longer soaking period yields benefit on oil recovery factor as heat could be transferred to oil better than cases with shorter soaking period. For the highest steam quality of 1.0, soaking period of 6 days yields the highest oil recovery of 31.76 percent. From previous case of low steam quality, the reason can be made for case of 4 days soaking period for high steam quality. However, at soaking period of 8 days, reduction of oil recovery factor compared to soaking period of 6 days is observed. At higher heat value carried by steam, reservoir oil obtained the transferred heat quickly due to temperature difference, allowing high driving force of heat transfer. With longer soaking period, production period is reduced

in this study. Longer soaking period of 8 days with high steam quality is therefore punished by shorter production period, resulting in slightly less oil recovery factor compared to soaking period of 6 days.

Nevertheless, oil recovery factor is not the only parameter that can judge effectiveness of the process. First, actual steam-oil ratio is considered as shown in Figure 5.6. From the figure, it can be obviously seen that higher steam quality yields the lowest steam-oil ratio. Since actual steam-oil ratio fluctuates with each cycle, average steam-oil ratio is plotted for the whole production period in Figure 5.7.

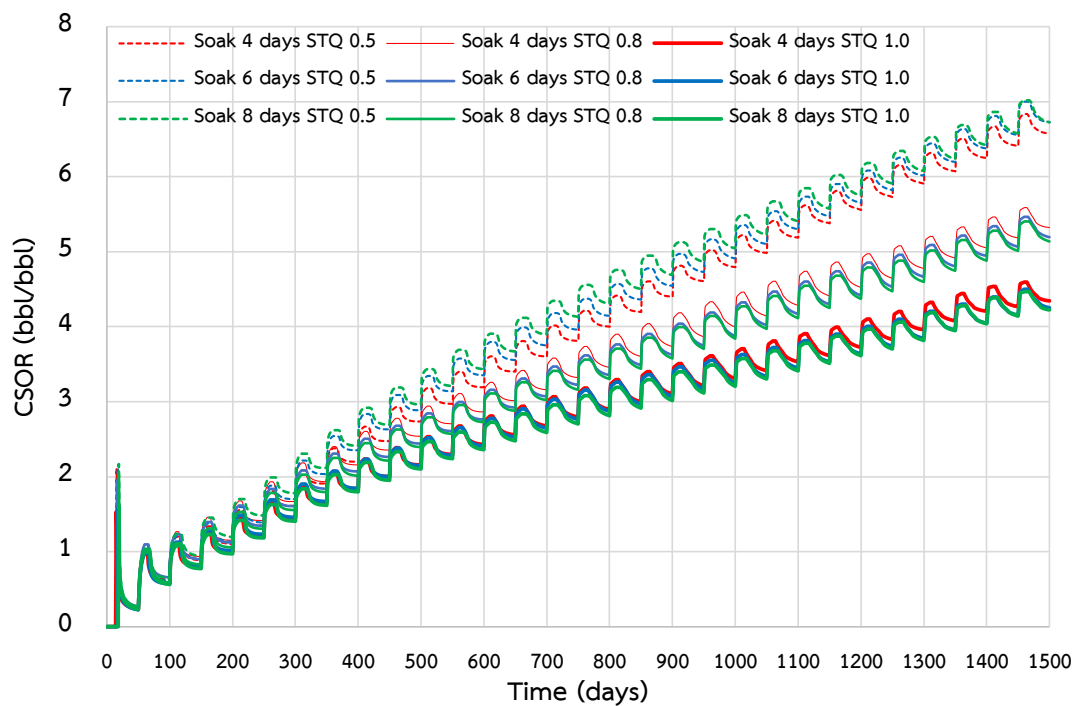


Figure 5.6 Actual steam-oil ratio for cases with different soaking period and steam quality as a function of time

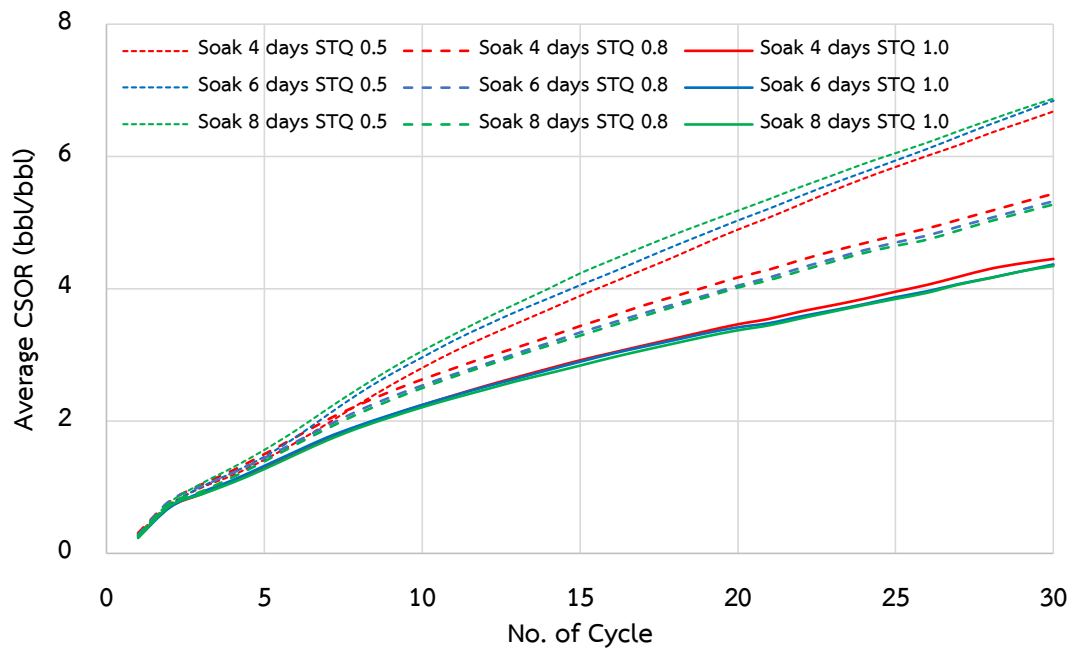


Figure 5.7 Average steam-oil ratio for cases with different soaking period and steam quality as a function of time

From Figure 5.7, steam quality of 1.0 yields the lowest values of steam-oil ratio. This value represents steam required per barrel of oil recovered. Therefore, the smallest value is more preferable. Comparing among the same steam quality, there is not exactly trend for each steam quality. At the lowest steam quality of 0.5, soaking period of 4 days yields the smallest steam-oil ratio. This could be explained that, at low steam quality, longer production period (soaking 4 days gains additional production period) results in higher steam efficiency.

However, when comparing steam-oil ratio to steam quality of 0.8 and 1.0, these two steam qualities showing the same trends, yields much lower steam-oil ratio. Longer soaking period tends to yields better steam-oil ratio. Since steam quality is higher, energy carried by steam is higher as well. Longer soaking period therefore results in better heat transfer to formation and reservoir fluids. Summary of cumulative steam-oil ratio is shown in Figure 5.8.

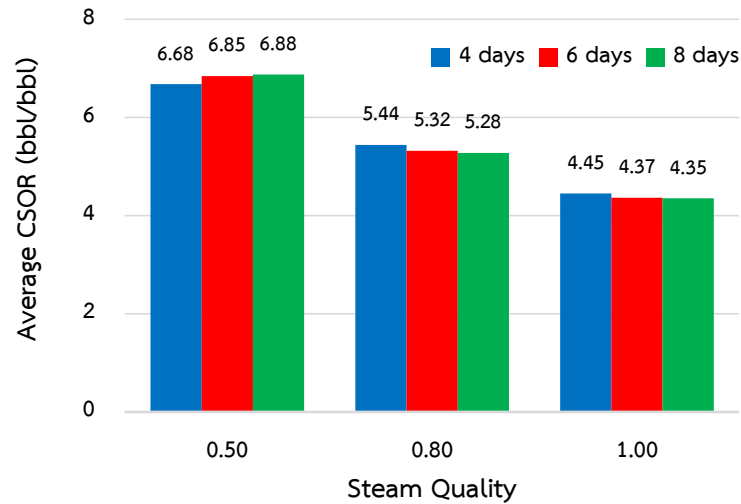


Figure 5.8 Summary of cumulative steam oil ratio at the end of production from whole cases.

From these results, it is obviously that high steam quality with long soaking period is suitable for CSI process. However, this consideration is based on amount of steam of which can be generated with different energy. Energy consumed per barrel of oil is therefore considered.

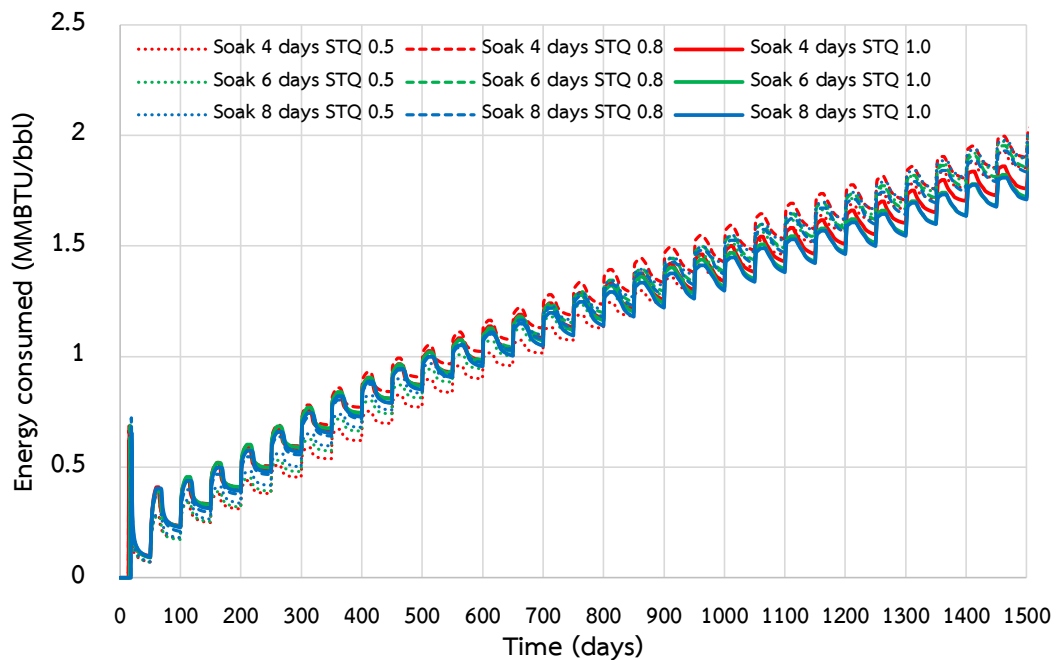


Figure 5.9 Energy consumed per barrel of oil for cases with different soaking period and steam quality as a function of time

From Figure 5.9 energy consumed is much higher for cases with higher steam quality at the start of process. As in initial period, quantity of steam injected into reservoir is quite limited due to low injectivity. Oil recovery is therefore not deviated much from case to case. High steam quality hence results in high consumption of energy. However, higher steam quality consumes less energy per barrel of oil since oil recovery is much higher at later stage. Figure 5.9 illustrates actual energy consumes which fluctuates with cycles. Hence, average energy consumed for each case is plotted in Figure 5.10 as a function of time for better comparison.

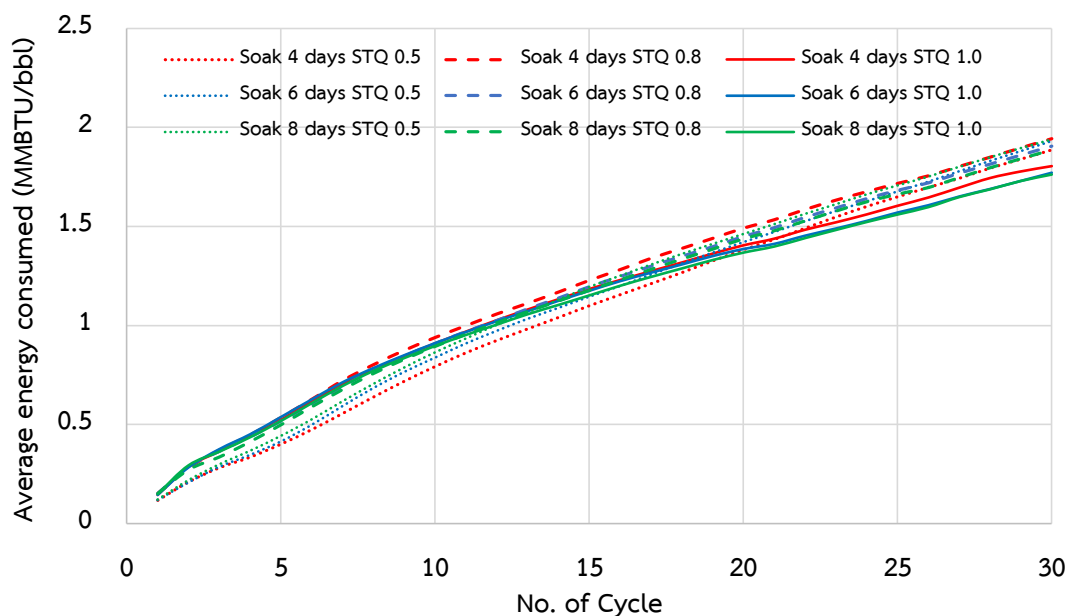


Figure 5.10 Average energy consumed per barrel of oil for cases with different soaking period and steam quality as a function of number of cycle

From Figure 5.10 average energy consumed per barrel of oil is the lowest in cases of high steam qualities. The figure clearly shows turn over period from high energy consumption to low energy consumption from the 5th to 20th cycle. Due to high oil recovery from heat dissipated in reservoir, oil recovery is much higher in cases of high steam quality. Summary of energy consumed per barrel of oil for the whole cases is shown in Figure 5.11.

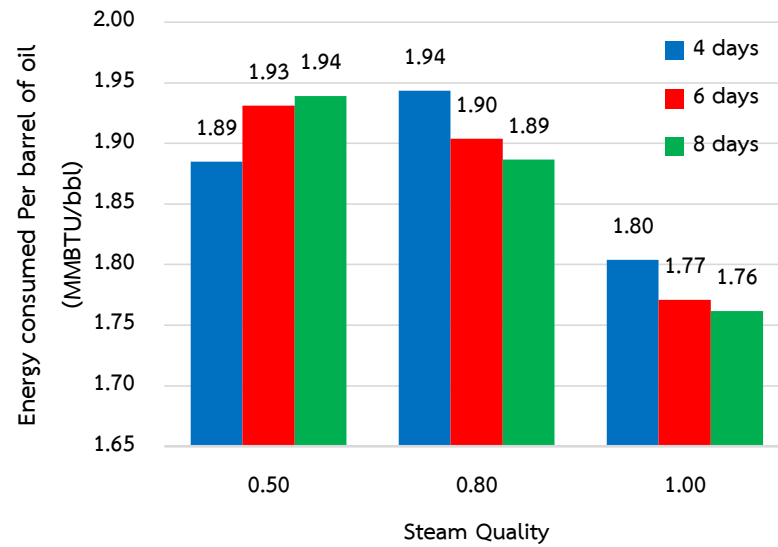


Figure 5.11 Summary of average energy consumed at the end of production from whole cases

From Figure 5.11 the case that yields the lowest energy consumed per barrel of oil is steam quality 1.0 with soaking period of 8 days. The result from this section is different from the best case that yields the highest oil recovery. Since maximum oil recovery is obtained from the soaking period of 6 days, steam is therefore injected at higher amount in following injection period, resulting in higher heat consumed in case of 6 days. Comparison between cumulative water injected (as steam) comparing between cases of soaking period 6 and 8 days (with steam quality 1.0) is depicted in Figure 5.12.

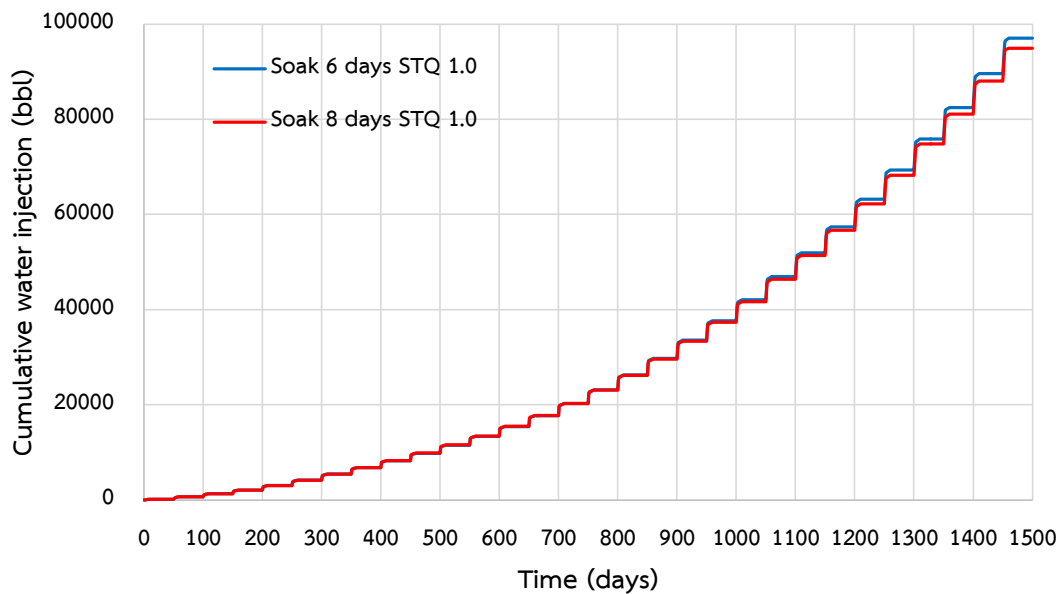


Figure 5.12 Comparison between cumulative water injected as steam to cases of steam quality of 1.0 with soaking period of 6 and 8 days.

From comparisons in terms of energy consumed per barrel of oil, the cases with steam quality of 1.0 and soaking period of 6 days and 8 days consumed almost the same energy (approximately 0.51 percent different). Consideration is therefore aimed at oil recovery among these two cases. Steam quality of 1.0 with soaking period of 6 days is hence chosen for the entire study due to higher oil recovery factor.

5.2 Effect of Reservoir Heterogeneity on Cyclic Steam Injection

From previous section, operating parameters from selected case yielding the best performance in terms of oil recovery factor and energy consumed are applied to all cases in this study as well as the entire study.

For reservoir heterogeneity in this study, models with different degrees of heterogeneity are constructed by varying permeability in each layer to create model with different Lorenz coefficient (L_k). Details of heterogeneity for each case are summarized in Table 4.2 in Chapter 4. Average permeability is 1,600 millidarcies. Permeability in top, median and bottom layers are also kept the same for all cases.

Oil recovery factors obtained from models with various Lorenz coefficients are shown in Figure 5.13.

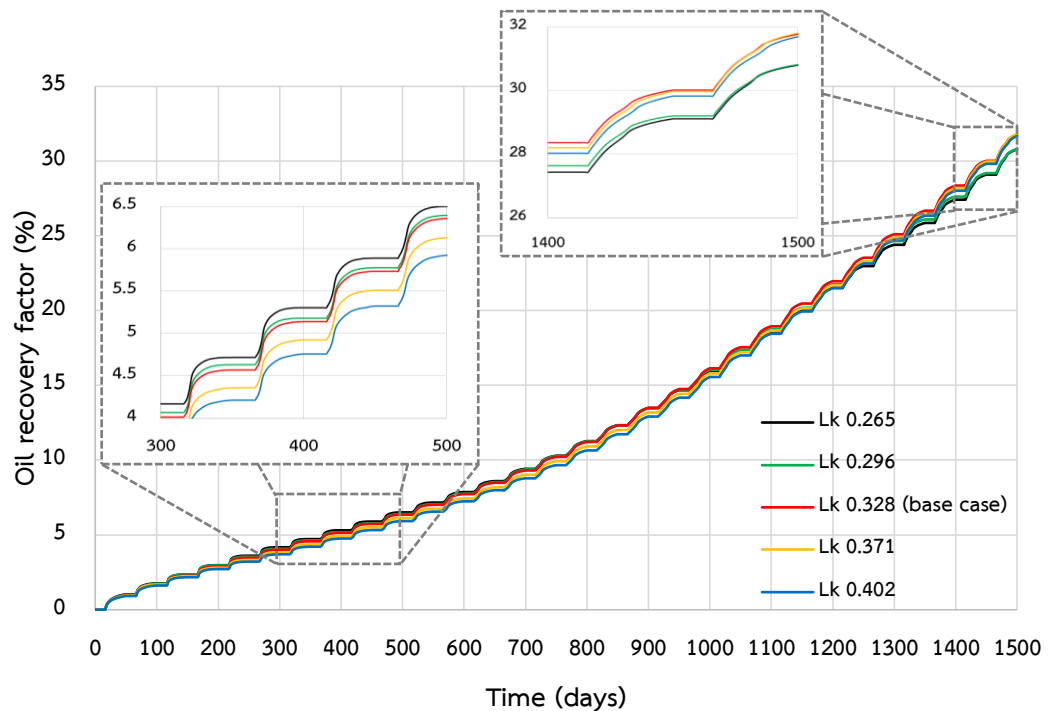


Figure 5.13 Oil recovery factors obtained from reservoir models with different degrees of heterogeneity as a function of time

From Figure 5.13, results obtained from reservoir models with different Lorenz coefficients do not show significant difference. In the first few cycles, lower heterogeneity tends to yield higher oil recovery factor. However, oil recovery factors from cases with higher heterogeneity are improved at later stage. For the model with small Lorenz coefficients, vertical permeability which is related to horizontal permeability is gradually decreased from top to bottom. In another word, permeability distribution in vertical direction is much better than cases with higher value of Lorenz coefficients. Comparison between vertical permeability of models with $L_k = 0.265$ (minimum value) and 0.406 (maximum value) is shown in Figure 5.14. Shading of color in case of L_k equals to 0.265 explains well distribution of vertical permeability.

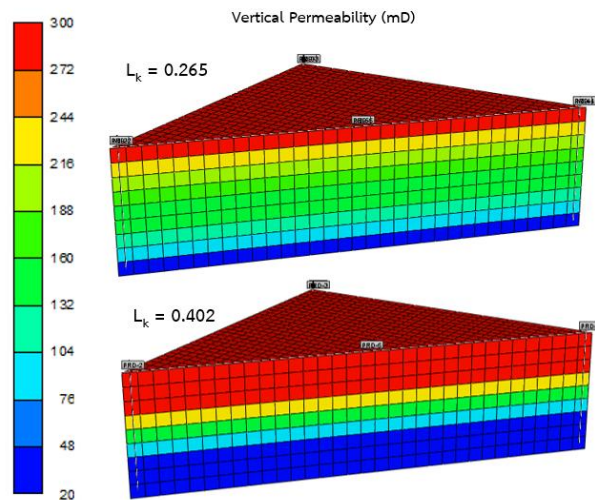


Figure 5.14 Distribution of vertical permeability of reservoir models with L_k 0.265 (minimum) and L_k 0.402 (maximum)

In early cycles, lower L_k value shows benefit on oil recovery since heat from injected steam can be delivered deeper at bottom layers. From Figure 5.15 both temperature and oil viscosity profile shows slightly bigger volume of reservoir that is affected from heat from steam in case of smaller L_k compared to case with larger L_k .

Oil mobility is improved as a result of oil viscosity reduction. Oil saturation profile in Figure 5.16 obviously shows location where oil is extracted from reservoir as similar explanation from temperature and oil viscosity profiles. Percolation of hot condensed water can be better observed from light blue color in three-phase fluid saturation profile in case of low L_k . Percolation of hot water during soaking period results in better heat distribution in low permeability zone in bottom layers since steam which is in a form of gas prefers to enter formation in top location where permeability is high. Therefore, good vertical permeability facilitates this percolation of hot water. From these reasons, recovery factor is slightly higher for reservoir model with smaller L_k compared to larger L_k .

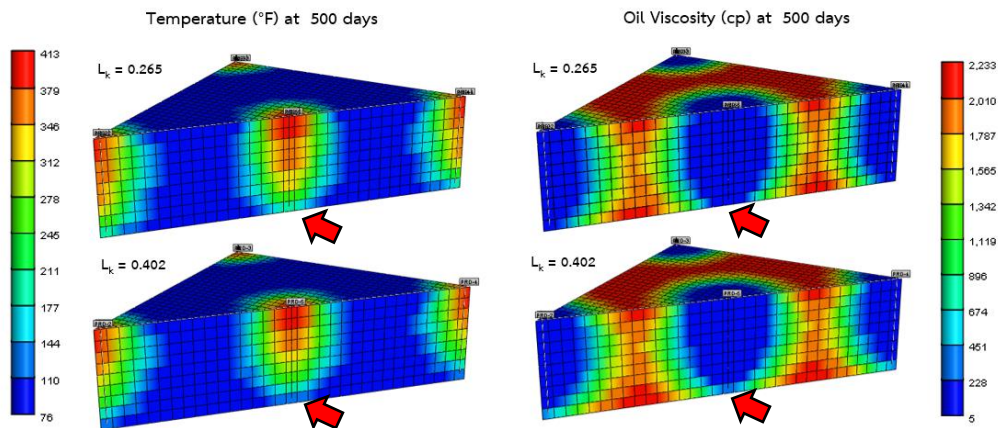


Figure 5.15 Temperature and oil viscosity profiles from reservoir model with L_k 0.265 (minimum) and L_k 0.406 (maximum) at 500 days

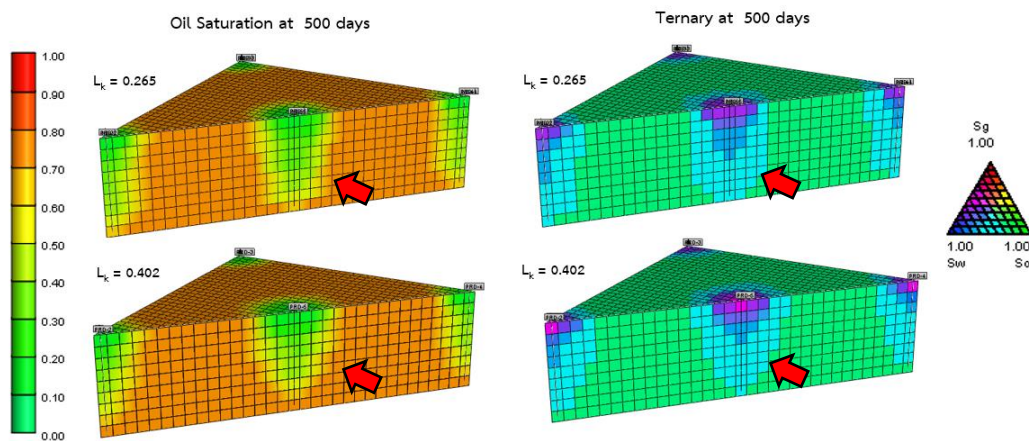


Figure 5.16 Oil saturation and three-phase fluid saturation profiles from reservoir model with L_k 0.265 (minimum) and L_k 0.406 (maximum) at 500 days

In later cycles, heat could be transferred better and steam could penetrate deeper into reservoir in both vertical and lateral directions. Temperature profiles in Figure 5.17 shows that in cases with L_k values of 0.328, 0.371 and 0.402, steam chamber in top most layers is expanded in slightly wider area than cases with L_k values of 0.265 and 0.296. This could be explained that larger horizontal permeability in top layers leads to faster expansion of steam chamber in top layer. A faster extent of steam chamber on top layer brings the heat transfer and percolation of water down to lower permeability zone in bottom layers. Summary of oil recovery is shown in Figure 5.18. The highest oil recovery is obtained from case with L_k of 0.371. As permeability

distribution is impoverished, steams better propagate to the upper zone of formation, expanding steam chamber. However, once steam is cooled down, condensed water hardly percolate down to bottom zone and this results in a turn over point for oil recovery factor from reservoir models with L_k 0.371 to L_k 0.402.

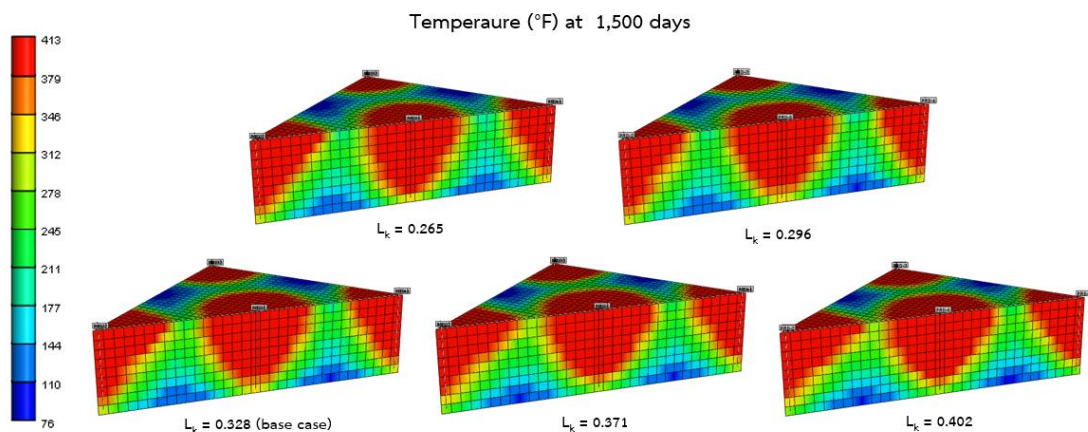


Figure 5.17 Comparison of reservoir temperature profile for reservoir models with different L_k values at the end of production

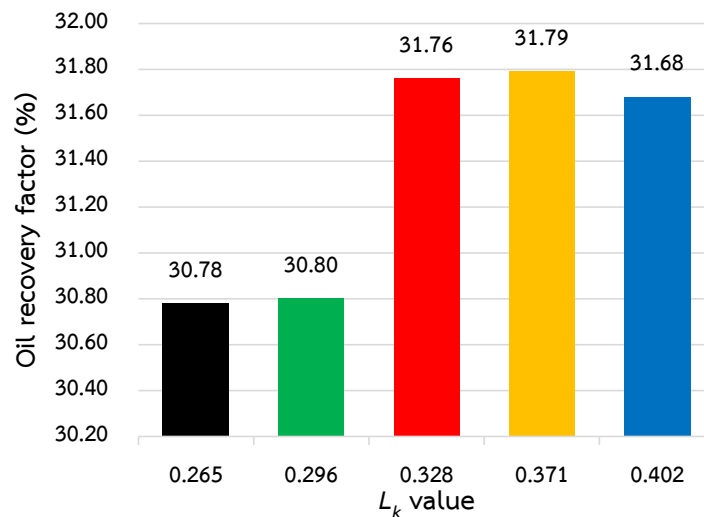


Figure 5.18 Summary of oil recovery factor for reservoir model with different L_k values at the end of production

Even cases with high L_k values yield higher oil recovery factor but energy consumed also becomes higher since more reservoir fluid is produced, steam injectivity is increased and as a consequent, higher amount of steam is injected into reservoir in

following cycles. Slightly higher in energy consumed is therefore observed in cases with high L_k values. The case with L_k value of 0.371 yields the highest oil recovery factor of 31.79 % which is approximately 0.03 percent higher than the case with L_k value of 0.328 (base case) but energy consumed per barrel of oil is also increased approximately 1.2 percent. The case with L_k value of 0.371 yields the highest oil recovery factor of 31.79 percent which approximately 1 percent higher than the case with L_k value of 0.265 but its energy consumed is also increased approximately 2.36 percent. Energy consumed for all cases with different L_k are shown in Figure 5.19 and Figure 5.20.

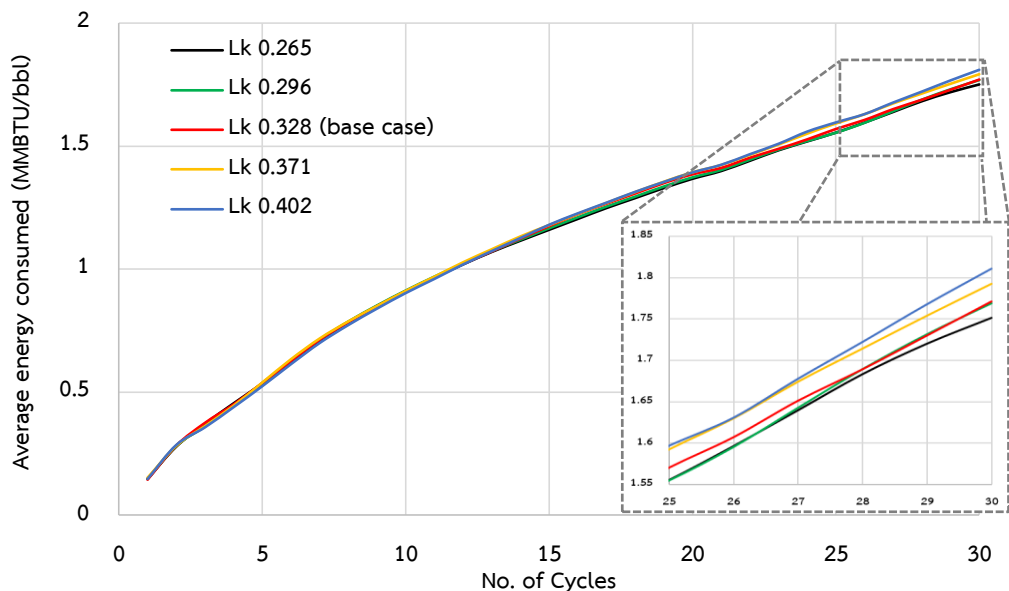


Figure 5.19 Energy consumed per barrel of oil obtained from reservoir models with different degrees of heterogeneity as a function of time

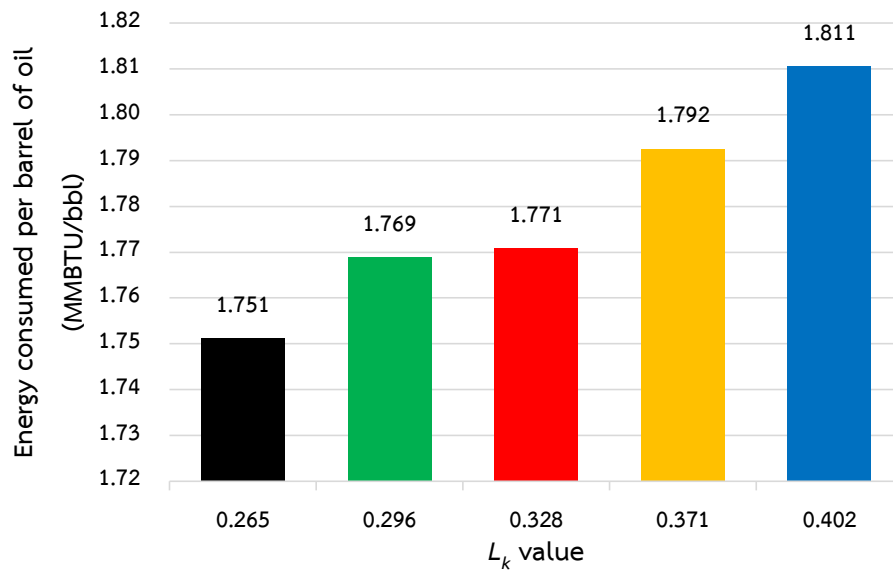


Figure 5.20 Summary of energy consumed per barrel of oil for reservoir model with different L_k values at the end of production

For the case with L_k value of 0.371 oil recovery is approximately 0.11 percent higher while energy consumed is approximately 1 percent lower than case with L_k value of 0.402 because of slightly lower cumulative water injection. Comparison of cumulative water injection between these two cases is shown in Figure 5.21. It could be explained that larger steam chamber is developed in higher heterogeneity case, resulting in removal of higher amount of oil from the steam chamber. However, as explained previously, higher vertical permeability in the case of lower L_k results in additional oil from condensed hot water. Condensed water itself occupied pore space due to irreducible water saturation. Higher oil recovery factor from the case of $L_k = 0.371$ is therefore observed and less water is therefore re-produced after the well is re-opened as illustrated in Figure 5.22. Nevertheless, injected steam only propagates to the chamber from previous cycle, making higher amount of steam injected in case of $L_k = 0.402$. This causes higher energy consumption in case of $L_k = 0.402$ while oil recovery factor is slightly less compared to case with $L_k = 0.371$.

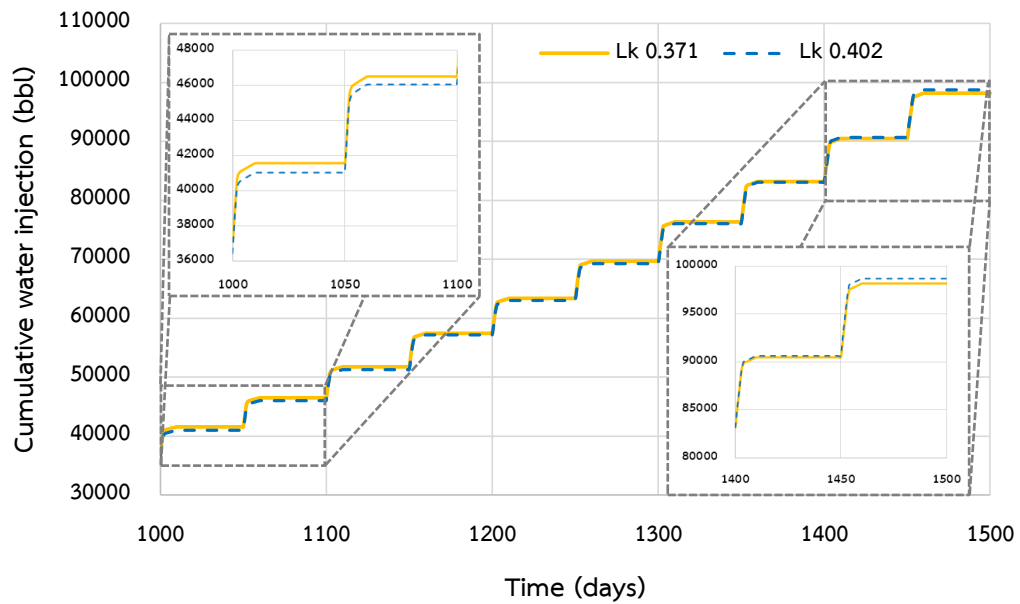


Figure 5.21 Cumulative water injected from reservoir model with L_k value of 0.371 and 0.402 at later cycles

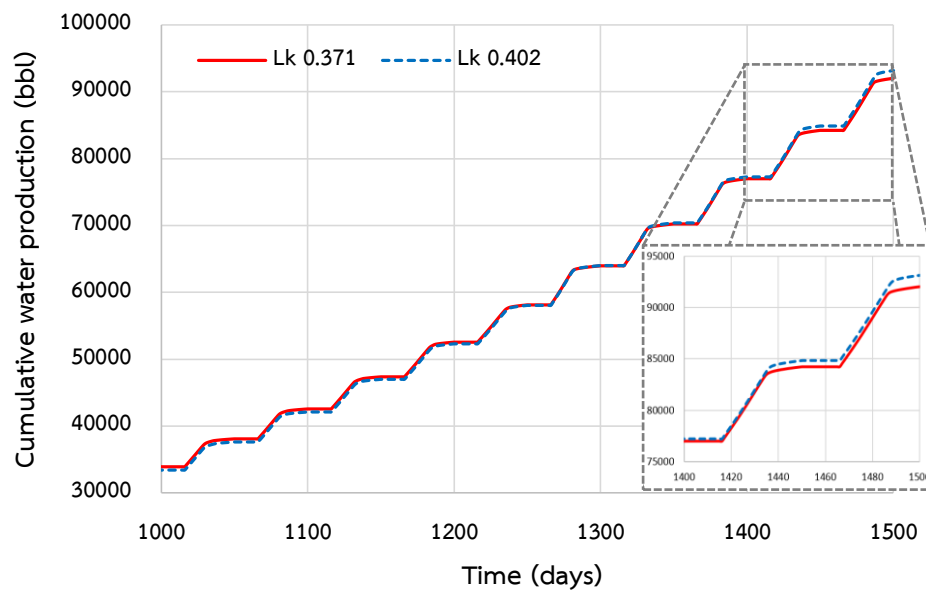


Figure 5.22 Cumulative water produced from reservoir model with L_k value of 0.371 and 0.402 at later cycles

It can be concluded that heterogeneity slightly affects effectiveness of CSI process. Reservoir with low degree of heterogeneity gains benefit from well distribution in vertical direction in early stage, resulting in better conformance of displacement.

Reservoir with higher degree of heterogeneity yields better results for longer production time due to steam propagation to deeper zone of reservoir. Ideal conditions for steam propagation in this case is therefore high horizontal permeability on top layers with also good vertical permeability, allowing hot condensed water during soaking period to percolate down to displace additional oil. L_k of 0.371 yields the highest oil recovery but if energy consumption is taken into account, this case might not yield the best benefit due to higher energy consumption. Moderate heterogeneity value (L_k of 0.328) tends to yield better benefit of both oil recovery and energy consumption since it obtains benefits from well distribution in vertical permeability in early cycles together with deeper steam propagation in later cycles.

In this section permeability sequence is coarsening upward where highest permeability is in upper layer and lower permeability is decreased in lower layers to bottom layer of reservoir. Effect of permeability sequence is described in section 5.6.

5.3 Effect of Vertical Permeability

In this section, heterogeneous reservoir model with L_k value of 0.328 (base case) is constructed with different vertical permeability values. Horizontal permeability values in all layers are as same as base case but vertical permeability values are varied by multiplying the ratio of vertical to horizontal permeability (k_v/k_h). Since k_v/k_h of heterogeneous base case is 0.1, variation of vertical permeability is constructed in both increasing and decreasing directions. Three additional values of k_v/k_h are 0.001, 0.01 and 0.2. Significant difference in oil recovery factors obtained from models with different vertical permeability is shown in Figure 5.23.

From the figure, it is shown that the case of $k_v/k_h = 0.2$ yields the highest oil recovery factor among all cases. Cases of $k_v/k_h = 0.01$ and 0.001 obtained very low oil recovery factors.

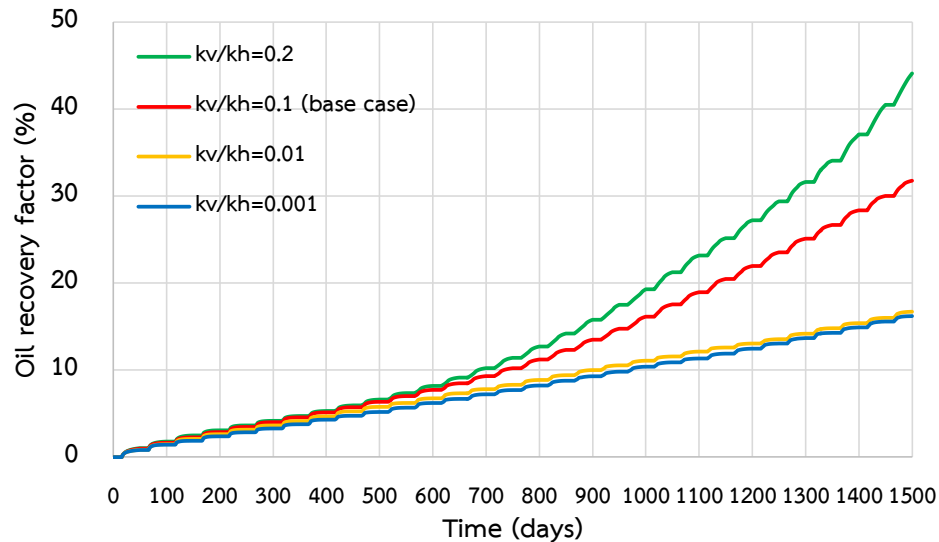


Figure 5.23 Oil recovery factors obtained from cases with different vertical permeability values as a function of time

Steam which is in gaseous phase normally flows up to upper layers after it is injected into reservoir due to its low density. For cases of low k_v/k_h (0.001 and 0.01), injected steam from lower layers of reservoir has difficulty to flow to top layers in vertical direction since vertical permeability is extremely low. Steam therefore, prefers to flow in lateral direction. Propagation of steam chamber in all cases with different vertical permeability values are illustrated in Figure 5.24.

It is obvious that in cases of very low vertical permeability, steam chamber grows mainly in middle of reservoir. As absolute permeability value in top layers are very high compared to middle layers, flowing back during production period results in both saturations of heated oil and condensed water around the wellbore. High saturation of both phases results in low effective permeability, causing difficulty for steam injection in the following cycles. In summary, steam propagation is more favorable in middle layers where horizontal permeability and effective permeability favor the lateral flow in two directions. Nevertheless, flowing in and out in the same layer is difficult to drain the heated oil to production well. Hence, oil recovery is quite low in these cases.

For cases of higher k_v/k_h (0.1 and 0.2), injected steam from lower layers easily flow to upper layers due to gravity and high vertical permeability. Steam chamber is formed in top of reservoir and start to expand to lower layers in both vertical and lateral directions.

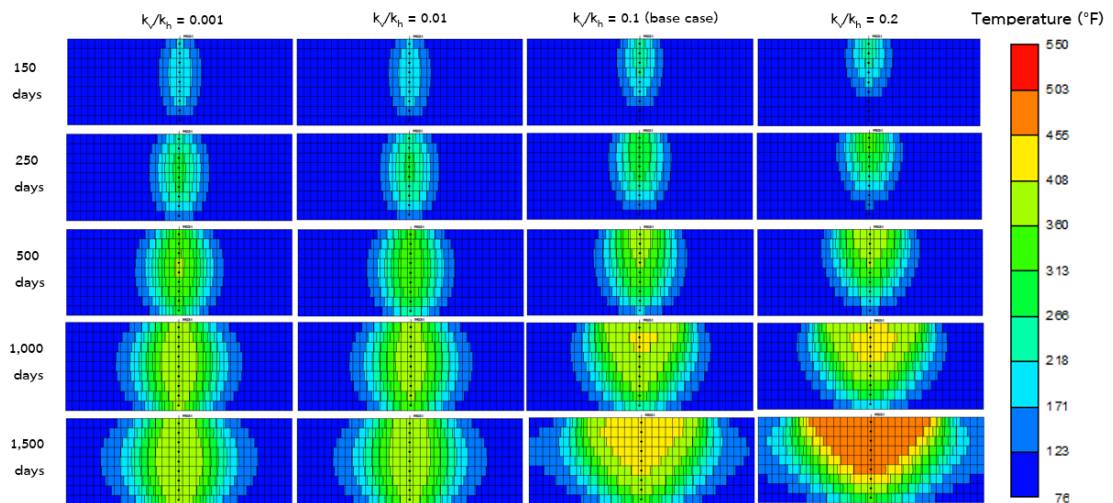


Figure 5.24 Temperature profiles of central well from reservoir models with different k_v/k_h values at different period, illustration steam propagation

Since steam chamber is formed near wellbore at the beginning and starts to propagate deeper into reservoir, this results in reduction of oil viscosity in larger area. High oil recovery factors from these cases are responsible from displacement from condensed water. Difference in shape of steam chamber significantly affects oil productions. Average oil production rate for all cases is shown in Figure 5.25.

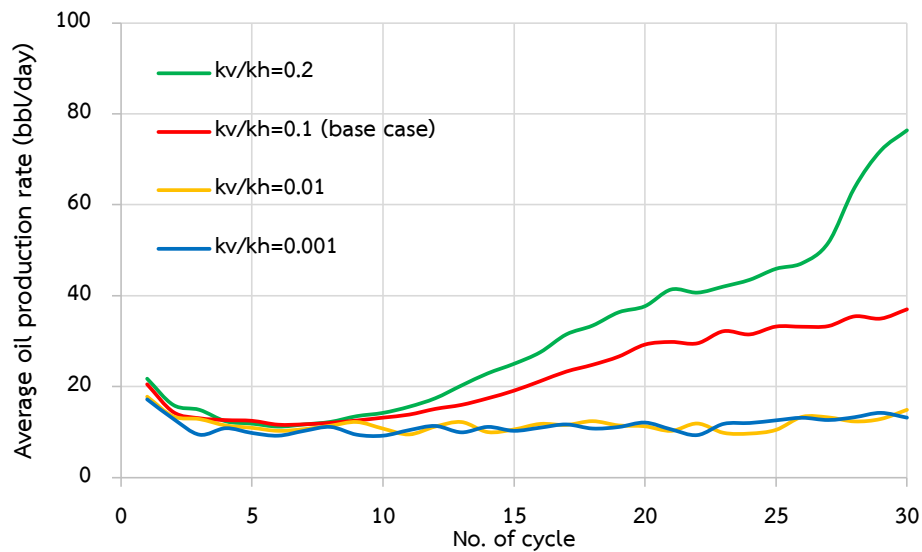


Figure 5.25 Average production rates obtained cases with different vertical permeability values as a function of time

As can be expected, reservoirs with low k_v/k_h values (0.001 and 0.01) yield fluctuation in oil production rates but in small range approximately around 11 barrels per day. Since steam chamber gradually expands into reservoir in lateral direction, heated oil hardly flows back to production well. For case of $k_v/k_h = 0.1$ and 0.2, oil production rate tends to increase more rapidly after 11th cycle. Since injected steam can easily flows to upper layers, condensed hot water percolates to lower layers, heating oil during soaking period and displacing oil when the well is re-opened.

Three-phase fluid saturation profiles and propagation direction of steam chamber for all cases are shown in Figure 5.26. Black solid arrows represent flow of steam, whereas red dashed arrows represent flow of condensed water. It can be obviously seen that increasing of vertical permeability results in higher propagation rate of steam chamber on top of reservoir. As explain previously, steam propagation into deeper zone facilitates contact between reservoir oil and injected steam as well as condensed hot water. From the figure, it can be observed also that at the same time of production, invaded reservoir volume by steam is much larger in case of reservoir with high vertical permeability.

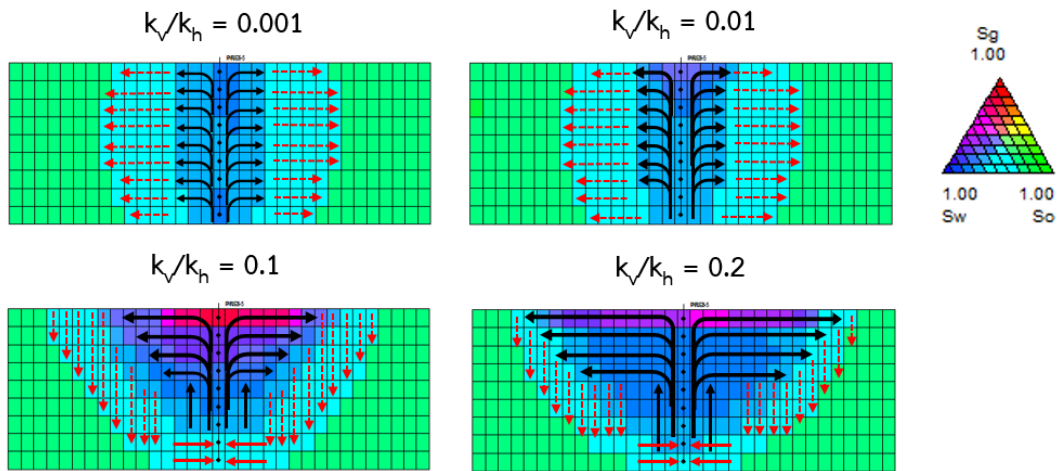


Figure 5.26 Three-phase fluid saturation profiles of the central well from reservoir models with different k_v/k_h values at 1,500 days, illustrating steam expansion direction and flow of condensed hot water direction

Fluid saturation profiles of all four wells are shown in Figure 5.27. From the figure, it can be seen that in case of $k_v/k_h = 0.2$, injecting steam from all wells at the same time results in encounter of steam chambers. Large amount of condensed water percolates down to lower layers as indicated by red arrows.

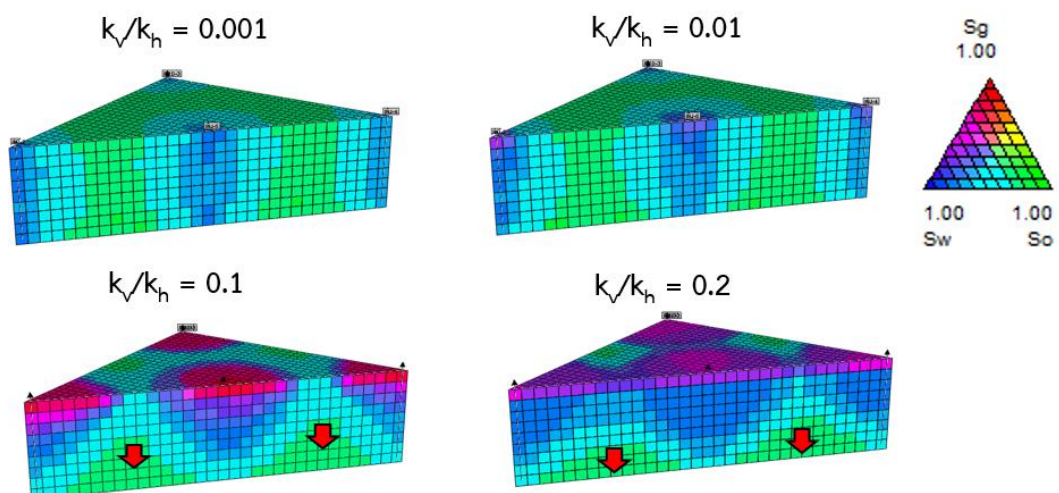


Figure 5.27 Three-phase fluid saturation profiles of reservoir models with different k_v/k_h values at 1,500 days

Since steam invasion is much higher in case of high vertical permeability, steam must be easily injected into reservoir and this should cause higher amount of injected steam. Therefore, comparison in terms of energy consumption is performed. Figure 5.28 illustrates energy consumed per barrel of oil recovered in different four cases as a function of time.

For cases of low k_v/k_h (0.001 and 0.01), oil recovery factor is mostly the same (approximately 16.21-16.71 percent) energy consumption from these two cases are slightly higher than other case since oil is hardly recovered. Energy consumed for cases of high k_v/k_h (0.1 and 0.2) is slightly lower due to much higher amount of produced oil. Even though higher amount of steam as same as energy required for steam propagation, higher amount of oil produced results in lower energy consumed in case of $k_v/k_h = 0.2$ especially for the last cycles where oil rate is rapidly increased from large invasion of steam chamber (as shown at the red arrow in Figure 5.28). Summary of oil recovery factor and energy consumed per barrel of oil obtained from all cases is shown in Figure 5.29.

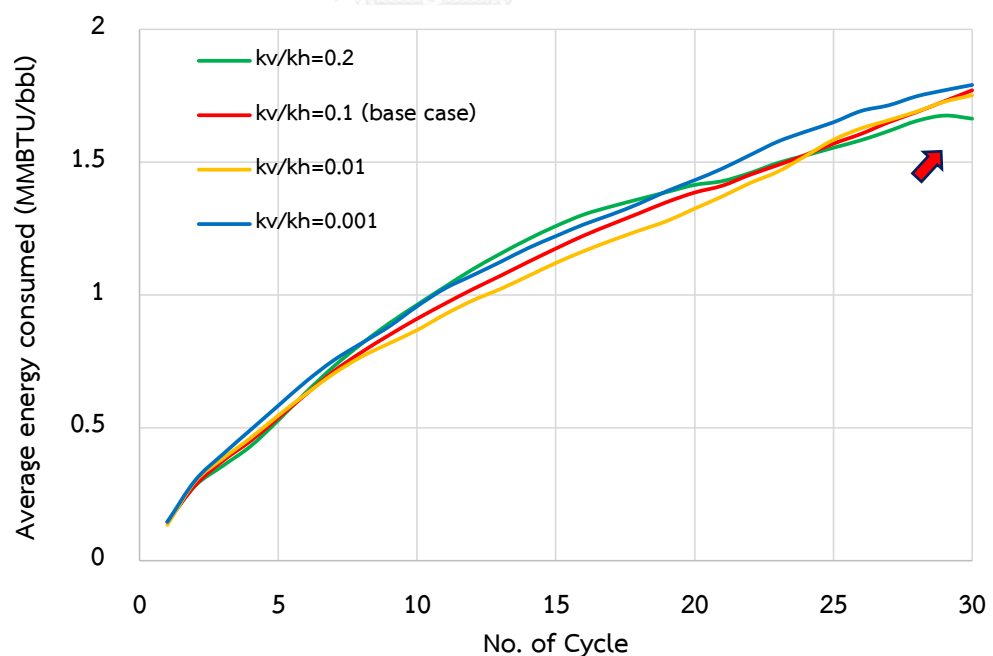


Figure 5.28 Energy consumed per barrel of oil obtained from reservoir models with different vertical permeability values as a function of time

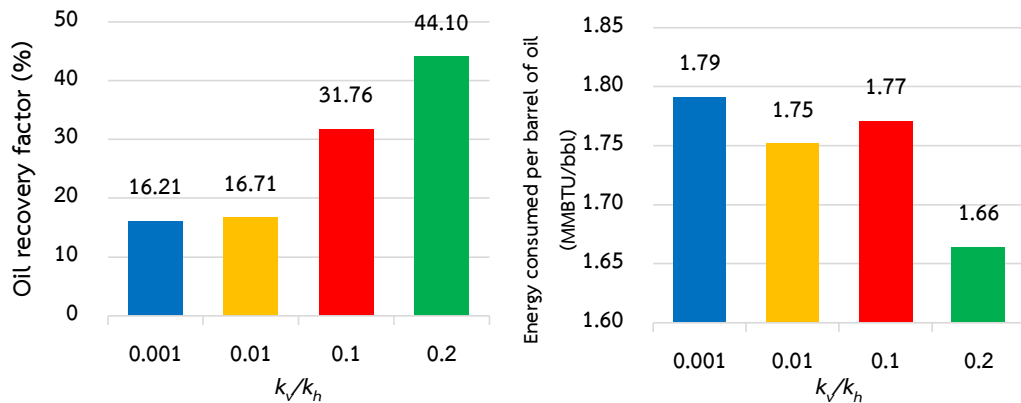


Figure 5.29 Summary of oil recovery factor and energy consumed per barrel of oil obtained from reservoir models with different vertical permeability values at the end of production

Vertical permeability greatly affects steam propagation as well as effectiveness of CSI process. Higher value of vertical permeability causes unequal propagation of steam in vertical profile due to good connection between reservoir layers. Steam chamber starts to form on top of reservoir, resulting in higher rate of steam invasion into deep area of reservoir. Vertical permeability also favors percolation of condensed hot water. Combination of these two mechanisms results in high oil recovery factors in every completion of each cycle.

5.4 Effect of Shale Volume

In order to study effects of shale percent on CSI process, reservoir models are constructed to have shale volume as structural shale. This type of shale is distributed within rock matrix without reduction of porosity but thermal properties of rock are altered due to the presence of shale. Therefore, porosity is kept constant for all models. Modification of thermal properties is hence accomplished on rock matrix only.

When rock matrix contains higher portion of shale, this affects both thermal conductivity and thermal capacity. As rock matrix (sandstone) contains higher percent of structural shale, overall thermal conductivity is proportionally decreased while thermal capacity is proportionally increased. Nevertheless, increasing higher portion of shale may cause in reduction of permeability but in order to avoid co-effect from

vertical permeability, reduction in permeability is neglected. Thermal properties of reservoir rock with different structural shale percent are summarized in Table 5.1.

Table 5.1 Thermal properties for reservoir rock with different structural shale volume

Percent of Sandstone	Percent of Shale	Volumetric Heat Capacity Btu/(ft ³ *F)	Thermal conductivity Btu/(ft ² *F)
1.00	0.00	24.71	60.00
0.90	0.10	27.44	55.38
0.85	0.15	28.81	53.07
0.80	0.20	30.17	50.76
0.75	0.25	31.54	48.45

Since reservoir rock for case without shale possesses the highest thermal conductivity, heat from injected steam could be conducted and transferred better than other cases. Average reservoir temperature for cases with different structural shale percent is shown in Figure 5.30

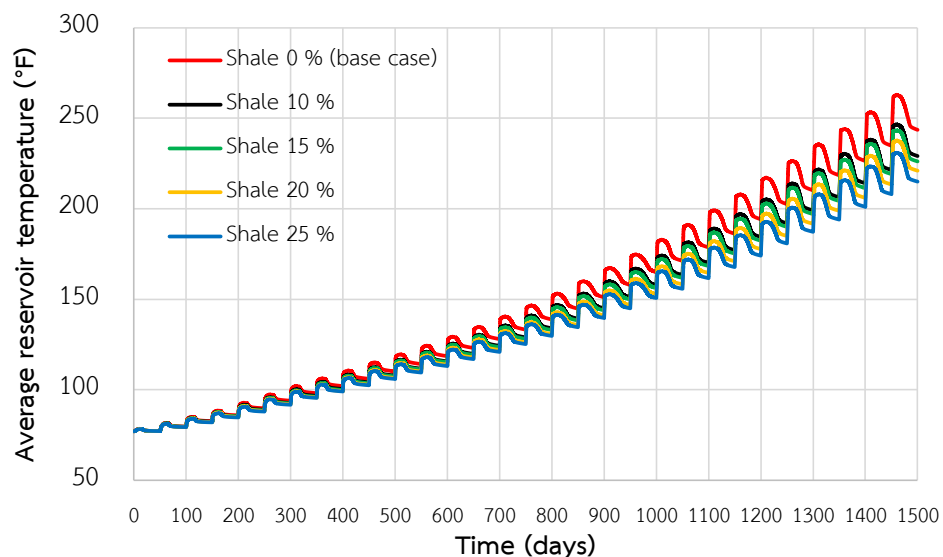


Figure 5.30 Average reservoir temperatures for cases with different structural shale percent as a function of time

Steam chamber of case without shale is slightly larger than the case with 25 shale percent at the same production period due to better heat conductivity. Comparison of reservoir temperature profile between case without structural shale percent and with structural shale percent is 25 percent is illustrated as Figure 5.31.

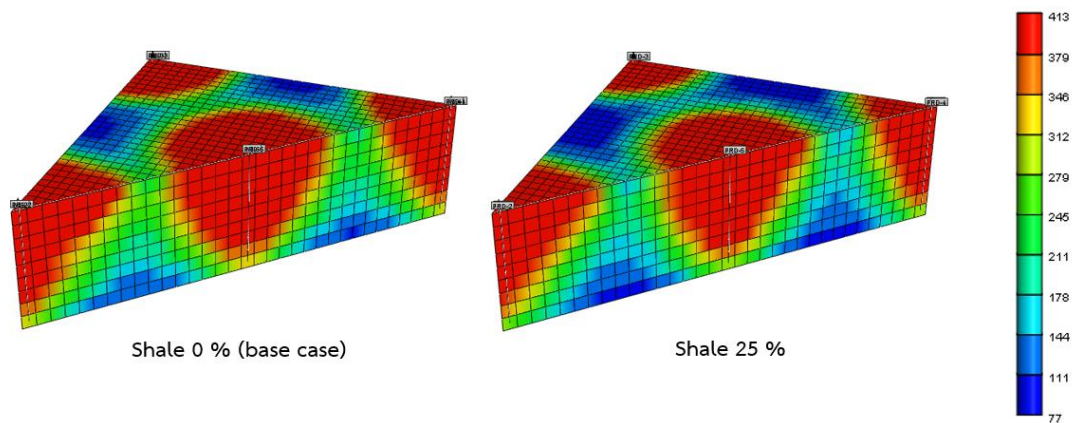


Figure 5.31 Comparison of reservoir temperature profile for reservoir models without structural shale volume and with structural shale volume of 25 percent (maximum) at the end of production

Theoretically, presence of shale tends to give benefit for CSI process in terms of heat accumulation which is the effect from higher thermal capacity. This should result in heat efficiency for the following cycle. However, in this study it shows that, higher oil recovery is obtained from lower percent shale volume. This is related to heat distribution in the reservoir since rock matrix with lower percent shale volume can transfer heat better than rock matrix with higher shale volume. Therefore, reservoir oil obtains heat at faster rate, resulting in higher oil recovery. Moreover, duration of each stage on CSI process (injection, soaking and production) may be too short in this study, causing insufficient retention time for heat to accumulate in each cycle. So, increment of thermal capacity with higher shale percent does not significantly improve effectiveness in terms of oil recovery. Case without shale obtains the highest oil recovery factor due to the highest thermal conductivity. Oil recovery factor for all cases with different structural shale percent is shown in Figure 5.32.

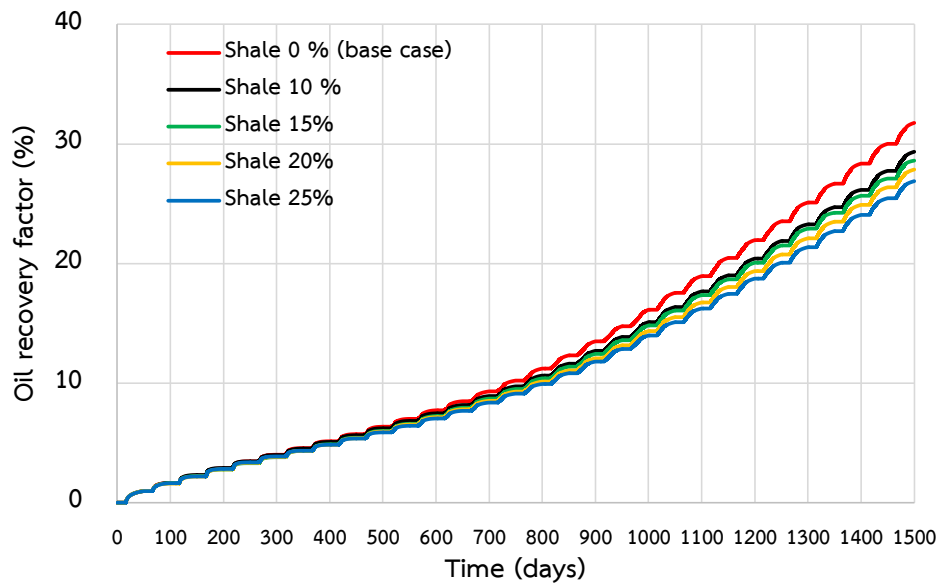


Figure 5.32 Oil recovery factors for cases with different structural shale percent as a function of time

It is obviously shown that case without structural shale volumes with better heat transfer property, yields the highest oil recovery. This high amount of produced oil results in lower energy consumption. Energy consumed per barrel of oil from models with different structural shale percent is shown in Figure 5.33.

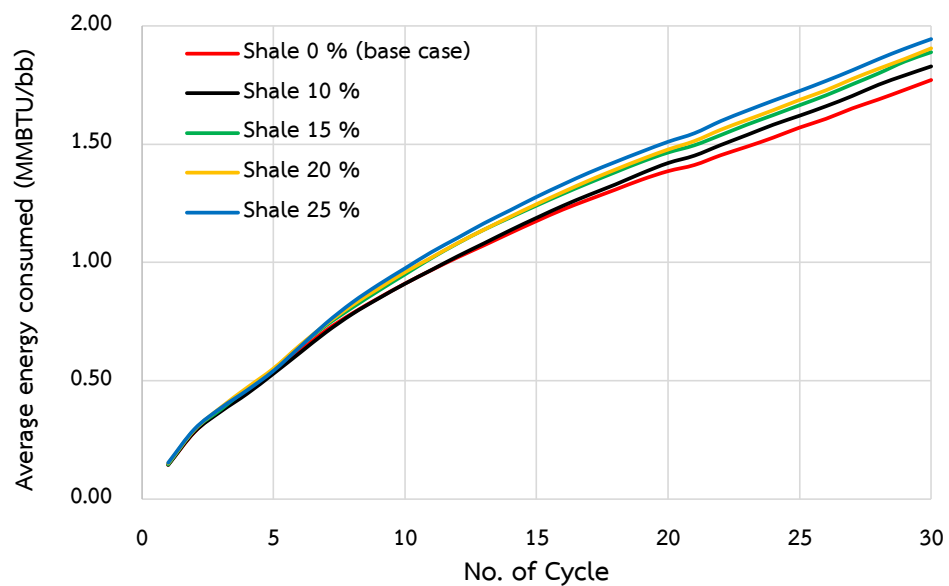


Figure 5.33 Energy consumed per barrel of oil obtained from reservoir models with different structural shale percent as a function of time

Increment of structural shale percent affects oil recovery mechanisms in CSI process. Increase of structural shale volume shows an adverse effect on oil recovery as a result of reduction in thermal conductivity. It could be summarized that low amount of structural shale is preferred for performing CSI process within short cycle life. Domination of thermal conductivity is observed in this study. With longer period of each cycle, effect from thermal capacity may dominate thermal conductivity which could turn the higher volume of structural shale to become more favorable case.

5.5 Effect of Relative Permeability

In this section, properties related to relative permeability are varied including Corey's exponents, end points of irreducible water and residual oil saturation before and after CSI process.

5.5.1 Corey's Exponent

Corey's exponent is expressed as curvaceous of relative permeability curves. Lower Corey's exponent value is described by less curvaceous of relative permeability curve. At any fluid saturation, lower Corey's exponent value corresponds to higher magnitude of relative permeability for every fluid compared to system with higher Corey's exponent value. Different values of Corey's exponent obviously affect flow ability of fluids. Relative permeability curves of oil/water and of gas/liquid systems for all cases are illustrated in Figure 5.34 and Figure 5.35, respectively.

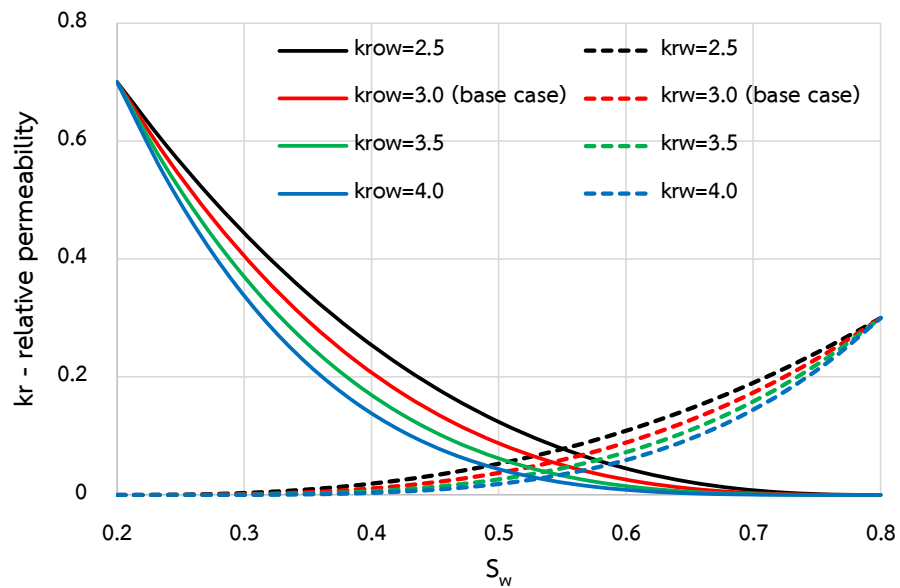


Figure 5.34 Relative permeability curves of oil/water system for reservoir models with different Corey's exponent values as a function of water saturation

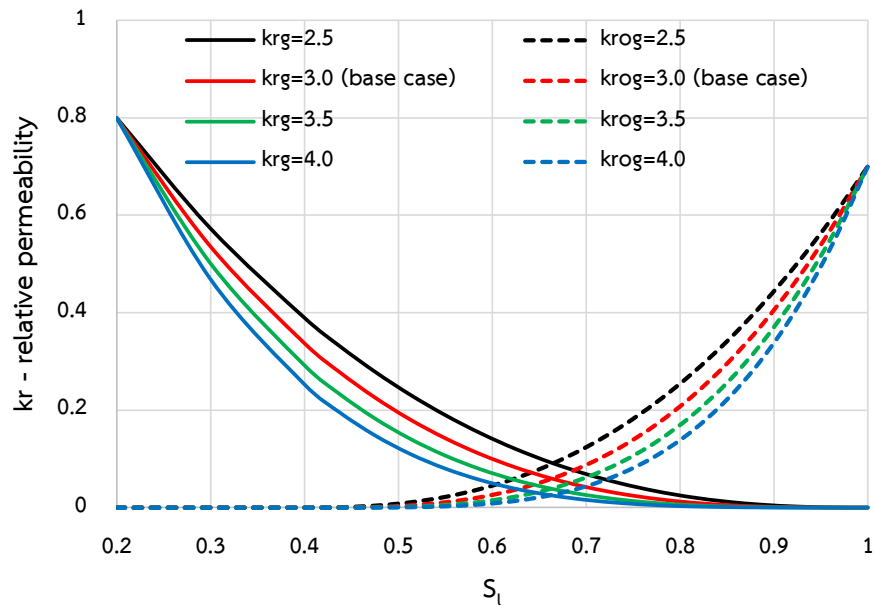


Figure 5.35 Relative permeability curves of gas/liquid system for reservoir models with different Corey's exponent values as a function of liquid saturation

Flow ability of fluid in reservoir is dependent on temperature since relative permeability curve changes with temperature. Relative permeability curves of oil/water systems at different temperatures for all cases are illustrated in Figure 5.36. As heated steam is injected into reservoir, increase in temperature leads all curves shift to the

right. As temperature is raised, relative permeability curves shift to the right hand side when plotting with water saturation. This greatly affects irreducible water saturation as well as residual oil saturation. In another word, at higher temperature, residual oil saturation is greatly reduced while irreducible water saturation is increased. In this section, magnitudes of relative permeability at end point saturations are kept constant to study effects of Corey's correlation.

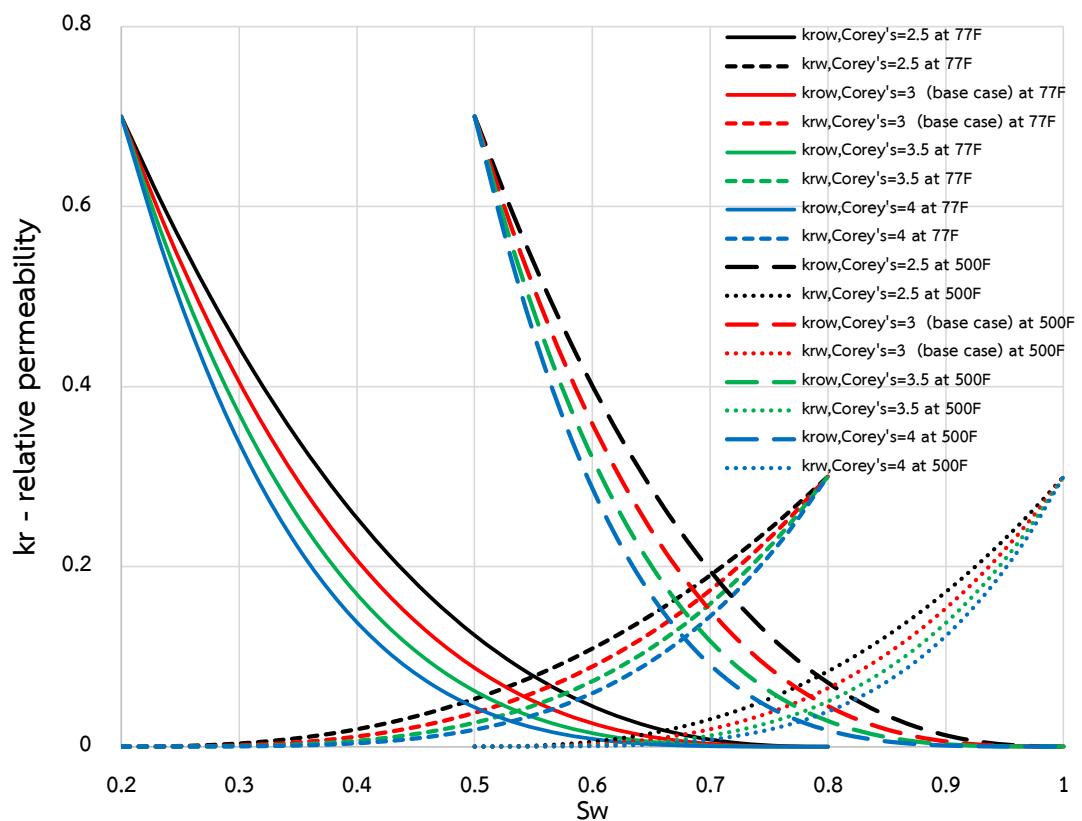


Figure 5.36 Relative permeability curves of oil/water system for reservoir models with different Corey's exponent values at different temperature as a function of water saturation

From these figures, it is obviously shown that lower Corey's exponent value yields higher magnitude of both relative permeability to oil and to water at any saturation. In early cycles of CSI process, water saturation around wellbore is higher after steam injection period. As absolute permeability values in upper layers of reservoir are much higher than that of lower layers, higher values of relative

permeability from cases with Corey's exponents of 2.5 and 3.0 results in high effective permeability to water in upper layers. So, injected steam prefers to flow into these upper layers. On the other hand, lower values of relative permeability to water in case of high Corey's exponents (3.5 and 4.0) results in lower effective permeability to water in upper layers. Therefore, difference of flow ability among layers of steam into formation is less compared to the cases of Corey's exponents of 2.5 and 3.0. Hence, injected steam enters every layer without a strong preference in high permeability layers.

Relative permeability to oil and saturation profile for all cases after injection period of 5th cycle is illustrated in Figure 5.37. Blue color in the profile of relative permeability to oil represents low flow ability of oil that is related to low oil saturation. This profile of relative permeability to oil also can refer to tendency of steam propagation (high water saturation) as shown by arrows.

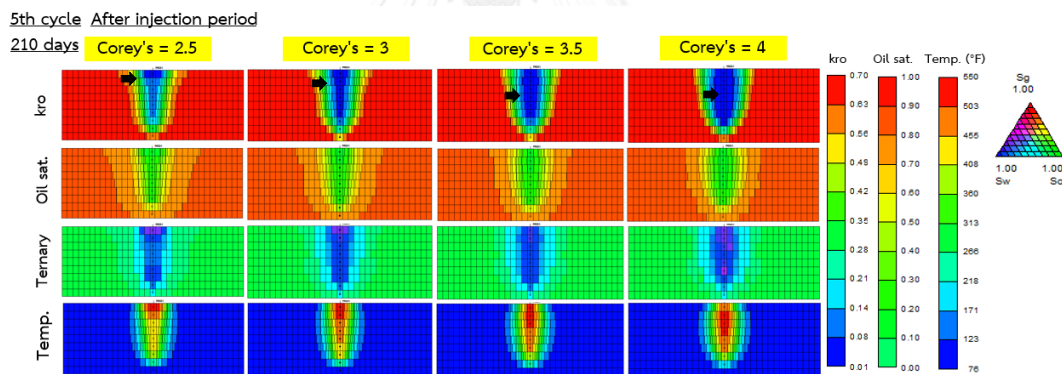


Figure 5.37 Profiles of relative permeability to oil, oil saturation, three-phase fluid saturation and temperature of the central well from cases with different values of Corey's exponents after the 5th injection cycle

After soaking period, well is re-opened to produce heated oil as well as condensed water. For cases with low Corey's exponent values (2.5 and 3.0), condensed water prefers to flow back through the zones with high effective permeability to water. Oil prefers to flow back and being produced in adjacent layers (lower layers) as less oil could flow due to high water saturation. This unequal in flow ability along layers results in tendency of steam propagation in top layers of reservoir. For cases with

higher Corey's exponent values (3.5 and 4.0), water flow back to the well followed by oil heat oil. Since flow ability is less in contrast along the vertical profile, propagation of steam is equal along the layers.

Relative permeability to oil and saturation profile for all cases after production period of 5th cycle is illustrated in Figure 5.38. In the profile of relative permeability to oil, area with high effective permeability to water or low effective permeability to oil is represented by blue color. High water saturation remains and so, injected steam in following cycles preferentially flow in area with this blue color.

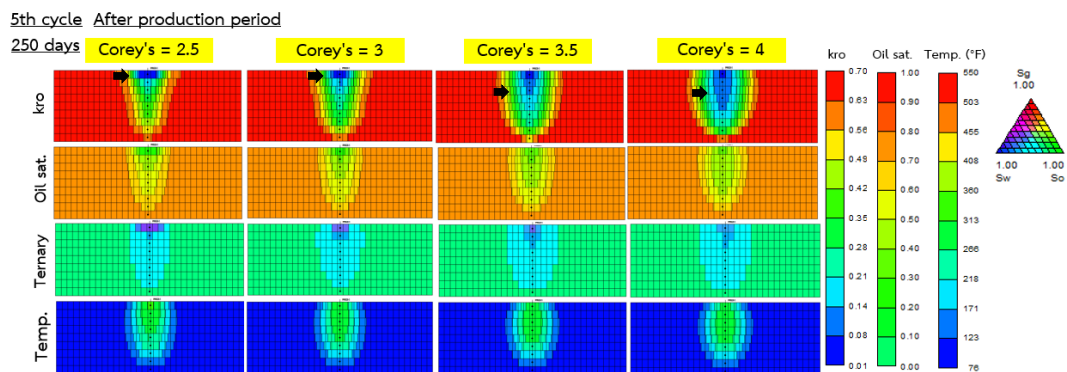


Figure 5.38 Profiles of relative permeability to oil, oil saturation, three-phase fluid saturation and temperature of the central well from cases with different values of Corey's exponents after the 5th production cycle

As injected steam in following cycles consequently prefers to flow in the zones where water saturation is high, propagation of steam among cases start to deviate from each other. In later cycles, flow ability and flow direction of water (steam) affects shape of steam chamber of each case. This is illustrated in several profiles in Figure 5.39, which is taken after the 20th injection cycle.

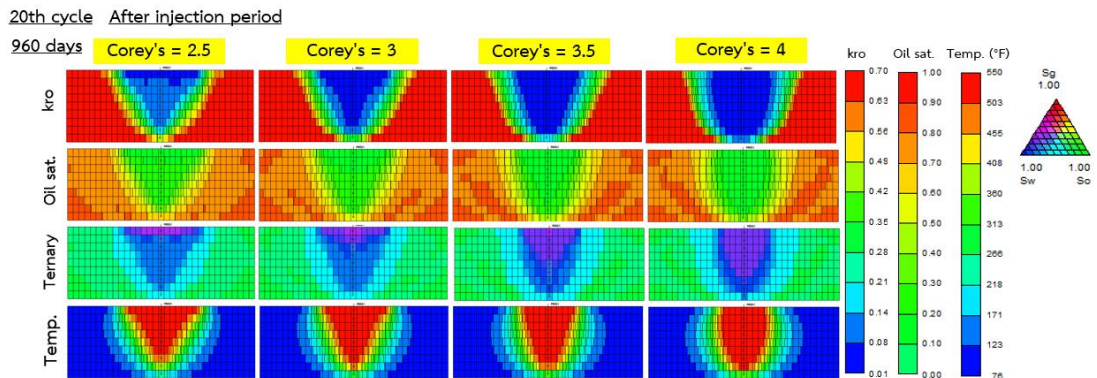


Figure 5.39 Profiles of relative permeability to oil, oil saturation, three-phase fluid saturation and temperature of the central well from cases with different values of Corey's exponents after the 20th injection cycle

Steam chamber for the case of Corey's exponent value of 2.5 early expands in upper layers. This causes hot condensed water to percolate down and steam chamber starts to expand deeper into reservoir as well as to lower adjacent layers in later cycles. The steam propagation/expansion is similar to effects of vertical permeability. For the case with Corey's exponent value of 4.0, steam chamber expands better in middle layers in early cycles and becomes larger in whole layers. Steam chamber profiles after the 20th production cycle for all cases are illustrated in Figure 5.40.

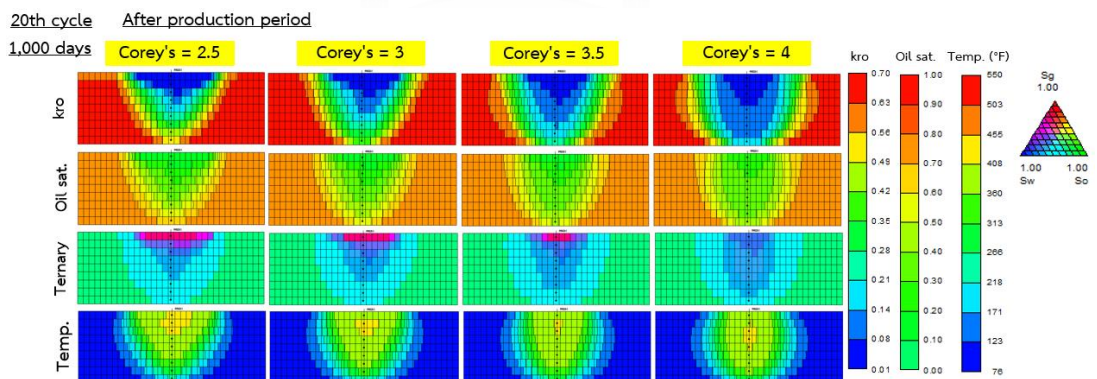


Figure 5.40 Profiles of relative permeability to oil, oil saturation, three-phase fluid saturation and temperature of the central well from cases with different values of Corey's exponents after the 20th production cycle

As high amount of injected steam propagates better only in upper layers in early cycles for case with Corey's exponent value of 2.5 and 3.0, water saturation is high in upper zone. This results in low relative permeability of oil. Less oil could flow back in this zone even at high temperature. Oil production rate during 1st to 16th cycles of CSI process is therefore quite low. Later, high amount of hot condensed water in upper layers starts to percolate down. Then, higher amount of oil is displaced and oil is produced faster than previous cycles. As average reservoir temperature is higher in case of low Corey's exponent value due to combined effect of steam chamber propagation and percolation of water, it results in improvement of flow ability. Average oil production rate and reservoir temperature for all cases are shown in Figure 5.41 and Figure 5.42 respectively.

For cases with Corey's exponent value of 3.5 and 4.0, injected steam does not have preference to expand in top layers during early cycles. Injected steam tends to flow into every layer and hence, temperature near wellbore is slightly high in all layers. Therefore, oil production rate is high from well thermal distribution in this period. After steam chamber starts to expand in later cycles, higher average reservoir temperature, production rate is gradually increased. However, since steam chamber is laterally developed, effect of hot water percolation is not well observed as in case of low Corey's exponent values.

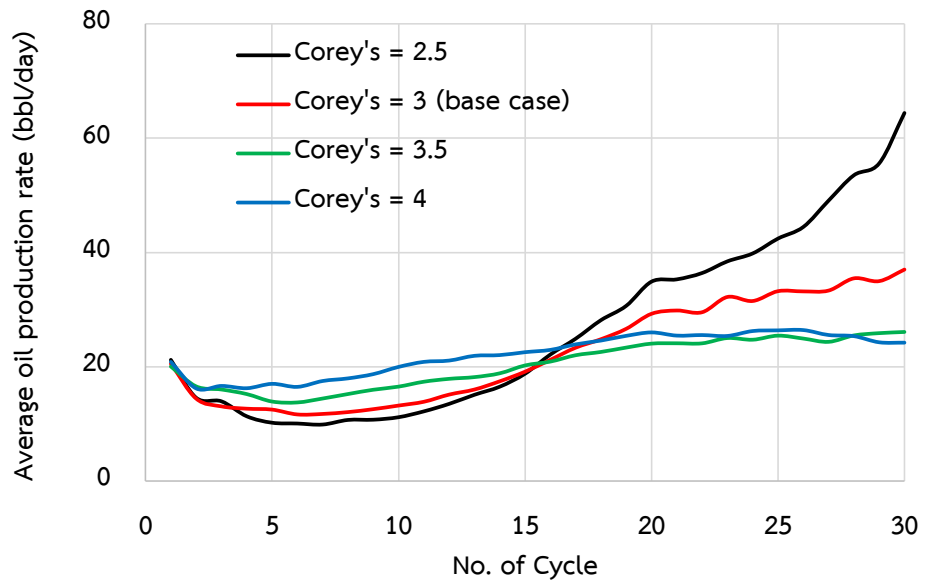


Figure 5.41 Average oil production rates for cases with different values of Corey's exponent as a function of time

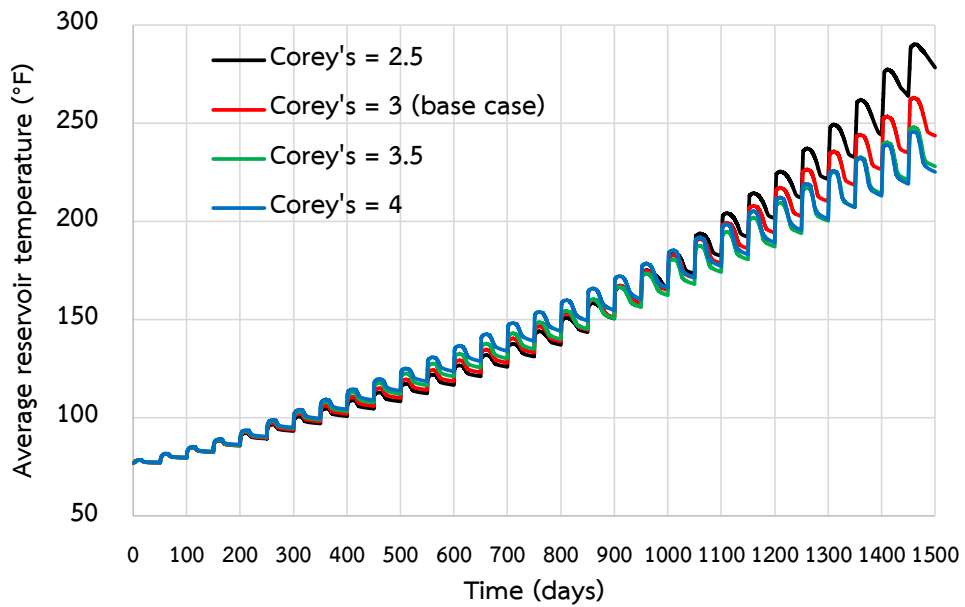


Figure 5.42 Average reservoir temperatures for cases with different values of Corey's exponent as a function of time

Larger volume of steam chamber for cases with low Corey's exponent values causes higher reservoir temperature, resulting in better flow ability of both oil and water. Hence, high amount of oil is produced in later cycles in this case. Oil recovery factor from case with Corey's exponent value of 2.5 at the end of production is the highest among all cases.

As same as in case with Corey's exponent value of 3.0, oil recovery factor increases slowly during early cycles for case with Corey's exponent of 2.5. Since reservoir temperature increases quickly in later cycles due to steam chamber expansion and percolation of hot condensed water, oil production rate sharply increases as well as oil recovery factor. Oil recovery factor obtained from case with Corey's exponent value of 3.0 is slightly higher than case with Corey's exponent value of 4.0 due to gradual increase in oil production rate. Oil recovery factors and energy consumed per barrel of oil for all cases with different values of Corey's exponents are shown in Figure 5.43 and Figure 5.44 respectively.

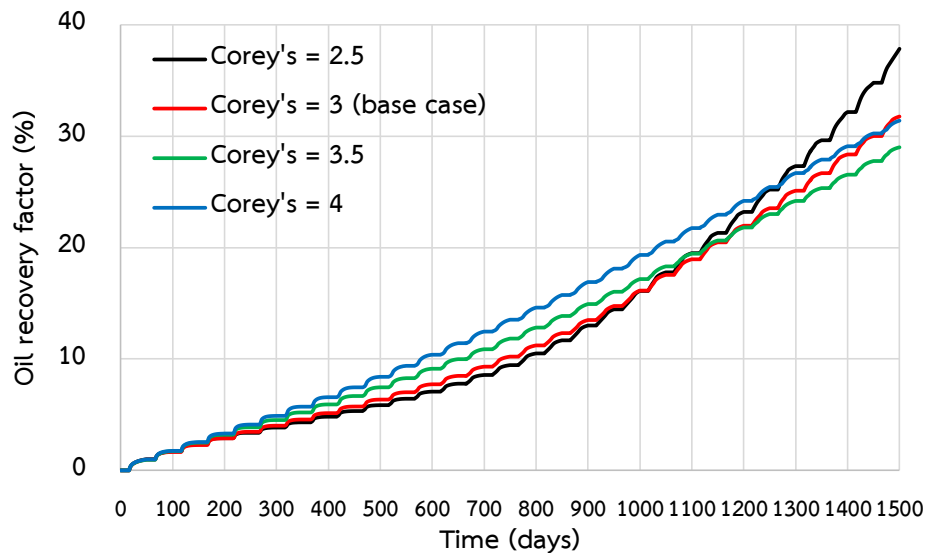


Figure 5.43 Oil recovery factors for cases with different values of Corey's exponent as a function of time

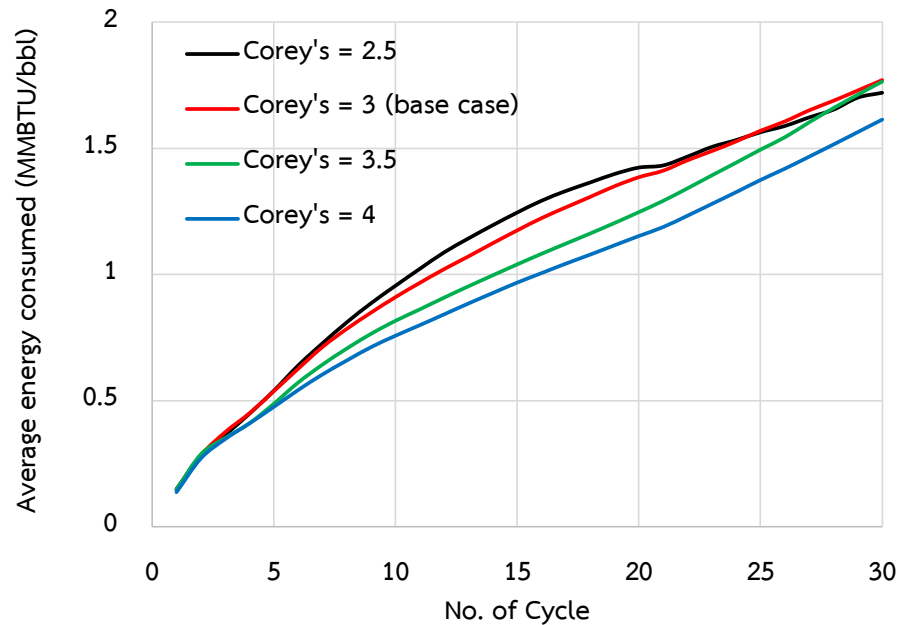


Figure 5.44 Energy consumed per barrel of oil obtained from reservoir models with different values of Corey's exponent as a function of time

Energy consumed per barrel of oil for cases with of low Corey's exponent values is obviously reduced at the end of production due to higher production of oil from combination of steam chamber expansion and hot water percolation. Comparison of oil that is produced in each layer between 5th and 30th cycle for case with Corey's exponent of 2.5 is shown in Figure 5.45. In 30th cycle, it is obvious that larger amount of oil is produced from 3rd layer and lower layers where condensed hot water tends to percolate down.

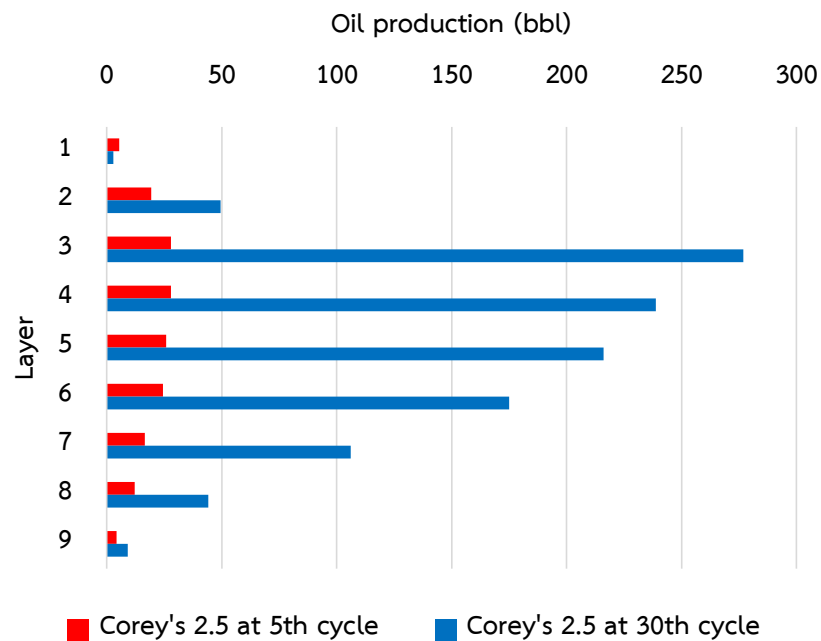


Figure 5.45 Comparison of oil produced in each layer between 5th and 30th cycle from a case with Corey's exponent value of 2.5 in each layer

Even though the case of Corey's exponent value of 2.5 yields the highest oil recovery factor but the overall energy consumed per barrel of oil is still higher than the case of Corey's exponent value of 4.0 since higher amount of steam is injected and less amount of oil is obtained in early cycles.

For the case with Corey's exponent value of 3.5, oil recovery factor is the lowest among all cases since higher Corey's exponent value results in lower flow ability of fluid. Part of injected steam flows to upper layers and condenses water percolates down slower than cases with lower Corey's exponent values (2.5 and 3.0). This results in slower oil displacement, leading to high energy consumed per barrel of oil at the end of production.

For case with Corey's exponent value of 4.0, energy consumed per barrel of oil slightly increases for whole production period. Even though the amount of injected steam is high, higher amount of oil is produced in later cycles. Comparison of oil produced in each layers between 5th and 30th cycle for case with Corey's exponent value of 4.0 is shown in Figure 5.46. From the figure, it can be seen that high amount

of oil is produced from middle layers in the 5th cycle. As condensed hot water percolates down in later cycles, more oil is produced in lower layers. Case with Corey's exponent value of 4.0 yields the lowest energy consumed per barrel of oil among all cases. Oil recovery factors and energy consumed for all cases are summarized in Figure 5.47.

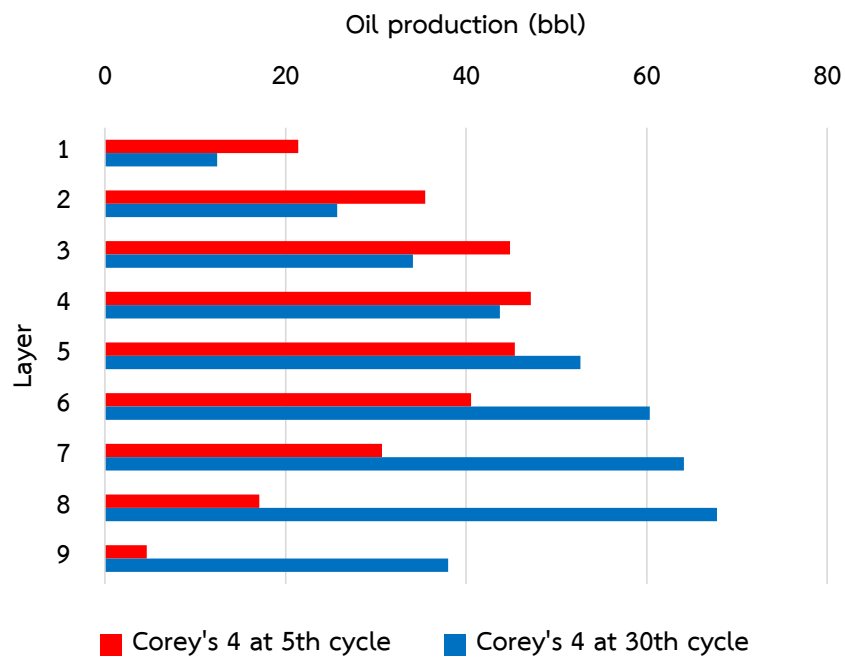


Figure 5.46 Comparison of oil produced from central well between 5th and 30th cycle for case with Corey's exponent value of 4.0 in each layer

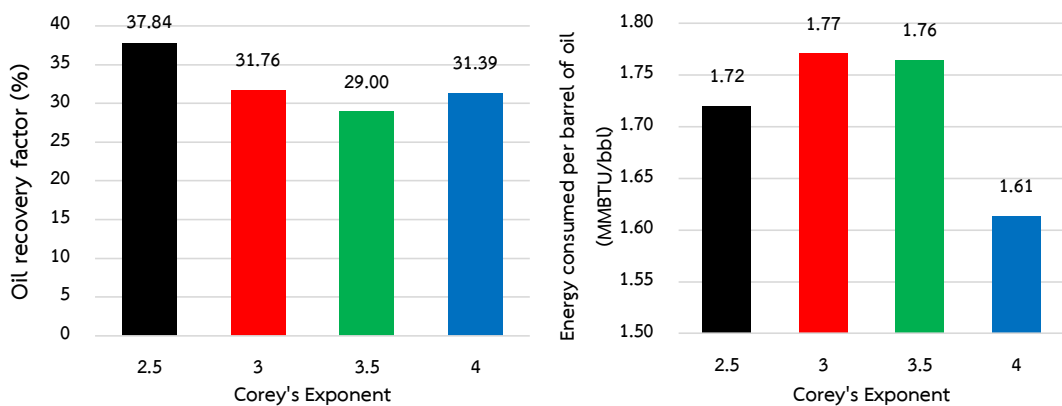


Figure 5.47 Summary of oil recovery factors and energy consumed at the end of production from whole cases

It is obvious that different values of Corey's exponent affect flow ability of all fluid in CSI process as magnitude of relative permeability of fluids is changed as a function of saturation and temperature during injection and production period. Different absolute permeability in each layer of heterogeneous reservoir model results in different effective permeability of fluids. Lower value of Corey's exponent results in higher summation of fluid flow ability at any fluid saturation. Preferential channel for steam to propagate into deep area of reservoir is observed on top of reservoir where summation of effective permeability is high. Together with percolation of hot condensed water due to gravity segregation, oil production rate and oil recovery factor rise up in later stage when steam expansion is large enough. Nevertheless, energy consumption is also dependent on amount of steam injected. As oil can be recovered, higher amount of steam can be easily injected, resulting in higher energy consumption.

5.5.2 End Point Saturations at Reservoir Temperature

In order to obtain effect of end point saturations at reservoir temperature, three set of relative permeability curves with end point saturations both irreducible water saturation and residual oil saturation at 77 °F modified while shape of relative permeability curves, magnitude of both relative permeability to oil and water, saturation end points of irreducible water and residual oil at 500 °F are kept constant. Values of three different end point saturations are summarized in Table 5.2 and constructed relative permeability curves of oil/water system for reservoir models with different saturation end points are shown in Figure 5.48.

Table 5.2 End point saturations of three different cases at reservoir temperature

End Point	Temperature (°F)					
	Case1		Base case		Case2	
	77	500	77	500	77	500
Irreducible water saturation (S_{wi})	0.15	0.50	0.20	0.50	0.25	0.50
Residual oil saturation (S_{or})	0.25	0	0.20	0	0.15	0

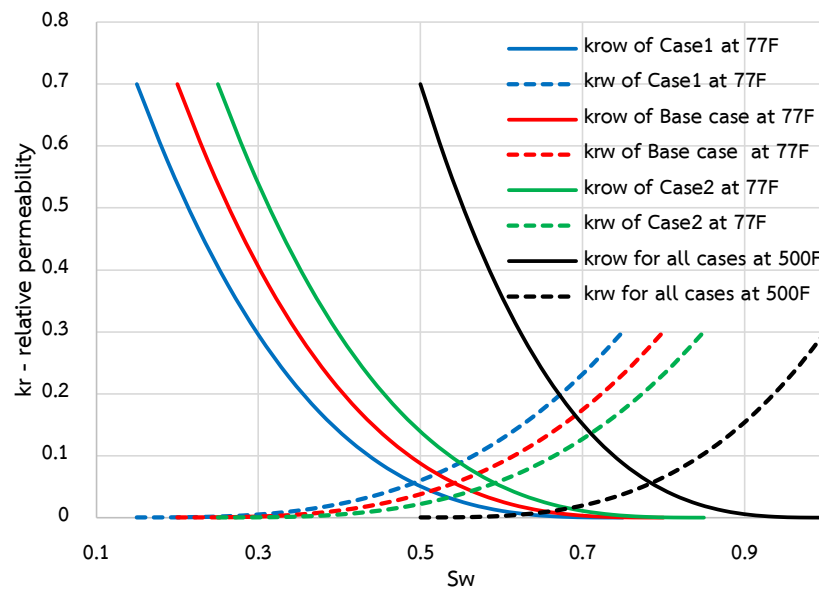


Figure 5.48 Relative permeability curves of oil/water system with different end point saturations at reservoir temperature as a function of water saturation

After soaking period, well is re-opened and both of heated oil and condensed water flow back due to pressurization. Case1 with the highest initial oil saturation (the lowest irreducible water saturation) obtains higher amount of produced oil among all cases. Higher amount of injected steam in the following cycles for case1 results in higher reservoir temperature. As oil viscosity decreases with temperature, oil mobility is improved especially around wellbore where temperature is very high. Case1 with the highest initial oil saturation yields best benefit on both oil recovery factor and energy consumed per barrel of oil at the end of production among all cases. Higher portion of oil is one desirable parameter for thermal recovery. Higher portion of heat is delivered to oil than absorbing by irreducible water. Oil recovery factors and energy consumed per barrel of oil obtained from models with different saturation end points are shown in Figure 5.49.

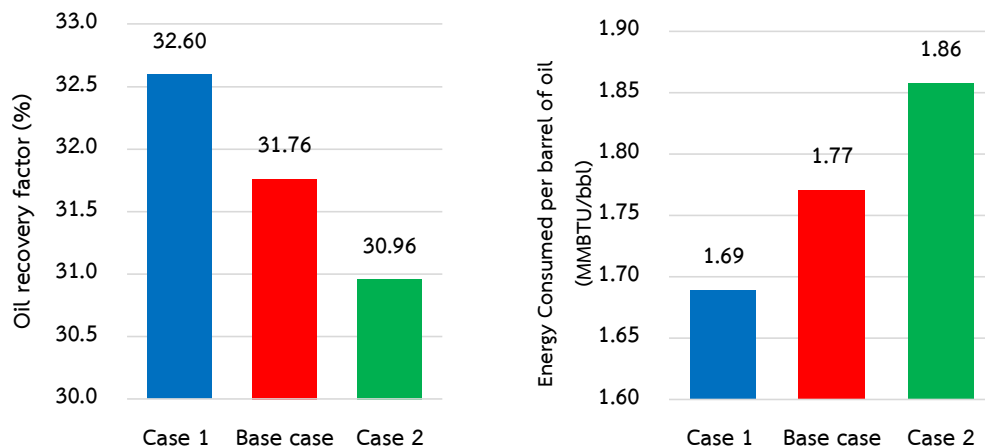


Figure 5.49 Summary of oil recovery factors and energy consumed per barrel of oil obtained from reservoir models with different end point saturation at reservoir temperature

Saturation end points of relative permeability affect initial exact oil in reservoir. Identifying of irreducible water saturation at reservoir condition is therefore important. As relative permeability curves all shift to right hand side at elevated temperature, effects of residual oil saturation is covered. Higher amount of initial oil saturation or lower amount of initial water saturation shows desirable results compared to others. Higher portion of oil results in better heat distribution to oil instead of to water.

5.5.3 End Point Saturations at Elevated Temperature

In this section, end point saturations of relative permeability to oil and water at elevated temperature (steam temperature) are varied while shape of relative permeability curves, magnitude of both relative permeability to oil and water, end point saturations at reservoir temperature are kept constant. Three different end point saturations are summarized in Table 5.3 and relative permeability curves of oil/water system for reservoir models different end point saturations are shown in Figure 5.50.

Table 5.3 End point saturations of three different cases at elevated temperature

End Point	Temperature (°F)					
	Case3		Case4		Base case	
	77	500	77	500	77	500
Irreducible water saturation (S_{wi})	0.20	0.40	0.20	0.45	0.20	0.50
Residual oil saturation (S_{or})	0.20	0.10	0.20	0.05	0.20	0

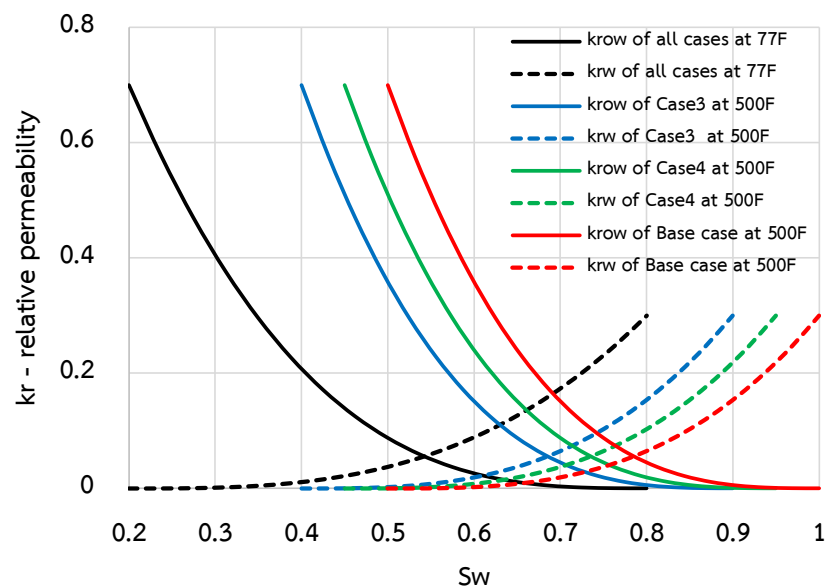


Figure 5.50 Relative permeability curves of oil/water system with different end point saturations at elevated temperature as a function of water saturation

As relative permeability to oil and water curves are shifted to the left at elevated temperature, system becomes lesser water wetness. Less amount of oil can be produced while less amount of water is stored in pore space as irreducible water saturation. From Figure 5.51, it is obvious that these shifted of oil-water relative permeability curves (case 3 and 4) result in lower oil recovery factor together with higher energy consumed per barrel of oil.

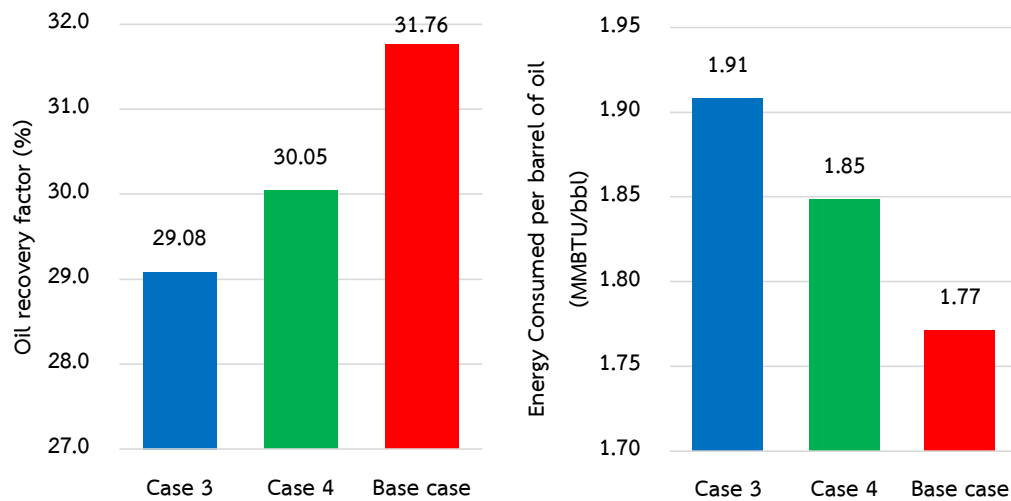


Figure 5.51 Summary of Oil recovery factors and energy consumed per barrel of oil obtained from reservoir models with different end point saturation at elevated temperature

As CSI process changes flow ability at the elevated temperature, relative permeability curves at this state is therefore very important. It is obvious that after CSI process, case with the least residual oil saturation (base case) results in the highest oil recovery factor as well as the lowest energy consumed per barrel of oil. Since only oil recovery factor is more emphasized, residual oil saturation at elevated temperature therefore affects the effectiveness of CSI process. Higher value of irreducible water saturation at elevated temperature is also desirable since condensed water can be stored back while leaving oil being produced.

From previous and this section, it can also be concluded that reservoir with less connate water or irreducible water saturation is desirable for CSI process. Moreover, residual oil saturation at elevated temperature should be as low as possible to recover the highest amount of oil.

5.6 Effect of Permeability Sequence

From previous sections, effects of reservoir heterogeneity and vertical permeability are studied with coarsening upward sequence where the highest permeability is located on top layer and lower permeability is at the bottom most one. Injected steam with low density tends to flow to upper layers of reservoir due to

gravity and it also prefers to flow to layers with high permeability. High amount of condensed hot water from upper layers significantly affects oil production. It is obvious that permeability in each layer affects flow ability of fluid as well as steam propagation/expansion. Permeability sequence is therefore one of important parameters on CSI process that can control shape of steam chamber. Fining upward sequence is constructed in this section while several conditions of permeability are kept constant. Permeability values in each layers of reservoir are summarized in Table 5.4.

Table 5.4 Permeability values in each layer of reservoir with coarsening and fining upward sequences

Layer	Permeability (mD)	
	Coarsening upward (base case)	Fining upward
1	3,000	200
2	2,650	550
3	2,300	900
4	1,950	1,250
5	1,600	1,600
6	1,250	1,950
7	900	2,300
8	550	2,650
9	200	3,000

As permeability in lower layers for case with fining upward sequence is high, injected steam prefers to flow into these layers. Basically, steam tends to flow to upper layer due to its low density. Since permeability in upper layers for this case is very low, steam is limited to flow in. Steam chamber therefore expands into middle layers during later cycles of CSI process. Comparison of temperature profiles between cases with fining and coarsening upward sequences at different times is illustrated in Figure 5.52.

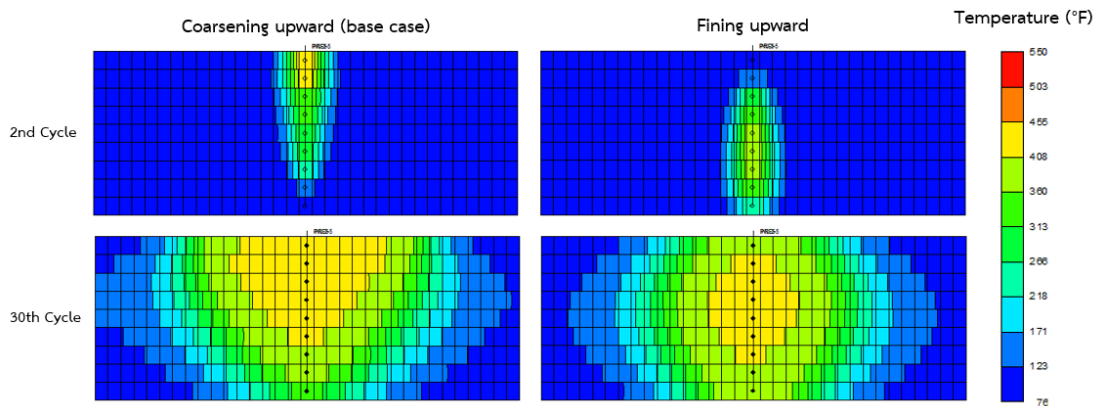


Figure 5.52 Comparison of temperature profiles between cases with fining and coarsening upward sequences at different time

In later cycles of CSI process, higher amount of condensed water for case with coarsening upward sequence percolates down to displaced oil in lower layers, resulting in higher amount of produced oil and higher oil production rate as well. Different of oil production rates between these two cases at later cycles is affected from different acceleration of oil displacement from hot condensed water from upper layers. Average oil production rates for cases with fining and coarsening upward sequences are shown in Figure 5.53.

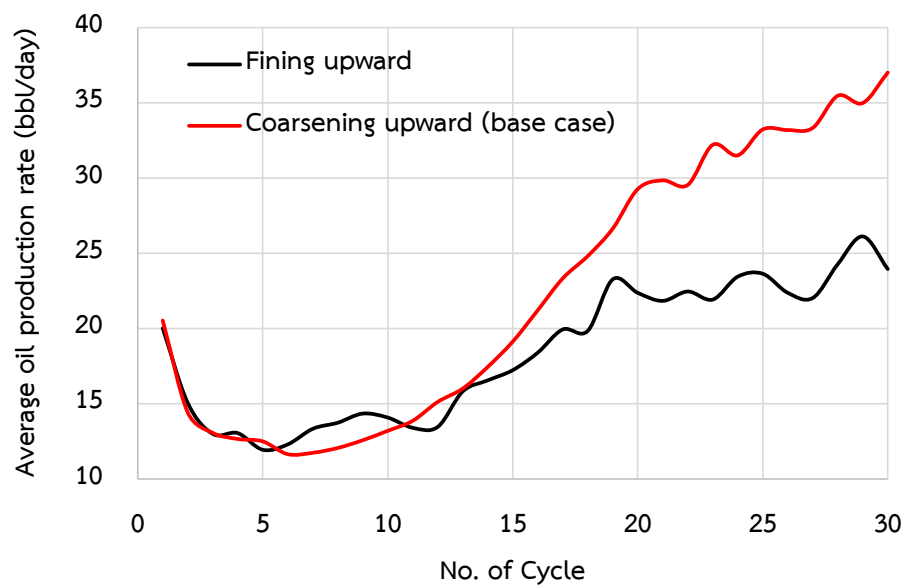


Figure 5.53 Average oil production rates for cases with fining and coarsening upward sequences as a function of time

It is obvious that permeability in each layer affects steam expansion and flow ability of fluid together with oil displacement direction. Oil recovery factors for cases with coarsening upward and fining upward sequences are 31.76% and 26.16% respectively. Oil recovery factors as a function of time for these two cases are illustrated in Figure 5.54.

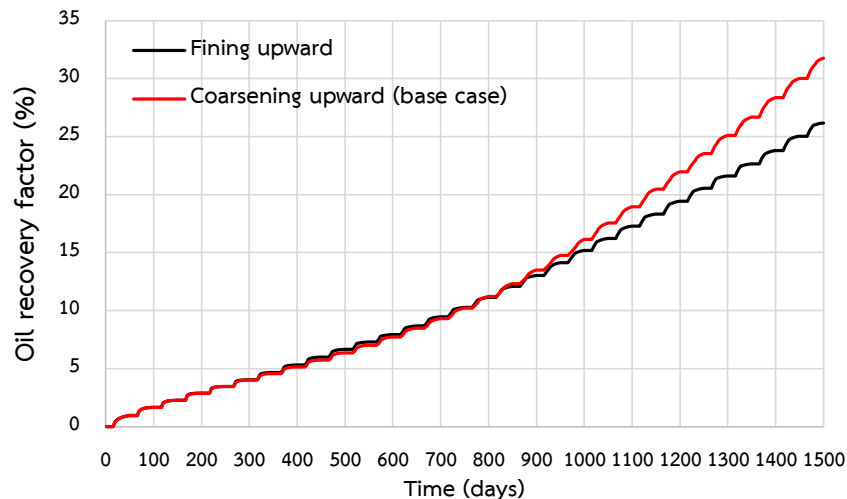


Figure 5.54 Oil recovery factors for cases with fining and coarsening upward sequences as a function of time

As explained previously, high permeability in upper layers for case with coarsening upward sequence (base case) causes higher amount of injected steam in following cycles. This results in higher energy consumed per barrel of oil. For case with fining upward sequence, injected steam is limited to flow to these high permeability layers especially in later stage where steam expansion is hardly occurred due to less percolation of hot condensed water. Comparison of cumulative water injection between these two cases is shown in Figure 5.55.

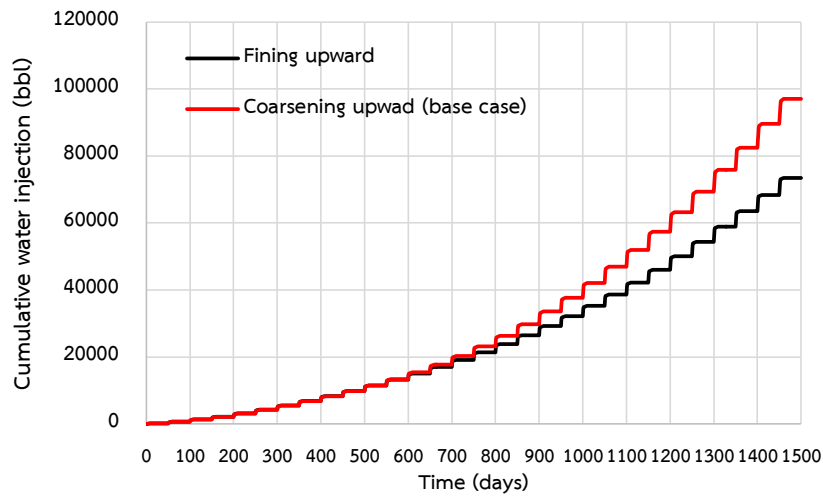


Figure 5.55 Cumulative water injection for reservoir models with fining and coarsening upward sequences as a function of time

At the end of production, energy consumed per barrel of oil for case with coarsening upward and fining upward sequence is 1.74 and 1.59 MMBTU/bbl respectively. Comparison of energy consumed per barrel of oil for these two cases is depicted in Figure 5.56.

Even the case of fining upward sequence obtains lower oil recovery factor (5.6% lower) but it consumed less injected steam due to less expansion of steam chamber and hence, less reservoir volume for injected steam in each cycle. Energy consumed per barrel of oil is approximately 8.85% lower than case of coarsening upward sequence.

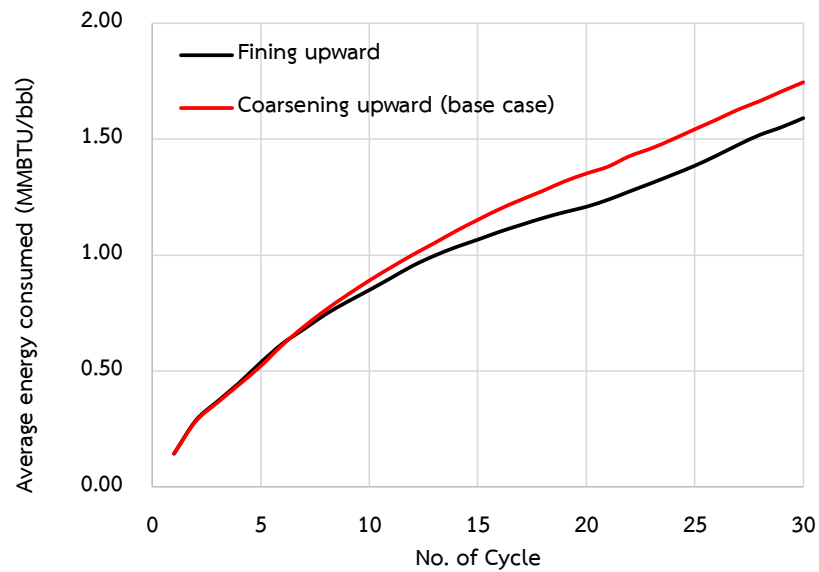


Figure 5.56 Energy consumed per barrel of oil obtained from reservoir models with fining and coarsening upward sequences as a function of time

In this section, it can be concluded that permeability sequence plays an important role on CSI process. Permeability significantly affects flow direction of fluid as well as shape of steam chamber shape. Coarsening upward sequence leads to well development of steam chamber on top of reservoir and this consequently results in percolation of hot condensed water to sweep down into lower layers. Oil recovery from this case is therefore much higher than the case of fining upward where steam expansion location is at the middle of reservoir where flow preference and gravity effect are intercepted.

CHAPTER VI

CONCLUSION AND RECOMMENDATION

Effects of operating parameters and reservoir parameters on cyclic steam injection process in multi-layered heterogeneous reservoir are summarized in this section together with recommendations for further study.

6.1 Conclusion

Results and discussion from previous chapter show that effectiveness of CSI process depends on many parameters. Study of interest reservoir parameters is useful to be a guideline by giving prime concerns for CSI process in reservoir with uncertain parameters and heterogeneity. Moreover, effects of these reservoir parameters also give a caution of acquiring data with more accuracy. Conclusions are summarized below.

1. Since production is performed in 5-spot pattern and all stages during CSI are performed at the same time, significant from CSI in this flood pattern occurs between these inter-well regions. Steam from each well tends to propagate deeper into reservoir in high permeability zone, resulting in steam chamber expansion. When steam chambers from different wells encounter each other, this causes higher amount of condensed water percolating down to lower layers. Combination of these two phenomena affects oil displacement especially in vertical direction.
2. Soaking period and steam quality are important operational parameters for designing production scheme of CSI process. Higher steam quality is more desirable as higher amount of heat is carried by steam. For lower value of steam quality, longer soaking period is required to compensate with longer contact to complete heat transferring. Based on oil recovery factor and energy consumed per barrel of oil recovered, steam quality of 1.0 and soaking period of 6 days is chosen as best condition for CSI process in reservoir with average heterogeneity value.

3. Reservoir heterogeneity in terms of Lorenz coefficient value does not show much significant effect on CSI process. Better distribution of permeability (lower heterogeneity or smaller Lorenz coefficient) tends to yields higher oil recovery factor in early cycles, whereas higher heterogeneity improves oil recovery factor in later cycles. In this study, reservoir model with L_k of 0.328 yields good results of both oil recovery factor and energy consumption since it obtains benefit from well distribution in vertical permeability in early cycles and deeper steam propagation in later cycles.
4. Vertical permeability significantly affects effectiveness of CSI process. High value of vertical permeability causes unequal propagation of steam in vertical profile due to good connection between reservoir layers. Higher vertical permeability is favorable since steam chamber can form on top of reservoir, resulting in higher rate of steam invasion into deep area of reservoir. Vertical permeability also favors percolation of condensed hot water. Combination of these two mechanisms results in high oil recovery factors in every completion of each cycle.
5. Higher portion of structural shale affects oil recovery mechanisms in CSI process as a result of reduction in thermal conductivity. Low amount of structural shale is favorable condition for performing CSI process within short cycle period. In this study, it is obvious that reduction in thermal conductivity dominates increment of thermal capacity.
6. Corey's exponent affects flow ability of all fluid in CSI process. Lower Corey's exponent results in preferential channel for steam to propagate into deep area of reservoir on top of reservoir where summation of effective permeability is high. Advantage of low Corey's exponent is observed in later stage when steam chamber developed on top of reservoir, favoring percolation of hot condensed water and as a result oil production rate and oil recovery factor rise up.
7. Saturation end points of relative permeability at reservoir and elevated temperature obviously affects oil recovery factor. Reservoir with less connate

water or irreducible water saturation is desirable for CSI process. Moreover, residual oil saturation at elevated temperature should be as low as possible to recover the highest amount of oil. Therefore, acquiring relative permeability curves should be as precise as possible.

8. Permeability sequence significantly affects flow direction of fluid as well as shape of steam chamber. Coarsening upward sequence leads to well development of steam chamber on top of reservoir, resulting in good percolation of hot condensed water to sweep down into lower layers. Oil recovery from case of coarsening upward is much higher than the case of fining upward where steam expansion prefers at middle of reservoir where flow preference and gravity effect are intercepted.

6.2 Recommendation

Several recommendations are provided for further study on CSI process

1. Wellbore heat loss of CSI process should be determined because this value also affects effectiveness of heat transfer by steam in terms of reduction of steam quality.
2. Laminated shale layer is one of another interesting reservoir parameter which may affect effectiveness of CSI process. However, more grid blocks are required to study effect of laminated shale as more sophisticated model construction is required. Since reservoir simulation program for this study is an academic license, number of grid block is limited.
3. Proper reservoir properties together with fluid properties such as oil gravity, solution gas-oil ratio and in-situ oil viscosity in specific area should be intensively considered as these properties affect overall operating conditions. Accurate values of fluid properties are required to construct more realistic reservoir model.

REFERENCES

- [1] Johannes Alvarez, S.H., Current Overview of Cyclic Steam Injection. **Journal of Petroleum Science Research** 2013. 2(3): p. 116-127.
- [2] Dietrich, J.K., Relative Permeability During Cyclic Steam Stimulation of Heavy-Oil Reservoirs. **Journal of Petroleum Technology**, 1981. 33(10).
- [3] Hascakir, B. and Kovscek, A.R. Reservoir Simulation of Cyclic Steam Injection Including the Effects of Temperature Induced Wettability Alteration. in **SPE Western Regional Meeting**. Anaheim, California, USA: Society of Petroleum Engineers, 2010.
- [4] Briggs, P.J. A Simulator for the Recovery of Heavy Oil From Naturally Fractured Reservoirs Using Cyclic Steam Injection. in **Middle East Oil Show**. Bahrain: Society of Petroleum Engineers, 1989.
- [5] Li, M., Astete, E.L., and Wang, H. A Simulation Study of a Cyclic Steam Stimulation Pilot in a Deep Carbonate Heavy Oil Reservoir in Oudeh Field, Syria. in **Canadian Unconventional Resources and International Petroleum Conference**. Calgary, Alberta, Canada: Society of Petroleum Engineers, 2010.
- [6] Chen, Q., Gerritsen, M.G., and Kovscek, A.R., Effects of Reservoir Heterogeneities on the Steam-Assisted Gravity-Drainage Process. **SPE Reservoir Evaluation & Engineering**, 2008. 11(5): p. 921 - 932.
- [7] Exploration, C. Project Indian. [Online]. Available from: <http://citadelexploration.com/project-indian/> [2014, August 1]
- [8] Sheng, J.J., Cyclic Steam Stimulation. in **Enhanced Oil Recovery Field Case Studies**: Gulf Professional Publishing, 2013
- [9] Latil, M., Enhance Oil Recovery. 1980, Paris, France: Technip.
- [10] R.M., B., Thermal Recovery of Oil and Bitumen. 1991, New Jersey: Prentice Hall.
- [11] Alpay, O.A., A Practical Approach to Defining Reservoir Heterogeneity. **Journal of Petroleum Technology**, 1972. 24(07): p. 841-848.

- [12] Permeability and Relative Permeability. [Lecture Notes]. 2014. Available from: <http://www.learningace.com/doc/2476843/d5264f55c59805a925a84afbd90a25d6/pet524-2c-permeability> [2014/08/01]
- [13] Glover, P., Petrophysics MSc Course Notes. in **Clay/Shale Effects on Porosity and Resistivity Logs**, pp. 270.





APPENDIX

จุฬาลงกรณ์มหาวิทยาลัย
CHULALONGKORN UNIVERSITY

APPENDIX

CMG Builder program with the section of STARS simulator are used. There are 5 sections required for the input of reservoir information including Reservoir, Components, Rock-Fluid, Initial conditions-Numerical and Wells and recurrent of simulator are involved with field unit and single porosity.

1. Reservoir

1.1 Create Cartesian Grid

Parameter	Value
Grid Type	Cartesian
K Direction	Down
Number of grid blocks	33, 33, 9
Block width (I direction)	33x5
Block width (J direction)	33x5

1.2 Array Properties

Parameter	Whole grid	Unit
Grid top (at layer 1)	1640	ft
Thickness	7	ft
Porosity	0.3	fraction
Permeability I	<i>vary with Lorenz coefficient</i>	
Permeability J	<i>vary with Lorenz coefficient</i>	
Permeability K	0.1*kh	
Water mole	1	fraction

1.3 Thermal Rocktype

1.3.1 Rock compressibility

Parameter	Value
Porosity reference pressure	725
Formation compressibility	0.000003 1/psi

1.3.2 Rock Thermal Properties

Parameter	Value
Volumetric Heat capacity	24.714 Btu/(ft ³ *F)
T-dependent Coefficient	0 Btu/(ft ³ *F*F)

1.3.3 Thermal conductivity

Parameter	Value
Thermal conductivity Phase mixing	Select COMPLEX
Reservoir rock	60 Btu/(ft*day*F)
Oil Phase	1.8 Btu/(ft*day*F)
Water Phase	8.58 Btu/(ft*day*F)
Gas Phase	0.32 Btu/(ft*day*F)

1.3.4 Overburden Heat Loss

	Volumetric Heat Loss	Thermal conductivity
Overburden	24.714 Btu/(ft ³ *F)	60 Btu/(ft*day*F)
Underburden	24.714 Btu/(ft ³ *F)	60 Btu/(ft*day*F)

2. Component

2.1 PVT Using Correlation

Parameter	Option	Value	Unit
Reservoir temperature		77	°F
Generate data up to max pressure of		1100	psi
Bubble point	Value Provided	294.859	psi
Oil density at STC (14.7 psia 60°F)	Stock tank oil gravity	9	API
Gas density at STC (14.7 psia 60°F)	Gas gravity (Air=1)	1.295	
Oil properties (bubble point, Rs, Bo) correlation	Standing		
Oil compressibility correction	Glaso		
Dead oil viscosity correlation	Ng and Egbogah		
Live oil viscosity correlation	Beggs and Robinson		
Gas critical properties correlation	Standing		
Set/update value of reservoir temperature, Fluid densities in dataset		Available	

2.2 Water Properties Using Correlation

Parameter	Option	Value	Unit
Reservoir temperature (TRES)		77	°F
Reservoir pressure (REFPW)		725	psi
Water bubble point pressure		-	
Water salinity		10000	ppm
Set/update value of reservoir temperature, Fluid densities in dataset		Available	

3. Rock-Fluid

3.1 Rock type Properties

Parameter	Value
Interpolation sets	Set#1, Set#2
Rock Fluid Properties	
Rock wettability	water wat
Method for evaluating 3-phase KRO	Stone's second method
Interpolation Component (INTCOMP)	Interpolation enabled
Relative permeability table	
Rock-fluid interpolation will depend on component:	Water
Phase from which component's composition will be taken:	gas mole fraction

3.2 Relative permeability table

End-point data and inputs required for construction of relative permeability curves of base case model

3.2.1 Generate Using Correlation

Parameter	Value
SWCON - Endpoint Saturation: Connate Water	0.2
SWCRIT - Endpoint Saturation: Critical Water	0.2
SOIRW - Endpoint Saturation: Irreducible Oil for Water-Oil Table	0.2
SORW - Endpoint Saturation: Residual Oil for Water-Oil Table	0.2
SOIRG - Endpoint Saturation: Irreducible Oil for Gas-Liquid Table	0
SORG - Endpoint Saturation: Residual Oil for Gas-Liquid Table	0.2
SGCON - Endpoint Saturation: Connate Gas	0
SGCRIT - Endpoint Saturation: Critical Gas	0
KROCW - K _{ro} at Connate Water	0.7
KRWIRO - K _{rw} at Irreducible Oil	0.3
KRGCL - K _{rg} at Connate Liquid	0.8
KROGCG - K _{rog} at Connate Gas	-
Exponent for calculating K _{rw} from KRWIRO	3
Exponent for calculating K _{row} from KROCW	3
Exponent for calculating K _{rog} from KROGCG	3
Exponent for calculating K _{rg} from KRGCL	3

Relative Permeability of Water-oil table			Relative Permeability of Liquid-Gas (Liquid saturation) table		
Sw	krw	krow	Sl	kr _g	krog
0.2	0	0.7	0.2	0.8	0
0.2375	7.32E-05	0.576782	0.3	0.535938	0
0.275	0.000586	0.468945	0.4	0.3375	0
0.3125	0.001978	0.375464	0.4375	0.278091	0.000171
0.35	0.004688	0.295312	0.475	0.226099	0.001367
0.3875	0.009155	0.227466	0.5125	0.181027	0.004614
0.425	0.01582	0.170898	0.55	0.142383	0.010938
0.4625	0.025122	0.124585	0.5875	0.109671	0.021362
0.5	0.0375	0.0875	0.625	0.082398	0.036914
0.5375	0.053394	0.058618	0.6625	0.060068	0.058618
0.575	0.073242	0.036914	0.7	0.042188	0.0875
0.6125	0.097485	0.021362	0.7375	0.028262	0.124585
0.65	0.126563	0.010938	0.775	0.017798	0.170898
0.6875	0.160913	0.004614	0.8125	0.0103	0.227466
0.725	0.200977	0.001367	0.85	0.005273	0.295312
0.7625	0.247192	0.000171	0.8875	0.002225	0.375464
0.8	0.3	0	0.925	0.000659	0.468945
			0.9625	8.24E-05	0.576782
			1	0	0.7

3.2.2 Relative permeability End point

a) Relative permeability Temperature Dependence

Parameter	Value		
Interpolation set	Set#1 & Set#2		
Temperature	Swr	Sorw	Sorg
77	0.2	0.2	0.2
500	0.5	0	0.05

b) Overwrite Critical Saturation and Endpoint

Parameter	Option	Value
Interpolation set		Set #2
Relative permeability to gas at connate liquid (KRGWCW)	Select Overwrite table value	0.9

3.2.3 Interpolation Set Parameter

Parameter	Value	
Phase Interpolation Parameters	Interpolation Set#1	Interpolation Set#2
Wetting Phase	0.2	0.6
Non-Wetting Phase	0.2	0.6

4. Initial conditions and Numerical

4.1 Initialization

Parameter	Value
Vertical Equilibrium Calculation methods	Depth-Average Capillary-Gravity method
Reference pressure (REFPRES)	725 psi
Reference depth (REFDEPTH)	1640
Water-Oil contact Depth (DWOC)	-

4.2 Numerical

Parameter	Value
Maximum Number of Timesteps (MAXSTEPS)	100000
First Time step size after well change (DTWELL)	1e-005 day
Isothermal Option (ISOTHERM)	OFF
Upstream calculation option (UPSTREAM)	KLEVEL
Linear solver iteration (ITERMAX)	200

5. Well and recurrent

5.1 Wells

5.1.1 Injector well 1-4

a) Perforation

Parameter	Value			
	well1	well 2	well3	well4
Radius	0.25 ft	0.25 ft	0.25 ft	0.25 ft
Perforation start	1,1,1	33,1,1	33,33,1	1,33,1
Perforation end	1,1,9	33,1,9	33,33,9	1,33,9

b) Well events

Name: INJ-1, INJ-2, INJ-3 and INJ-4

Type: INJECTOR MOBWEIGHT EXPLICIT

Constraint	Parameter	Limit/Mode	Value	Action
OPERATE	BHP bottom hole pressure	MAX	900 psi	CONT REPEAT
OPERATE	STW surface water rate	MAX	250 bbl/day	CONT REPEAT

5.1.2 Injector well 5

a) Perforation

Parameter	Value
Radius	0.25 ft
Perforation start	17,17,1
Perforation end	17,17,9

b) Well events

Name: INJ-5

Type: INJECTOR MOBWEIGHT EXPLICIT

Constraint	Parameter	Limit/Mode	Value	Action
OPERATE	BHP bottom hole pressure	MAX	900 psi	CONT REPEAT
OPERATE	STW surface water rate	MAX	1000 bbl/day	CONT REPEAT

5.1.3 Producer well 1-4

a) Perforation

Parameter	Value			
	well1	well 2	well3	well4
Radius	0.25 ft	0.25 ft	0.25 ft	0.25 ft
Perforation start	1,1,1	33,1,1	33,33,1	1,33,1
Perforation end	1,1,9	33,1,9	33,33,9	1,33,9

b) Well events

Name: PRD-1, PRD-2, PRD-3 and PRD-4

Type: PRODUCER

Constraint	Parameter	Limit/Mode	Value	Action
OPERATE	BHP bottom hole pressure	MIN	300 psi	CONT REPEAT
OPERATE	STL surface liquid rate	MAX	50 bbl/day	CONT REPEAT

5.1.4 Producer well 5

a) Perforation

Parameter	Value
Radius	0.25 ft
Perforation start	17,17,1
Perforation end	17,17,9

b) Well events

Name: PRD-5

Type: PRODUCER

Constraint	Parameter	Limit/Mode	Value	Action
OPERATE	BHP bottom hole pressure	MIN	300 psi	CONT REPEAT
OPERATE	STL surface liquid rate	MAX	200 bbl/day	CONT REPEAT

5.2 Groups

Cycling groups have been set, one group consists of one injection well and one production well at the same location. Parameters for each cyclic group are defined below.

5.2.1 Injection well constrains

Parameter	Value		Unit
Group name:	Group 1 to Group 4	Group 5	
Maximum bottom hole pressure	900	900	psi
Maximum injection water rate	250	1000	STB/D
Steam Temperature	500	500	°F
Steam quality	Varied (0.5, 0.8, 1.0)		Fraction

5.2.2 Production wells constrains

Parameter	Value		Unit
Group name:	Group 1 to Group 4	Group 5	
Minimum bottom hole pressure	300	300	psi
Maximum liquid rate	100	400	STB/D

5.2.3 Injection and production rate for all groups at different period of cycle

Cycle	Injection period		Production period	
	Maximum injection rate (STB/D)		Maximum liquid rate (STB/D)	
	Group 1 to Group 4	Group 5	Group 1 to Group 4	Group 5
1 - 20	250	1000	25	100
21 - 25	250	1000	37.5	150
26 - 30	250	1000	50	200

VITA

Worawanna Panyakotkaew was born on November 1st, 1987 in Chiangmai, Thailand. She received a Bachelor degree in Electrical Engineering from Faculty of Engineering, Chiangmai University in 2009. After obtaining her first degree, she spent three years working as a quality assurance engineer for Nikon Thailand Co., Ltd, Phra Nakhon Si Ayutthaya, Thailand. After that, she continued her further study in the Master's Degree program in Petroleum Engineering at the Department of Mining and Petroleum Engineering, Faculty of Engineering, Chulalongkorn University since the academic year 2013.

